POLYMERIC MICELLE NANOCARRIERS FOR THE TREATMENT OF DISSEMINATED CANDIDIASIS

by

Ronak Vakil

A dissertation submitted in partial fulfillment of

the requirements for the degree of

Doctor of Philosophy

(Pharmaceutical Sciences)

at the

UNIVERSITY OF WISCONSIN – MADISON

2006

AWPP
V134p
2006

POLYMERIC MICELLE NANOCARRIERS FOR THE TREATMENT OF DISSEMINATED CANDIDIASIS

Ronak Vakil

Under the supervision of Associate Professor Glen S. Kwon

At the University of Wisconsin – Madison

This dissertation evaluated the potential of polymeric micelles formed from a PEG-phospholipid as nanocarriers for amphotericin B (AmB). AmB is the primary drug used to treat life-threatening invasive candidiasis. The clinical utility of this antifungal drug has been limited by poor patient tolerance and an acute loss in kidney function at therapeutic doses. AmB monomers are thought to be selectively toxic to fungal cells. The drug causes toxicity to mammalian cells above its critical aggregation concentration. Since the drug's selectivity is influenced by extent of self-association, it was proposed that carriers which deaggregate AmB through polymer-drug interactions and slowly release monomeric drug may result in superior selectivity compared to its current formulation with sodium deoxycholate (D-AmB).

We could solubilize high levels of deaggregated AmB in micelles formed from PEG-phospholipids. In this form, AmB demonstrated reduced toxicity to mammalian cells while retaining potent antifungal efficacy, in vitro. While these micelles released AmB slowly in saline solutions, bovine serum albumin was found to have a destabilizing effect on these micelles causing encapsulated drug to be rapidly dissociated from the nanocarrier, a likely situation in vivo. Cholesterol co-incorporation influenced properties of PEG-phospholipid micelles and slowed AmB

release in serum albumin raising promise as long-circulating carriers for AmB delivery.

Novel polymeric micelles formed from PEG-phospholipid and PEG-b-poly(ε-caprolactone) are interesting for drug delivery due to biocompatibility, small size and high thermodynamic stability. These mixed polymeric micelles encapsulated clinically relevant levels of AmB, which was released in buffer in a composition-dependent manner. However, these micelles were unable to prevent AmB association with serum albumin raising questions about the utility of these carriers for AmB delivery.

In contrast with D-AmB, AmB in PEG-phospholipid micelles was stable against precipitation in saline when combined with 5-fluorocytosine (5-FC) and solubilized rapamycin. Hence, AmB solubilized in PEG-phospholipid micelles represents an interesting alternative to D-AmB particularly for combination therapy involving AmB, in conjunction with sodium supplementation. In vitro susceptibility studies exploring the interactive effects of AmB, 5-FC and rapamycin as pair-wise and three-drug combinations suggested indifferent or moderately synergistic activity for the isolates tested.

Dedication

I dedicate this dissertation to my grandmother, parents and sister.

Thank you for your guidance, support, love and enthusiasm.

You have been so close, from so far away.

Acknowledgements

I express my gratitude to Dr. Glen Kwon for mentoring my research and guiding me through a very productive graduate school experience. Thank you for the patience and kindness you have shown through these years.

I want to thank my thesis committee members Dr. Ralph Albrecht, Dr. Timothy Heath, Dr. Sandro Mecozzi and Dr. Lian Yu for their time, valuable advice and constructive criticisms.

I thank the faculty of the School of Pharmacy, especially in Drug Delivery for their instructive courses. Thank you for laying a solid foundation that has put me in a position so that I may contribute productively to the health sciences.

I would like to thank Dr. Thomas Stringfellow for help with the NMR experiments described in chapter 4.

I want to thank Dr. David Andes and Karen Marchillo for their time and expert advice with the fungal susceptibility studies. I would like to acknowledge Kayla Knilans and Laura Sewall for their assistance with fungal susceptibility studies detailed in chapter 5.

This work has been partially funded by the National Institutes of Health (AI043346-08). I thank the School of Pharmacy for funding from the Pfizer fellowship in my first year and teaching assistantships in the subsequent years. I also thank the drug delivery faculty for awarding me a travel grant for attending the AAPS, Annual meeting in October 2006.

I thank my friends in the Kwon Lab, especially Dr. Scott Croy, Dr. Anuj Kumar, Dr. Karen Jette (Kostick), Dr. Laird Forrest and Sheng Tu for their encouragement, criticisms and advice.

I thank Dr. Melgardt de Villiers, Dr. Judy Thompson and Bonnie Fingerhut for being so wonderful to work with. I have certainly learnt a lot from them and in working as a teaching assistant.

I thank the staff at Business and the Dean's office for their help. Special thanks to Tom O'Connor, Joni Mitchell, Linda Frei and Karen Steinle.

Thank you to Dr. Sheetal Muley, Dr. Lingyun Xiao, Joseph Su, Adam Alani, Deepa Rao and other graduate students of the School of Pharmacy, past and present, for their conversations and friendship.

Lastly, I thank my dear friends Anand Nilekar, Dr. Anish Khandekar, Bupendra Shah, Kavita Patil, Jinesh Shah, Murali Rajaa, Soujanya Jamapala and Dr. Niyati Mehta for their friendship and many memorable experiences I have shared with them over the past five years.

Table of Contents

Dedication i

Acknowledgements ii

Table of contents iv

List of tables viii

List of figures ix

List of abbreviations xii

Chapter 1: Introduction 1

1.1 Introduction 2
1.2 Long-circulating characteristics of polymeric micelles 3
1.3 Drug solubilization by polymeric micelles 4
1.4 Polymeric micelles formed from PEG-lipid conjugates 5
1.5 Mixed micellar systems in drug delivery 8
1.6 Systemic fungal diseases due to *Candida* pathogens 9
1.7 Drugs used in the treatment of invasive candidiasis 10
1.8 Amphotericin B 12
1.8.1 Structural aspects 12
1.8.2 Membrane-level activity of AmB 13
1.8.3 Associated toxicities 14
1.9 Strategies to decrease AmB related toxicities 15
1.9.1 Lipid formulations 15
1.9.2 Surfactant formulations 15
1.9.3 Polymeric micelle based formulations 16
1.9.4 Sodium supplementation 17
1.9.5 Continuous infusion 17
1.10 Treatment of systemic candidiasis using drug combinations 18
1.11 Research proposal 20
1.12 Specific aims 21
1.13 References 22

Chapter 2: PEG-phospholipid micelles for the delivery of amphotericin B 30

2.1 Introduction 31
2.2 Materials 31
2.3 Incorporation of AmB in PEG-DSPE micelles 32
2.4 Micelle characterization 32
2.4.1 Dynamic light scattering 32
2.4.2 Spectroscopic analysis of AmB 33
2.4.3 Size exclusion chromatography 33
2.5 Evaluation of *in vitro* toxicity of PEG-DSPE encapsulated AmB 33
2.5.1 Hemolytic activity of AmB against murine erythrocytes 33
2.5.2 Cell-viability studies using HK-2 cells 34
2.6 *In vitro* susceptibility of yeast isolates against PEG-DSPE incorporated AmB 35
2.7 Results and Discussion 36
2.7.1 Micelle characterization and drug loading 36
2.7.2 AmB self-aggregation in PEG-DSPE micelles 37
2.7.3 In vitro toxicity and efficacy studies 41
2.8 Conclusions 44
2.9 References 45

Chapter 3: Structuring effect of cholesterol on PEG-phospholipid micelles: amphotericin B solubilization and *in vitro* release studies 47

3.1 Introduction 48
3.2 Materials 50
3.3 Micelle preparation and incorporation of AmB 50
3.4 Micelle characterization 50
3.4.1 Dynamic light scattering 50
3.4.2 Core microviscosity measurements using P3P 51
3.4.3 ^{1}H NMR spectroscopy 51
3.4.4 AmB release from PEG-DSPE micelles using equilibrium dialysis 52
3.4.5 Electronic absorption kinetics 53
3.5 Results and Discussion 54
3.5.1 Micelle preparation and characterization 54

3.5.2 AmB release from PEG-DSPE micelles using equilibrium dialysis 61
3.5.3 Electronic absorption kinetics 63
3.5.4 *In vitro* toxicity and efficacy studies 64
3.6 Conclusions 66
3.7 References 67

Chapter 4: Characterization of mixed polymeric micelles formed from PEG-b-poly(ε-caprolactone) and PEG-phospholipid **71**

4.1 Introduction 72
4.2 Materials 75
4.3 Preparation of mixed PEG-DSPE|PEG_{5000}-b-PCL_x micelles 75
4.4 Micelle characterization 76
4.4.1 Size exclusion chromatography 76
4.4.2 Dynamic light scattering 76
4.4.3 Critical micellar concentration and core polarity using pyrene fluorescence 77
4.4.4 Core microviscosity measurements using P3P 77
4.4.5 Diffusion coefficients using pulsed field gradient (PFG) spin echo 78
4.4.6 Spin lattice relaxation (T_1) measurements 78
4.4.7 NOE measurements 79
4.8 AmB incorporation and *in vitro* release studies 79
4.8.1 AmB incorporation into PEG-DSPE, PEG_{5000}-b-PCL_{4000} and PEG-DSPE| PEG_{5000}-b-PCL_{4000} micelles 79
4.8.2 HPLC assay for estimation of AmB content 80
4.8.3 *In vitro* release study of micelle encapsulated AmB using equilibrium dialysis 80
4.8.4 Electronic absorption kinetics 81
4.9 Results, Analysis and Discussion 81
4.9.1 Micelle characterization 81
4.9.2 AmB encapsulation and release 93
4.9.3 Electronic absorption kinetics 95
4.10 Conclusions 98
4.11 References 99

Chapter 5: Polymeric micelles for combination antifungal therapy involving amphotericin B, rapamycin and 5-fluorocytosine **103**

5.1 Introduction 104
5.2 Materials 107
5.3 Micelle preparation and incorporation of AmB and rapamycin 107
5.4 Micelle characterization 108
5.4.1 Dynamic light scattering 108
5.4.2 Size exclusion chromatography 108
5.5 Solution turbidity measurements 109
5.6 *In vitro* susceptibility measurements 109
5.6.1 Estimation of minimum inhibitory concentration (MIC) 109
5.6.2 Interactive effects of drug combinations 110
5.7 Results and Discussion 112
5.7.1 Micelle characterization 112
5.7.2 *In vitro* susceptibility studies 116
5.8 Conclusions 126
5.9 References 128

Chapter 6: General discussion and conclusions **132**

6.1 Conclusions and primary findings 133
6.2 Suggestions for future research 137
6.2.1 Determination of serum lipoprotein distribution of AmB 137
6.2.2 *In vivo* dose escalation studies for AmB in PEG-DSPE|Cholesterol micelles 137
6.2.3 *In vivo* biodistribution and pharmacokinetic studies with AmB in PEG-DSPE and PEG-DSPE|Cholesterol micelles 138
6.2.4 *In vivo* toxicity studies with PEG-DSPE micelle encapsulated AmB with slow infusion in conjunction with sodium supplementation 138
6.2.5 *In vivo* toxicity and efficacy studies of pair-wise and three-drug combinations in a murine model of systemic candidiasis 139
6.3 References 140

List of Tables

Chapter 2:

Table 2.1 Solubilization of AmB by PEG-DSPE micelles..... 36

Table 2.2 Minimum Inhibitory Concentration (MIC) of AmB against *Candida albicans*..... 44

Chapter 3:

Table 3.1 Solubilization of AmB by PEG-DSPE and PEG-DSPE|Cholesterol micelles..... 59

Table 3.2 Fit parameters for AmB release from PEG-DSPE micelles at 25 °C..... 62

Table 3.3 Fit parameters for absorbance change for PEG-DSPE incorporated AmB at 412 nm in 4 % bovine serum albumin..... 66

Chapter 4:

Table 4.1 Particle sizing of one-component and mixed micelles using DLS. 83

Table 4.2 Diffusion-coefficient measurements using pulsed-field gradient echo attenuation data..... 86

Table 4.3 Spin-lattice relaxation (T_1) measurements for one-component and mixed micelles in D_2O at 25 °C..... 91

Table 4.4 AmB loading into PEG-DSPE| PEG_{5000}-b-PCL_{4000} mixed micelles..... 94

Table 4.5 Fit parameters for absorbance change at 412 nm on addition of mixed micelle encapsulated AmB to 4 % bovine serum albumin.. 97

Chapter 5:

Table 5.1 Solubilization of AmB and rapamycin in PEG-DSPE micelles..... 113

Table 5.2 Minimum Inhibitory Concentration (MIC) of AmB against *Candida albicans* isolates..... 116

Table 5.3 Best fit parameters for fungal growth inhibition to median-effect equation..... 117

Table 5.4 Range of combination index and fractional inhibitory concentration index and associated descriptions 119

Table 5.5 Fractional inhibitory concentration analysis for AmB|PEG-DSPE – rapamycin|PEG-DSPE – 5-FC combinations..... 120

List of Figures

Chapter 1:

Figure 1.1 Chemical structure of PEG-DSPE..... 6
Figure 1.2 Chemical structure of AmB..... 13
Figure 1.3 Membrane activity of monomeric and aggregated AmB..... 14

Chapter 2:

Figure 2.1 Absorption spectra of monomeric and self-aggregated AmB..... 38
Figure 2.2 Absorption spectra of AmB solubilized by PEG-DSPE at varied mole ratios of PEG-DSPE to AmB..... 38
Figure 2.3 SEC-HPLC of AmB in PEG-DSPE micelles..... 40
Figure 2.4 Hemolytic activity of AmB against murine erythrocytes..... 42
Figure 2.5 HK-2 cell viability on exposure to AmB..... 43

Chapter 3:

Figure 3.1 Effect of cholesterol content on size of PEG-DSPE|Cholesterol micelles..... 54
Figure 3.2 ^{1}H NMR spectra for PEG-DSPE and PEG-DSPE|Cholesterol (1:1) micelles in D_2O at 25 °C..... 56
Figure 3.3 I_M/I_E ratios for P3P fluorescence emission in PEG-DSPE|Cholesterol micelles..... 57
Figure 3.4 Chemical structure of cholesterol..... 58
Figure 3.5 Absorption spectra of AmB solubilized by PEG-DSPE and PEG-DSPE|Cholesterol micelles..... 60
Figure 3.6 AmB release profiles at 25 °C in 5 mM HEPES and 4 % bovine serum albumin..... 62
Figure 3.7 Absorbance spectra of micelle encapsulated AmB in 4 % bovine serum albumin **a.** Unencapsulated AmB **b.** AmB in PEG-DSPE micelles **c.** AmB in PEG-DSPE|Cholesterol micelles..... 65

Chapter 4:

Figure 4.1 Chemical structures of PEG_{5000}-b-PCL_x and PEG-DSPE..... 72
Figure 4.2 SEC-HPLC for one-component and mixed micelles **a.** Simple mixing of PEG-DSPE and PEG_{5000}-b-PCL_{4000} **b.** PEG-DSPE| PEG_{5000}-b-PCL_{4000} mixed micelles after sonication for 20 min **c.** PEG-DSPE and PEG_{5000}-b-PCL_{4000}micelles..... 82
Figure 4.3 Pulsed-field gradient echo attenuation for PEG_{5000}-b-PCL_{4000} micelles in D_2O..... 85

Figure 4.4 Effect of PCL block length on critical micellar concentration of PEG-DSPE| PEG_{5000}-b-PCL_{6000} (1:1) micelles..... 87

Figure 4.5 Effect of PEG-DSPE: PEG_{5000}-b-PCL_{6000} ratio on effective critical micellar concentration of PEG-DSPE| PEG_{5000}-b-PCL_{6000} micelles..... 87

Figure 4.6 Core micropolarity of PEG-DSPE| PEG_{5000}-b-PCL_{6000} micelles... 89

Figure 4.7 I_M/I_E ratios for P3P fluorescence emission in PEG-DSPE| PEG_{5000}-b-PCL_{4000} micelles at 25 °C..... 90

Figure 4.8 Contour plot of the NOE spectrum at 25 °C of PEG-DSPE| PEG_{5000}-b-PCL_{4000} (1:1) micelles in D_2O..... 92

Figure 4.9 SEC-HPLC of AmB encapsulated in PEG-DSPE| PEG_{5000}-b-PCL_{4000} (1:1) mixed micelles..... 94

Figure 4.10 AmB release from PEG-DSPE| PEG_{5000}-b-PCL_{4000} mixed micelles under sink conditions at 37 °C..... 95

Figure 4.11 Absorbance spectra of micelle encapsulated AmB in 4 % bovine serum albumin **a.** AmB in PEG-DSPE micelles **b.** AmB in PEG-DSPE| PEG_{5000}-b-PCL_{4000} (1:1) micelles **c.** PEG-DSPE| PEG_{5000}-b-PCL_{4000} (5:1) micelles..... 96

Chapter 5:

Figure 5.1 Light scattering on admixing a. D-AmB with 0.9 % NaCl b. D-AmB with 5 % dextrose c. AmB|PEG-DSPE with rapamycin|PEG-DSPE and 5-FC in 0.9 % NaCl..... 114

Figure 5.2 SEC-HPLC of AmB|PEG-DSPE, rapamycin|PEG-DSPE and 5-FC in 0.9 % NaCl..... 115

Figure 5.3 Sizing of AmB|PEG-DSPE, rapamycin|PEG-DSPE and 5-FC in 0.9 % NaCl using DLS..... 115

Figure 5.4 Combination index values for **a.** 5-FC – AmB|PEG-DSPE **b.** 5-FC – rapamycin|PEG-DSPE **c.** rapamycin|PEG-DSPE – AmB|PEG-DSPE combinations against C. *albicans* 98-17..... 123

Figure 5.5 Combination index values for 5-FC – AmB|PEG-DSPE – rapamycin|PEG-DSPE combinations for AmB|PEG-DSPE: rapamycin|PEG-DSPE **a.** 1:2 **b.** 2:1 for *C. albicans* 98-17..... 123

Figure 5.6 Combination index values for **a.** 5-FC – AmB|PEG-DSPE **b.** 5-FC – rapamycin|PEG-DSPE **c.** rapamycin|PEG-DSPE – AmB|PEG-DSPE combinations against C. *albicans* 98-234..... 124

Figure 5.7 Combination index values for 5-FC – AmB|PEG-DSPE – rapamycin|PEG-DSPE combinations for AmB|PEG-DSPE: rapamycin|PEG-DSPE **a.** 1:2 **b.** 2:1 for *C. albicans* 98-234..... 124

Figure 5.8 Combination index values for **a.** 5-FC – AmB|PEG-DSPE **b.** 5-FC – rapamycin|PEG-DSPE **c.** rapamycin|PEG-DSPE – AmB|PEG-DSPE combinations against C. *albicans* K-1..... 125

Figure 5.9 Combination index values for 5-FC – AmB|PEG-DSPE – rapamycin|PEG-DSPE combinations for AmB|PEG-DSPE: rapamycin|PEG-DSPE **a.** 1:2 **b.** 2:1 for *C. albicans* K-1..... 125

List of Abbreviations

ABC.....amphiphilic block copolymers
AIDS.....acquired immunodeficiency syndrome
AmB.....amphotericin B
AmB|PEG-DSPE.....amphotericin B encapsulated in PEG-DSPE micelles
ATCC.....American Type Culture Collection
ATP.....adenosine triphosphate
BSA.....bovine serum albumin
CFU.....colony forming units
CH_3-.....methyl
CI.....combination index
CMC.....critical micellar concentration
D-AmB.....amphotericin B solubilized in sodium deoxycholate
DLS.....dynamic light scattering
DMEM.. .....Dulbecco® Modified Eagle's Minimal Essential Medium
DMF.....dimethylformamide
DMSO.....dimethylsulfoxide
D_2O.....deuterium oxide
DPPC..... .....dipalmitoyl phosphatidyl choline
EDTA.....ethylenediaminetetraacetic acid
5-FC.....5-fluorocytosine
FDA.....United States Food and Drug Administration
FIC(I).....fractional inhibitory concentration (index)
FID.....free induction decay
FTIR..... .....fourier-transformed infrared
HDL.....high density lipoprotein
HEPES..... .....4-(2-hydroxyethyl)-1-piperazineethanesulfonic acid
HK-2.....human proximal tubule kidney cell line
HPLC.....high performance liquid chromatography
I/IV.....ratio of intensities at peak I and peak IV in the absorbance spectrum of AmB

IV.....intravenous

L-AmB.....liposomal AmB

LD_{50}.....lethal dose in 50 % of subjects

LDL.....low density lipoprotein

mol.....mole

MIC.....minimum inhibitory concentration

MTS.....3-(4,5-dimethylthiazol-2-yl)-5-(3-carboxymethoxyphenyl)-2-(4-sulfophenyl)-2H-tetrazolium)

MWCO.....molecular weight cut-off, for semi-permeable membranes

NaCl.....sodium chloride

NCCLS.....National Committee for Clinical Laboratory Standards

NMR..... nuclear magnetic resonance

NOE.....Nuclear Overhauser effect

OD_{650nm}.....optical density at 650 nm

P3P.....1,3-(1,1'-dipyrenyl) propane

PBS.....phosphate-buffered saline

PC.....phosphatidyl choline

PCL.....poly(ε-caprolactone)

PEG.....polyethylene glycol, also known as polyethylene oxide

PEG-DSPE.....1,2-Distearoyl-*sn*-glycero-3-phosphoethanolamine-N-methoxy(polyethylene glycol)$_{5000}$

PEG-DSPE|Cholesterol.....PEG-DSPE micelles with co-incorporated cholesterol

PEG_{5000}-b-PCL_x.....methoxy(polyethylene glycol)$_{5000}$-b-poly(ε-caprolactone)

PEG-DSPE|PEG_{5000}-b-PCL_x.....mixed micelles formed from PEG-DSPE and PEG_{5000}-b-PCL_x

PFG.....pulsed field gradient

Rapamycin|PEG-DSPE.....rapamycin encapsulated in PEG-DSPE micelles

RBC.....red blood cell

RPM.....revolutions per minute

RPMI-1640.....Roswell Park Memorial Institute medium 1640

SDA.....Sabouraud dextrose agar

SEC.....size exclusion chromatography

$t_{1/2}$.....release half life

THF.....tetrahydrofuran

Chapter 1:

Introduction

1.1 Introduction

Delivery of potent, yet poorly water-soluble drugs using polymers is a growing area of research. Several innovative carriers such as water soluble polymer-drug conjugates, polymeric pro-drugs and polymeric micelles have been studied with a goal to improve drug solubility and influence biodistribution, metabolism and excretion (1, 2). Amphiphilic polymers assemble into nanoscopic supramolecular core-shell structures, micelles, which are under extensive study for drug delivery (3-5). The shell of polymeric micelles consists of poly(ethylene glycol) (PEG), a non-toxic, water-soluble polymer, which prevents protein adsorption and cellular adhesion, and the cores of these micelles consist of a smaller hydrophobic block or moiety, varying in drug delivery due to requirements of low toxicity, compatibility with the companion drug, usually a poorly water-soluble compound, and stability of the polymeric micelle in blood. In drug delivery, a goal is to study the potential of polymeric micelles as 'nanocarriers' for potent, toxic and poorly water-soluble drugs.

Many existing drugs used in the treatment of life-threatening diseases and many compounds coming out of massive drug discovery efforts have poor water-solubility due to hydrophobicity, low hydrogen bond capacity and large size (6). Adjustments in pH, co-solvents, cyclodextrins and surfactants are the primary methods used for drug solubilization (7). However, these methods are often unable to realize adequate levels of drug in solution for parenteral administration at target doses. In addition, parenteral excipients often exert toxicity. For example, Cremophor® EL, a nonionic surfactant commonly used for drug solubilization, causes

hemolysis, hypersensitivity reactions, neurotoxicity and hyperlipidemia on intravenous administration (8).

1.2 Long circulating characteristics of polymeric micelles

Micelles formed from amphiphilic polymers have attracted intense interest for drug delivery due to their small size and potential for prolonged circulation in blood. Since the size of polymeric micelles is typically in the 10 – 100 nm range, these are larger than the renal threshold but small enough to be quite effective in penetrating fine capillaries and hence may offer a highly effective tissue distribution (9, 10). Particles larger than 200 nm are removed from circulation in the spleen, an effect seen with microparticulate and liposomal delivery systems (11). The PEG exterior of polymeric micelles has a low affinity for interaction with proteins facilitating evasion from the reticuloendothelial system (12). Hence polymeric micelles may circulate in the body for prolonged periods of time. The clearance of polymeric micelles from the circulation may occur by a gradual disassembly process into constituent unimers, which may be cleared via the kidneys.

Small size and stability on dilution are important advantages offered by polymeric micelles for development of poorly water-soluble compounds. Since polymeric micelles have low critical micellar concentrations, encapsulated drugs may remain solubilized for prolonged periods of time on extensive dilution, reducing the risk of embolism due to drug precipitation – an important criterion for compounds which need slow infusion, such as amphotericin B. Moreover, the small size of these carriers may permit facile on-site sterilization via a simple filtration step.

1.3 Drug Solubilization in Polymeric Micelles

Drugs may be solubilized in the hydrophobic core of polymeric micelles by chemical conjugation or physical entrapment. For chemical conjugation, the drug is covalently linked with the hydrophobic block via degradable linkages. Several degradable linkages have been investigated in the context of polymeric micelles, such as ester, amide and hydrazone (5). Degradation of polymer-drug linkages in the core of polymeric micelles may be substantially slower compared with polymer-drug conjugates, resulting in slower drug release (13). However, preparation of drug-polymer conjugates may be synthetically challenging and there is potential for decrease in drug activity on chemical manipulation.

A large fraction of poorly soluble drugs are solubilized in the core of polymeric micelles via non-covalent interactions. In this case, the structure of the hydrophobic block influences the solubilization and release characteristics of an encapsulated drug. Structural similarity between a poorly water-soluble drug and the core-forming block often indicates compatibility (5, 14). Several hydrophobic blocks have been investigated for drug delivery. Poloxamers, poly(ester)s, poly(L-amino acid)s and phospholipid represent structural diversity for drug solubilization. Various aspects of poloxamers of interest for drug delivery have been reviewed in detail by Kabanov and Alakhov (15). Similarly, the utility of polymeric micelles formed from PEG-*b*-poly(ester)s and PEG-*b*-poly(L-amino acid)s has been reviewed by Kwon (5) and more recently by Aliabadi and Lavasanifar (16). Physical incorporation of drugs into polymeric micelles is accomplished using direct dissolution, dialysis, oil/water emulsion, complexation, freeze-drying and solvent evaporation procedures. These

procedures have been reviewed by Aliabadi and Lavasanifar (16). It is noted that the extent of drug loading and physical attributes of polymeric micelles such as size is sensitive to the method of preparation and drug incorporation.

1.4 Polymeric micelles formed from PEG-lipid conjugates

PEG-phospholipids are amphiphilic polymers consisting of a PEG chain conjugated with a relatively short but very hydrophobic diacyl phospholipid. PEG-phospholipids have been approved for use in humans by the FDA. 1,2-Distearoyl-*sn*-glycero-3-phosphoethanolamine-N-methoxy(polyethylene glycol) (PEG-DSPE, Figure 1.1) has been shown to have very low toxicity and is currently used in the clinic as a surface-modifier in long-circulating liposomal doxorubicin, Doxil® . Most studies concerning drug delivery have focused on PEG-derivatives of saturated lipids with long diacyl chains i.e. dipalmitoyl and distearoyl, since these polymers form micelles with low critical micellar concentrations (2.2 μM for PEG_{5000}-DSPE and 1.6 μM for PEG_{2000}-DSPE).

Though PEG-DSPE is not a block copolymer, micelles formed from PEG-DSPE have attracted attention for solubilization and delivery of various poorly water-soluble diagnostic and therapeutic agents. PEG-phospholipid micelles have been used to solubilize several poorly water-soluble compounds such as dequalinium (17, 18) ellipticine (19) m-porphyrin (18, 20), tamoxifen (18, 20) and paclitaxel (18, 20) using a solvent evaporation procedure. The solvent evaporation method consists of co-precipitating PEG-DSPE with the hydrophobic drug as a thin film, which is then dissolved in a suitable buffer. The solvent evaporation method is preferred method for

incorporation of drugs in PEG-DSPE micelles, since it results in higher drug loading compared with direct dissolution.

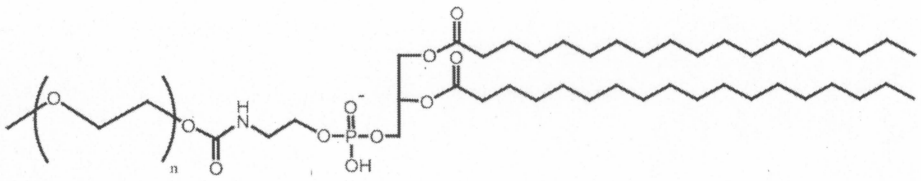


Figure 1.1 Chemical structure of PEG-DSPE

Since the diacyl lipid chains in PEG-phospholipid are extremely hydrophobic, Torchilin has suggested that incorporation of poorly soluble drugs into these polymeric micelles is primarily driven by structural similarity and hydrophobic interactions. Incorporation of molecules which have structural resemblance to diacyl lipid chains in PEG-DSPE (e.g. lipid derivative of rhodamine) result in stable incorporation in PEG-DSPE micelles. Incorporation of highly non-polar compounds, which are structurally unrelated to PEG-DSPE leads to the formation of large water-soluble aggregates (e.g. diphenylhexatriene) or an initial solubilization in PEG-DSPE micelles, followed by exclusion and precipitation (e.g. camptothecin, paclitaxel) (4). The level of drug solubilized by PEG-DSPE micelles is also governed by polymer drug – interactions. Low levels (ca. 4 %) of highly non-polar compounds (e.g. ellipiticine) could be incorporated into PEG-DSPE micelles, compared with ca. 33 % incorporation of rhodamine-PE, which is structurally related to PEG-DSPE.

Zhang et al. have prepared parenteral formulations of benzoporphyrin derivatives in PEG-DSPE micelles for photodynamic therapy (21). The B-ring isomers are particularly difficult to formulate due to high degree of hydrophobicity and tendency to self-associate. The extent of benzoporphyrin derivative B self-aggregation, according to absorbance spectroscopy, depended on the ratio of polymer to photosensitizer and the pH of the medium used to prepare the micellar solution. For long-term storage, PEG-DSPE micelles containing benzoporphyrin derivatives could be freeze-dried and reconstituted with the photosensitizer in a monomeric state.

Torchilin et al. have studied the incorporation of chelates of diethylenetriamine pentaacetic acid (DTPA) with metals such ^{111}In and ^{64}Gd in PEG-phospholipid micelles for applications as contrast agents in imaging (22). PEG-phospholipid micelles incorporating chelated ^{111}In demonstrated higher accumulation at tumor sites compared with non-target tissue, such as muscle (18). Due to their small size compared with liposomal carriers, PEG-phospholipid micelles may be effective for delivery of therapeutic agents to tumors with fine vasculature, such as the Lewis lung carcinoma (LLC) model in mice (23). PEG-phospholipids conjugated with antibodies have been explored for tumor-specific drug delivery. On self-assembly, the micelle exterior presents conjugated antibodies and facilitates further selectivity. Paclitaxel loaded in these micelles led to a significant reduction in tumor size, compared with free paclitaxel or paclitaxel in PEG-phospholipid micelles (24).

Researchers have studied incorporation of additives in PEG-DSPE micelles with an aim to modify micelle properties and enhance drug loading. Onyuksel et al. have used phosphatidylcholine (PC) as a co-additive in an attempt to modify

properties of PEG-DSPE micelles. The size of the PEG-DSPE micelles increased on incorporation of PC. Higher levels of paclitaxel (25) and diazepam (26) could be solubilized in these micelles, presumably due to a larger volume for drug solubilization. PEG-DSPE micelles with α-tocopherol had larger size and lower core polarity compared to PEG-DSPE micelles and could solubilize higher levels of rapamycin (27).

In this dissertation, PEG-DSPE micelles have been studied in the context of amphotericin B delivery due to proven biocompatibility of the polymer and presumed compatibility with drug. Results related to amphotericin B solubilization and drug release have been presented in chapters 2 and 3.

1.5 Mixed micellar systems in drug delivery

Binary surfactant mixtures may form aggregates with greater thermodynamic stability through a cooperative interaction between components (28). Polymeric micelles formed from mixtures of several poloxamers have been studied for solubilization of poorly water-soluble compounds (29). Mixed Pluronic® P-105 and PEG-DSPE micelles have been investigated for the delivery of the poorly water-soluble antineoplastic doxorubicin. These mixed micelles resulted in greater tumor accumulation of doxorubicin compared to Pluronic® P-105 micelles alone (30, 31). Lee et al. have prepared mixed micelles from PEG-b-poly(L-lactic acid) and folate-PEG-b-poly(L-histidine). The release rate of doxorubicin from these mixed polymeric micelles showed an interesting dependence on pH as well as fraction of PEG-b-poly(L-lactic acid) in the mixed polymeric micelle (32).

PEG-b-poly(ε-caprolactone) micelles have been studied for delivery of several hydrophobic compounds such as cyclosporine A (33), rapamycin (34), ellipticine (35), FK506 (36), dihydrotestosterone (37) and geldanamycin (38) as these micelles have high microviscosity and are expected to be stable carriers in blood. In this dissertation, mixed micelles formed from PEG-DSPE and PEG-b-poly(ε-caprolactone) have been studied in the context of amphotericin B delivery, since these novel carriers may possess interesting characteristics such as higher stability via cooperative interactions between hydrophobic blocks or chain entanglement. Results from this study are presented in chapter 4.

1.6 Systemic fungal diseases due to *Candida* pathogens

Newer technologies, such as organ-transplants which employ aggressive regimens that lead to immune suppression have become common at many medical centers (39). The AIDS epidemic has led to a further increase in the patient population with compromised host-defense mechanisms. These immunocompromised patients are very susceptible to infections caused by organisms such as fungi that are otherwise considered non-pathogenic. Simultaneously, the use of invasive monitoring devices, assisted ventilation and long-dwelling catheters for parenteral nutrition has risen, especially in critical-care units. Hence, it is not surprising that the incidence of nosocomial fungal infections has increased dramatically over the past two decades, with a consequent increase in both mortality and prolonged hospitalizations. By an estimate, the annual incidence of systemic fungal infections is likely to be greater than 60,000 cases/year in the United States (40). *Candida albicans* is the fourth most

common bloodstream pathogen accounting for 8-10% of all bloodstream infections. Infections due to non-*albicans* species such as *C. parapsilosis, C. tropicalis, C. krusei and C. lusitaniae* are gaining incidence and are of growing concern. Bloodstream infections due to *Candida* species cause a spectrum of disease ranging from thrush to more serious conditions such as endocarditis, meningitis or fungemia (41). Fungal infections in immunocompromised patients are severe, rapidly progressive and difficult to diagnose or treat. The estimated mortality attributable to candidemia is ca. 40 % (40, 42-44).

1.7 Drugs used in the treatment of invasive candidiasis

Since fungi are eukaryotic cells, they are similar to host cells in many aspects; hence relatively few drugs are available for treating fungal infections, compared with bacterial infections. The FDA has approved the use of several antifungal agents belonging to different chemical classes for the treatment of systemic fungal diseases. However, the treatment is often complicated by high toxicity, low tolerability or a narrow spectrum of activity. These drugs primarily act on the cytoplasmic membrane, cell wall or block fungal DNA and protein synthesis. The action, toxicity and resistance of several antifungal drugs has been presented in reviews by Dismukes and Ghannoum (45, 46).

The polyene antifungals have been in clinical use for approximately 50 years against a wide variety of yeast and mould infections. While nystatin is not approved for systemic administration, amphotericin B (AmB) is considered a first-line antifungal agent against disseminated candidiasis and is administered intravenously.

Solubilized AmB demonstrates rapid cidal activity against virtually all strains of *Candida albicans*. Although AmB has a wide-spectrum of activity, its use is limited due to severe toxicities. AmB has been shown to exert activity at the membrane level by inducing the formation of cellular membrane pores, which leads to the leakage of cellular contents and eventual cell death. Several aspects of AmB have been reviewed in greater depth later in this chapter.

Although polyene antibiotics clearly have superior *in vitro* activity against *Candida* species, the triazole antifungals have been extensively studied due to their superior toxicity profile. The triazole antifungals disrupt the synthesis of ergosterol, a critical sterol component in fungal membranes. The four triazoles approved for systemic use are fluconazole, itraconazole, voriconazole and ketoconazole. All triazoles exert fungistatic activity, leading to frequent relapses upon termination of therapy (47). It is estimated that 5-20 % of *Candida albicans* strains in the United States are resistant to azole therapy (48). Despite problems of resistance, fluconazole is a preferred first-line antifungal in the treatment of disseminated candidiasis in non-neutropenic patients due to safety, efficacy and cost considerations (40).

5-Fluorocytosine (5-FC) is an analogue of cytosine that interferes with fungal DNA and protein synthesis. Upon cellular uptake, 5-FC is converted to 5-fluorouracil by cytosine deaminase, an enzyme selectively present in fungal cells. The 5-fluorouracil blocks synthesis of fungal DNA and proteins, which leads to cell death. 5-FC is a widely used antifungal agent; however, its use is restricted by narrow spectrum of activity and drug resistance (45).

Caspofungin is a newly approved antifungal agent belonging to a novel class of drugs called echinocandins. This class of drugs exert antifungal activity by inhibiting $\beta_{1,3}$-glucan synthase, a key enzyme in fungal cell wall synthesis. In a recent study, caspofungin was as effective as AmB for the treatment of patients with invasive *Candida* infections (49). Hence it has recently been recommended as a first-line antifungal against candidiasis. Since these antifungals have recently been introduced in treating systemic fungal infections, issues relating to drug resistance are not fully understood.

1.8 Amphotericin B

1.8.1 Structural aspects

Amphotericin B (AmB) is a polyene macrolide consisting of a hydrophobic system of seven conjugated double bonds which represents the hydrophobic portion of the molecule, while numerous hydroxyl groups are located on the opposite side of the macrolide ring (Figure 1.2). This asymmetric distribution of hydrophobic and hydrophilic portions imparts amphiphilicity to the molecule. Additionally, the presence of ionizable carboxyl and amino groups makes the molecule zwitterionic at physiological pH. Due to the amphiphilic nature of the molecule, the drug is poorly soluble in aqueous media and has a tendency to self-associate in water above a threshold concentration known as the critical aggregation concentration, which is ca. 1 μM (50). Due to its poor water-solubility, AmB is most commonly solubilized as a mixture with sodium deoxycholate in phosphate buffer (D-AmB), and is marketed by Bristol-Myers Squibb company, under the trade name Fungizone®.

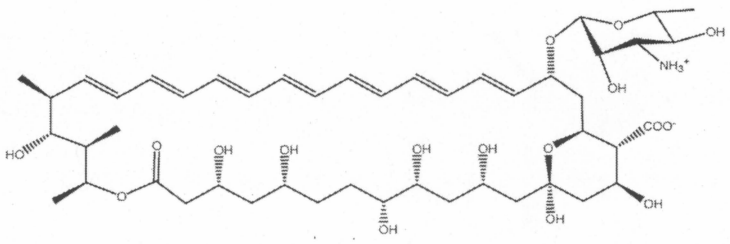


Figure 1.2 Chemical structure of AmB

1.8.2 Membrane-level activity of AmB

The potential for AmB to selectively damage fungal cells has been ascribed to the differences in the major sterol component between fungal and mammalian cell-membranes. According to the widely accepted model proposed by Bolard et al. monomers of the drug interact with the ergosterol in fungal membranes, assisting the formation trans-membrane pores that allow for significant Na^+ influx and K^+ efflux, generating a severe electrolyte imbalance. This imbalance is thought to impose high energy demand in terms of ATP utilization, eventually leading to cell death (51). On the other hand, it has been shown that AmB induces leakage of K^+ through cholesterol containing membranes only beyond a certain threshold of concentration, which corresponds to the formation of self-associated water-soluble species of AmB (52, 53).

Since deoxycholate is a surfactant with high CMC, AmB is partly dissociated in D-AmB, which forms a mixture of water-soluble monomers, oligomers and insoluble aggregates. The proportions of these different species and their state of

aggregation would depend on many factors, including temperature and total concentration of AmB (50). The various chemical species interact with membrane sterols to evoke changes in membrane permeability as described. In this context, stable carriers that inhibit self-aggregation and release AmB in a monomeric form may exert greater selectivity compared with D-AmB.

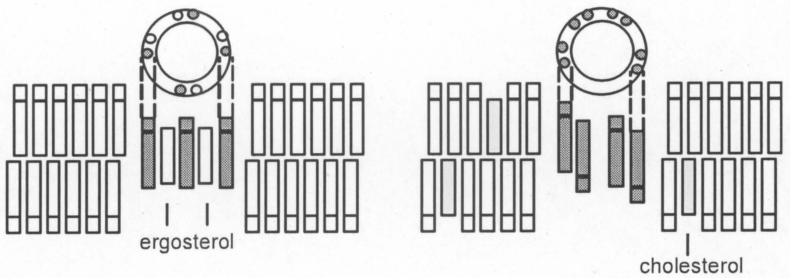


Figure 1.3 Membrane activity of monomeric and aggregated AmB.

1.8.3 Associated toxicities

D-AmB has activity against a broad spectrum of fungal pathogens, however, therapeutic doses of D-AmB often cause severe side effects, including pain at the site of injection, fever, rigors, hypotension, nausea and electrolyte imbalances. Clinicians attempt to address these toxicities by pre-treating with antipyretics, antihistamines and corticosteroids with some success (54). The drug's dose limiting complication is renal toxicity. Some patients experience a severe impairment of kidney function, due to which antifungal therapy must be discontinued. Drug related nephrotoxicity is characterized by a reduction in the glomerular filtration rate (GFR) and urine concentration ability (54, 55).

1.9 Strategies to decrease AmB related toxicities

1.9.1 Lipid formulations

The three major lipid formulations for AmB products approved by the FDA for treatment of systemic candidiasis are AmB in a lipid complex (Abelcet), as a colloidal dispersion (Amphotec) and in liposomes (AmBisome) (63-65). Lipid based AmB formulations are less toxic compared to D-AmB allowing for dose-escalation and improved tolerability. However, liposomal AmB (L-AmB) has lower antifungal activity at equal doses necessitating significantly higher doses for comparable efficacy, raising doubts about a meaningful increase in the therapeutic index (66). Notably, L-AmB has not had a significant impact on mortality rates compared to D-AmB (67). Currently, the lipid based amphotericin B products are only indicated for patients with refractory fungal infections or who are intolerant to D-AmB. Due to the prohibitively high drug-acquisition costs and a questionable improvement in outcome, lipid based AmB has not displaced D-AmB as first-line therapy (68, 69).

1.9.2 Surfactant formulations

Since AmB toxicity is mediated by its aggregation state, low molecular weight surfactants such as sodium deoxycholate, lauryl sucrose and Myrj 59 (PEG-derivative of stearic acid) have been evaluated for AmB solubilization and deaggregation (70, 71). *In vitro* hemolysis and cell-viability studies suggest correlation between polyene deaggregation and decreased toxicity. However, there is poor correlation between *in vivo* and *in vitro* toxicity results. Although the reasons for this are not entirely clear, it is proposed that these surfactants are not entirely non-toxic and that the high levels of

these surfactants used to deaggregate AmB are likely to be too toxic for parenteral use.

1.9.3 Polymeric micelle based formulations

PEG-*b*-p(N-hexyl-L-aspartamide) block copolymers can be esterified to incorporate acyl chains of varied lengths to tailor properties of polymeric micelles and optimize drug encapsulation (72). In these studies, the length of the acyl side chain attached on PEG-*b*-p(N-hexyl-L-aspartamide) was found to govern the extent of interaction, incorporation, and release of AmB (73). In particular, the stearic acid ester of PEG-*b*-p(N-hexyl-L-aspartamide) was most efficient in deaggregating AmB and also caused the least *in vitro* hemolysis. It is noted that the efficacy of the polymeric micelle encapsulated AmB was comparable to D-AmB in a neutropenic model of disseminated candidiasis (74).

Mixed micelles formed from poly(ε-caprolactone) and poloxamer 188 have been studied for the delivery of AmB. AmB in this formulation demonstrated potent *in vitro* activity against test isolates, while reducing *in vitro* and *in vivo* toxicities (75). More recently, polymeric micelles formed from PEG-b-poly(ε-caprolactone-co-trimethylene carbonate) have been investigated for the delivery of AmB. These poly(ester) micelles could solubilize moderate levels of AmB in a deaggregated form. AmB encapsulated in these polymeric micelles exerted low levels of hemolysis, but possessed lower *in vitro* efficacy, compared with D-AmB (76). In this dissertation, polymeric micelles formed from PEG-DSPE were studied for solubilization and deaggregation of AmB. These results are presented in chapters 2 and 3.

1.9.4 Sodium supplementation

Saline loading represents a simple and inexpensive procedure which lowers kidney toxicity associated with AmB therapy. An exhaustive clinical study found that patients who received 1 L of 0.9 % NaCl prior to AmB therapy had unchanged serum creatinine levels compared to patients who received a similar volume of 5 % dextrose, as placebo (56). While the exact mechanism of nephroprotection is not clear, it has been suggested that sodium blocks tubuloglomerular feedback induced by D-AmB (57). D-AmB cannot be administered with NaCl in the same aqueous vehicle, owing to the precipitation of the drug, necessitating sequential infusion of 0.9 % NaCl followed by D-AmB (58). To avoid hazardous drug precipitation, special care must be taken to thoroughly rinse the IV line with 5 % dextrose prior to addition of D-AmB. Dynamic light scattering, size-exclusion chromatography and solution turbidity measurements have been used to study precipitation of AmB from PEG-DSPE micelles in saline. AmB solubilized in PEG-DSPE micelles did not precipitate for prolonged periods enabling simultaneous administration of NaCl and AmB via a single IV access-line.

1.9.5 Continuous infusion

Continuous infusion of D-AmB is another simple nephroprotective measure that has gained popularity (59). In a recent open-label study, continuous infusion of D-AmB resulted in a lower incidence of nephrotoxicity and fewer infusion related side effects, compared to the standard 4 h infusion at an equal dose (60). More recently, 17 patients with hematological malignancies having fever of unknown

origin with possible invasive fungal infection were treated with D-AmB as a continuous infusion, and no infusion-related side effects were found, contrasting with the control group of D-AmB infused over 2 to 6 hrs (61). It is proposed that continuous infusion of D-AmB produces a constant soluble "bioactive" fraction of AmB and lower accumulation at deep tissue sites, compared to the 4 h infusion (62). Regardless of the mechanism, it is becoming increasingly clear that the continuous infusion of D-AmB reduces toxic manifestations of this important antifungal drug. There is some concern about the physical and chemical stability of D-AmB. PEG-DSPE micelles solubilize AmB in a form that is stable to extensive dilution for prolonged periods of time, which is of significant advantage for continous infusion compared to D-AmB.

1.10 Treatment of systemic candidiasis using drug combinations

There is a renewed interest in studying combinations of antifungal drugs to explore potential advantages such as broad-spectrum efficacy and additive or synergistic potency (77, 78). The most common rationale behind studying drug combinations is based on combining agents with sufficiently different mechanisms or spectrum of activity. Not all combinations are beneficial; drug combinations may be antagonistic and could result in reduced activity or raise potential for drug interactions and toxicities. While pharmacokinetics may have a significant impact on the activity of a drug combination *in vivo*, *in vitro* susceptibility studies are valuable in screening drug combinations before validation in animal models.

Combination therapy involving AmB has been restricted by poor physical stability and compatibility with antifungal drugs and vehicles, especially in the form of D-AmB. Significantly, AmB solubilized in PEG-DSPE micelles is stable against precipitation in a saline solution over prolonged periods raising promise for use in combination with other antifungal drugs. Rapamycin and 5-FC are antifungal agents with unique mechanisms of activity, with potential for cooperative interaction with AmB.

Rapamycin exerts potent cidal activity by inhibiting fungal TOR kinases (79, 80). Early animal experiments showed effectiveness against *Candida* infection. However, enthusiasm for use as an antifungal agent were lowered on emergence of potent immunosuppression in hosts (81). The TOR signaling cascade represents a conserved pathway across yeasts, involved in eliciting cell response to a wide variety of stimuli including nutrients and external stress (82). Considering the unique mechanism of action, this class of antifungal antibiotics has unexplored potential for treatment of systemic fungal disease, particularly in combination with AmB.

5-FC is selectively converted to toxic 5-fluorouracil in fungal cells. The *in vitro* antifungal effects of the combination of D-AmB and 5-FC have been studied before and have been reported as synergistic or additive, depending on the species of *Candida* (78). It is hypothesized that AmB potentiates 5-FC activity by increasing the penetration of 5-FC across fungal membranes, highlighting the value of exposing the fungal pathogens to 5-FC at the same time or after exposure to AmB (83).

The potential for PEG-DSPE micelle solubilized AmB for use in combination therapy has been assessed in chapter 5. Since rapamycin has limited aqueous

solubility, it has been solubilized in PEG-DSPE micelles. Interactive effects between AmB, rapamycin and 5-FC were determined using broth microdilution method (84), using a checkerboard layout.

1.11 Research Proposal

Amphotericin B (AmB) is a poorly soluble antifungal drug used to treat systemic fungal diseases, despite severe toxicities. AmB toxicity is thought to be mediated by the relative aggregation state of the drug. This proposal seeks to explore the utility of polymeric micelles formed from PEG-DSPE to solubilize AmB and to reduce its toxicity without an appreciable loss in antifungal activity. It is hypothesized that PEG-DSPE based micelles may serve as long-circulating nanocarriers and may increase the therapeutic index of AmB by sustained release or changes in the self-aggregation state.

There is renewed interest in studying combinations of antifungal drugs to explore potential advantages such as enhanced potency or activity. Rapamycin and 5-FC are antifungal agents with unique mechanisms of action, with potential for cooperative interaction with AmB. It is hypothesized that AmB will remain solubilized in PEG-DSPE micelles when mixed with 5-FC and solubilized rapamycin enabling evaluation of the potential of drug combinations in treating systemic fungal diseases.

1.12 Specific Aims

To address the above research proposal, the following specific aims for this work are presented:

1. Determine the effects of relative proportions of PEG-DSPE and AmB on level of drug solubilized and extent of self-aggregation
2. Evaluate toxicity of micelle encapsulated AmB relative to free drug, *in vitro*, using erythrocytes and kidney cells. Assess *in vitro* fungicidal activity of micelle encapsulated AmB relative to free drug
3. Study and compare AmB release from PEG-DSPE micelles in buffer and serum albumin. In this context,
    a. Examine the effects of cholesterol incorporation on the properties of PEG-DSPE micelles and AmB release in serum albumin
    b. Investigate formation of mixed polymeric micelles from PEG-b-poly(ε-caprolactone) and PEG-DSPE and evaluate potential for these assemblies for AmB solubilization and slow release
4. Investigate compatibility of PEG-DSPE encapsulated AmB with rapamycin and 5-FC in a saline vehicle
5. Examine interactive effects between AmB and rapamycin in PEG-DSPE micelles when combined with 5-FC, *in vitro*

1.13 References

1. Vicent, M., Duncan, R., Polymer conjugates: Nanosized medicines for treating cancer. Trends Biotechnol., 2006. **24**(1): p. 39-47.

2. Sinha, R., Kim, G., Nie, S., Shin, D., Nanotechnology in cancer therapeutics: bioconjugated nanoparticles for drug delivery. Mol. Cancer Ther., 2006. **5**(8): p. 1909-17.

3. Kataoka, K., Kwon, G., Yokoyama, M., Okano, T., Sakurai, Y., Block copolymer micelles as vehicles for drug delivery. J. Controlled Release, 1993. **24**(1-3): p. 119-132.

4. Torchilin, V., Structure and design of polymeric surfactant-based drug delivery systems. J. Controlled Release, 2001. **73**(2-3): p. 137-72.

5. Kwon, G., Polymeric micelles for delivery of poorly water-soluble compounds. Crit. Rev. Ther. Drug Carrier Syst., 2003. **20**(5): p. 357-403.

6. Lipinski, C., Drug-like properties and the causes of poor solubility and poor permeability. J. Pharmacol. Toxicol. Methods, 2000. **44**(1): p. 235-49.

7. Jonkman-De Vries, J., Flora, K., Bult, A., Beijnen, J., Pharmaceutical development of (investigational) anticancer agents for parenteral use. A review. Drug Dev. Ind. Pharm, 1996. **22**: p. 475.

8. Gelderblom, H., Verweij, J., Nooter, K., Sparreboom, A., Cremophor EL: the drawbacks and advantages of vehicle selection for drug formulation. Eur. J. Cancer, 2001. **37**(13): p. 1590-8.

9. Stolnik, S., Illum, L., Davis, S., Long circulating microparticulate drug carriers. Adv. Drug Del. Rev., 1995. **16**(2-3): p. 195-214.

10. Papisov, M., Modeling in vivo transfer of long-circulating polymers (two classes of long circulating polymers and factors affecting their transfer in vivo). Adv. Drug Del. Rev., 1995. **16**(2-3): p. 127-139.

11. Schiffelers, R., Bakker-Woudenberg, I., Snijders, S., Storm, G., Localization of sterically stabilized liposomes in Klebsiella pneumoniae-infected rat lung tissue: influence of liposome characteristics. Biochim. Biophys. Acta, 1999. **1421**(2): p. 329-39.

12. Kwon, G., Kataoka, K., Block copolymer micelles as long-circulating drug vehicles. Adv. Drug Del. Rev., 1995. **16**(2-3): p. 295-309.

13. Yokoyama, M., Polymeric micelles for the targeting of hydrophobic drugs, in Polymeric drug delivery systems, G. Kwon, Editor. 2005. p. 533-575.

14. Nagarajan, R., Barry, M., Ruckenstein, E., Unusual selectivity in solubilization by block copolymer micelles. Langmuir, 1986. **2**: p. 210-215.

15. Kabanov, A., Alakhov, V., Pluronic block copolymers in drug delivery: from micellar nanocontainers to biological response modifiers. Crit. Rev. Ther. Drug., 2002. **19**: p. 1-72.

16. Aliabadi, H., Lavasanifar, A., Polymeric micelles for drug delivery. Expert Opinion in Drug Delivery, 2006. **3**(1): p. 139-162.

17. Weissig, V., Whiteman, K., Torchilin, V., Accumulation of protein-loaded long-circulating micelles and liposomes in subcutaneous Lewis lung carcinoma in mice. Pharm. Res., 1998. **15**(10): p. 1552-6.

18. Lukyanov, A., Gao, Z., Torchilin, V., Micelles from polyethylene glycol/phosphatidylethanolamine conjugates for tumor drug delivery. J. Controlled Release, 2003. **91**(1-2): p. 97-102.

19. Lasic, D., Liposomes: from physics to applications. 1993: Elsevier.

20. Gao, Z., Lukyanov, A., Singhal, A., Torchilin, V., Diacyllipid-polymer micelles as nanocarriers for poorly water soluble anticancer drugs. Nano Letters, 2002. **2**(9): p. 979-982.

21. Zhang, J., Hansen, C., Allen, T., Boey, A., Boch, R., Lipid-derivatized poly(ethylene glycol) micellar formulations of benzoporphyrin derivatives. J. Controlled Release, 2003. **86**(2-3): p. 323-38.

22. Trubetskoy, V., Frank-Kamenetsky, M., Whiteman, K., Wolf, G., Torchilin, V., Stable polymeric micelles: Lymphangiographic contrast media for gamma scintigraphy and magnetic resonance imaging. Acad. Radiol., 1996. **3**(3): p. 232-8.

23. Lukyanov, A., Torchilin, V., Micelles from lipid derivatives of water-soluble polymers as delivery systems for poorly soluble drugs. Adv. Drug Deliv. Rev., 2004. **56**(9): p. 1273-89.

24. Torchilin, V., Lukyanov, A., Gao, Z., Papahadjopoulos-Sternberg, B., Immunomicelles: Targeted pharmaceutical carriers for poorly soluble drugs. Proc. Natl. Acad. Sci., 2003. **100**(10): p. 6039-44.

25. Krishnadas, A., Rubinstein, I., Onyuksel, H., Sterically stabilized phospholipid mixed micelles: in vitro evaluation as a novel carrier for water-insoluble drugs. Pharm. Res., 2003. **20**(2): p. 297-302.

26. Ashok, B., Arleth, L., Hjelm, R., Rubinstein, I., Onyuksel, H., In vitro characterization of PEGylated phospholipid micelles for improved drug solubilization: effects of PEG chain length and PC incorporation. J. Pharm. Sci., 2004. **93**(10): p. 2476-2487.

27. Forrest, M., Kwon, G., unpublished.

28. Nagarajan, R., Thermodynamics of nonionic polymer-micelle association. Colloids Surf., 1985. **13**: p. 1-17.

29. Oh, K., Bronich, T., Kabanov, A., Micellar formulations for drug delivery based on mixtures of hydrophobic and hydrophilic Pluronic block copolymers. J. Controlled Release, 2004. **94**(2-3): p. 411-22.

30. Gao, Z., Fain, H., Rapoport, N., Ultrasound-enhanced tumor targeting of polymeric micellar drug carriers. Mol. Pharm., 2004. **1**(4): p. 317-330.

31. Gao, Z., Fain, H., Rapoport, N., Controlled and targeted tumor chemotherapy by micellar-encapsulated drug and ultrasound. J. Controlled Release, 2005. **102**(1): p. 203-222.

32. Lee, E., Na, K., Bae, Y-H.,, Polymeric micelle for tumor pH and folate-mediated targeting. J. Controlled Release, 2003. **91**(1-2): p. 103-113.

33. Aliabadi, H., Brocks, D., Lavasanifar, A., Polymeric micelles for the solubilization and delivery of cyclosporine A: Pharmacokinetics and biodistribution. Biomaterials, 2005. **26**(35): p. 7251-7259.

34. Forrest, M., Won, C., Malick, A., Kwon, G., In vitro release of the mTOR inhibitor rapamycin from poly(ethylene glycol)-b-poly(epsilon-caprolactone) micelles. J. Controlled Release, 2006. **110**(2): p. 370-7.

35. Liu, J., Xiao, Y., Allen, C., Polymer-drug compatibility: A guide to the development of delivery systems for the anticancer agent, ellipticine. J. Pharm. Sci., 2004. **93**(1): p. 132-43.

36. Allen, C., Eisenberg, A., Mrsic, J., Maysinger, D., PCL-b-PEO micelles as a delivery vehicle for FK506: Assessment of a functional recovery of crushed peripheral nerve. Drug Delivery, 2000. **7**(3): p. 139-145.

37. Allen, C., Han, J., Yu, Y., Maysinger, D., Eisenberg, A., Polycaprolactone-b-poly(ethylene oxide) copolymer micelles as a delivery vehicle for dihydrotestosterone. J. Controlled Release, 2000. **63**(3): p. 275-286.

38. Forrest, M., Zhao, A., Won, C., Malick, A., Kwon, G., Lipophilic prodrugs of Hsp90 inhibitor geldanamycin for nanoencapsulation in poly(ethylene glycol)-b-poly(epsilon-caprolactone) micelles. J. Controlled Release, 2006.

39. Wisplinghoff, H., Bischoff, T., Tallent, S., Seifert, H., Wenzel, R., Edmond, M., Nosocomial bloodstream infections in US hospitals: Analysis of 24,179 cases from a prospective nationwide surveillance study. Clin. Infect. Dis., 2004. **39**(3): p. 309-17.

40. Spellberg, B., Filler, S., Edwards, J., Current treatment strategies for disseminated candidiasis. Clin. Infect. Dis., 2006. **42**(2): p. 244-51.

41. Fridkin, S., Jarvis, W., Epidemiology of nosocomial fungal infections. Clin. Microbiol. Rev., 1996. **9**(4): p. 499-511.

42. Jarvis, W., Epidemiology of nosocomial fungal infections, with emphasis on Candida species. Clin. Infect. Dis., 1995. **20**(6): p. 1526-30.

43. Wenzel, R., Nosocomial candidemia: Risk factors and attributable mortality. Clin. Infect. Dis., 1995. **20**(6): p. 1531-4.

44. Edmond, M., Wallace, S., Mcclish, D., Pfaller, M., Jones, R., Wenzel, R., Nosocomial bloodstream infections in United States hospitals: a three-year analysis. Clin. Infect. Dis., 1999. **29**(2): p. 239-44.

45. Dismukes, W., Introduction to antifungal drugs. Clin. Infect. Dis., 2000. **30**(4): p. 653-7.

46. Ghannoum, M., Rice, L., Antifungal agents: mode of action, mechanisms of resistance, and correlation of these mechanisms with bacterial resistance. Clin. Microbiol. Rev., 1999. **12**(4): p. 501-17.

47. Baddley, J., Moser, S., Emerging fungal resistance. Clin. Lab. Med., 2004. **24**(3): p. 721-35, vii.

48. Pfaller, M., Jones, R., Messer, S., Edmond, M., Wenzel, R., National surveillance of nosocomial blood stream infection due to Candida albicans: frequency of occurrence and antifungal susceptibility in the SCOPE Program. Diagn. Microbiol. Infect. Dis., 1998. **31**(1): p. 327-32.

49. Mora-Duarte, J., Betts, R., Rotstein, C., Colombo, A., Thompson-Moya, L., Smietana, J., Lupinacci, R., Sable, C., Kartsonis, N., Perfect, J., Comparison of caspofungin and amphotericin B for invasive candidiasis. N. Engl. J. Med., 2002. **347**(25): p. 2020-9.

50. Brajtburg, J., Bolard, J., Carrier effects on biological activity of amphotericin B. Clin. Microbiol. Rev., 1996. **9**(4): p. 512-31.

51. Zager, R., Polyene antibiotics: Relative degrees of in vitro cytotoxicity and potential effects on tubule phospholipid and ceramide content. Am. J. Kidney Dis., 2000. **36**(2): p. 238-49.

52. Bolard, J., Legrand, P., Heitz, F., Cybulska, B., One-sided action of amphotericin B on cholesterol-containing membranes is determined by its self-association in the medium. Biochemistry, 1991. **30**(23): p. 5707-15.

53. Legrand, P., Romero, E., Cohen, B., Bolard, J., Effects of aggregation and solvent on the toxicity of amphotericin B to human erythrocytes. Antimicrob. Agents Chemother., 1992. **36**(11): p. 2518-22.

54. Slain, D., Lipid-based amphotericin B for the treatment of fungal infections. Pharmacotherapy, 1999. **19**(3): p. 306-23.

55. Ceylan, E., Akkan, H., Tutuncu, M., Agaoglu, Z., Nephrotoxic effect of amphotericin B administered in different doses and infusion modes in dogs. Acta Vet. Brno, 2003. **72**: p. 229-234.

56. Llanos, A., Cieza, J., Berando, J., Effect of salt supplementation on amphotericin nephrotoxicity. Kidney Int., 1991. **40**: p. 302-308.

57. Gerkins, J., Branch, R., The influence of sodium status and furosemide on canine acute amphotericin b nephrotoxicity. J. Pharmacol. Exp. Ther., 1980. **214**: p. 306-311.

58. Jurgens, R., Deluca, P., Papadimitriou D., Compatibility of amphotericin b with certain large-volume parenterals. Am. J. Hospital Pharm., 1981. **38**: p. 377-378.

59. Eriksson, U., Seifer, B., Schaffner, A., Comparison of effects of amphotericin b deoxycholate infused over 4 to 24 hours: Randomized controlled trial. Br. Med. J., 2001. **322**: p. 579-582.

60. Imhof, A., Walter, R.B., Schaffner, A., Continuous infusion of escalated doses of amphotericin b deoxycholate: an open-label observational study. Clin. Infect. Dis., 2003. **36**: p. 943-951.

61. Schulenburg, A., Sperr, W., Rabitsch, W., Knobl, P., Thalhammer, F., Brief report: Practicability and safety of amphotericin b deoxycholate as continuous infusion in neutropenic patients with hematological malignancies. Leukemia & Lymphoma, 2005. **46**: p. 1163-1167.

62. Lewis, R., Wiederhold, N., The solubility ceiling: a rationale for continuous infusion of amphotericin b therapy? Clin. Infect. Dis., 2003. **37**: p. 871-872.

63. Brajtburg, J., Powderly, W., Kobayashi, G., Medoff, G., Amphotericin B: Delivery systems. Antimicrob. Agents Chemother., 1990. **34**(3): p. 381-4.

64. Mehta, R., Liposomes as drug carriers for polyene antibiotics. Adv. Drug Del. Rev., 1989. **3**(3): p. 283-306.

65. Abu-Salah, K., Amphotericin B: An update. Br. J. Biomed. Sci., 1996. **53**(2): p. 122-33.

66. Dupont, B., Overview of the lipid formulations of amphotericin B. J. Antimicrob. Chemother., 2002. **49 Suppl. 1**: p. 31-6.

67. Walsh, T., Finberg, R., Arndt, C., Hiemenz, J., Schwartz, C., Bodensteiner, D., Pappas, P., Seibel, N., Greenberg, R., Dummer, S., Schuster, M., Holcenberg, J., Dismukes, W., Liposomal amphotericin B for empirical therapy in patients with persistent fever and neutropenia. N. Engl. J. Med., 1999. **340**(10): p. 764-771.

68. Wong-Beringer, A., Jacobs, R., Guglielmo, B., Lipid formulations of amphotericin B: clinical efficacy and toxicities. Clin. Infect. Dis., 1998. **27**(3): p. 603-18.

69. Cannon, J., Garey, K., Danziger, L., A prospective and retrospective analysis of the nephrotoxicity and efficacy of lipid-based amphotericin B formulations. Pharmacotherapy, 2001. **21**(9): p. 1107-14.

70. Barwicz, J., Christian, S., Gruda, I., Effects of the aggregation state of amphotericin B on its toxicity to mice. Antimicrob. Agents Chemother., 1992. **36**(10): p. 2310-2315.

71. Tasset, C., Preat, V., Roland, M., The influence of Myrj 59 on the solubility, toxicity and activity of amphotericin B. J. Pharm. Pharmacol., 1991. **43**(5): p. 297-302.

72. Adams, M., Kwon, G., The effects of acyl chain length on the micelle properties of poly(ethylene oxide)-block-poly(N-hexyl-L-aspartamide)-acyl conjugates. J. Biomater. Sci., Polym. Ed., 2002. **13**(9): p. 991-1006.

73. Adams, M., Kwon, G., Relative aggregation state and hemolytic activity of amphotericin B encapsulated by poly(ethylene oxide)-block-poly(N-hexyl-L-aspartamide)-acyl conjugate micelles: effects of acyl chain length. J. Controlled Release, 2003. **87**(1-3): p. 23-32.

74. Adams, M., Andes, D., Kwon, G., Amphotericin B encapsulated in micelles based on poly(ethylene oxide)-block-poly(L-amino acid) derivatives exerts reduced in vitro hemolysis but maintains potent in vivo antifungal activity. Biomacromolecules, 2003. **4**(3): p. 750-757.

75. Espuelas, M., Legrand, P., Campanero, M., Appel, M., Cheron, M., Gamazo, C., Barratt, G., Irache, J., Polymeric carriers for amphotericin B: In vitro activity, toxicity and therapeutic efficacy against systemic candidiasis in neutropenic mice. J. Antimicrob. Chemother., 2003. **52**(3): p. 419-27.

76. Vandermeulen, G., Rouxhet, L., Arien, A., Brewster, M., Preat, V., Encapsulation of amphotericin B in poly(ethylene glycol)-block-poly(epsilon-caprolactone-co-trimethylenecarbonate) polymeric micelles. Int. J. Pharm., 2006. **309**(1-2): p. 234-40.

77. Johnson, M., Macdougall, C., Ostrosky-Zeichner, L., Perfect, J., Rex, J.,, Combination antifungal therapy. Antimicrob. Agents Chemother., 2004. **48**(3): p. 693-715.

78. Mukherjee, P., Sheehan, D., Hitchcock, C., Ghannoum, M., Combination treatment of invasive fungal infections. Clin. Microbiol. Rev., 2005. **18**(1): p. 163-94.

79. Vezina, C., Kudelski, A., Sehgal, S., Rapamycin (AY-22,989), a new antifungal antibiotic I. Taxonomy of the producing streptomycete and isolation of the active principle. J. of Antibiotics, 1975. **28**: p. 721-726.

80. Baker, H., Sidorowicz, A., Sehgal, S.., Vezina, C., Rapamycin (AY-22,989), a new antifungal antibiotic III. In vitro and in vivo evaluation. J. Antibiotics, 1978. **31**: p. 539-545.

81. Kahan, B., Camardo, J., Rapamycin: clinical results and future opportunities. Transplantation, 2001. **72**: p. 1181-1193.

82. Rohde, J., Heitman, J., Cardenas, M., The TOR kinases link nutrient sensing to cell growth. J. Biol. Chem., 2001. **276**(13): p. 9583-6.

83. Medoff, G., Kobayashi, G., Kwan, C., Schlessinger, D., Venkov, P., Potentiation of rifampicin and 5-fluorocytosine as antifungal antibiotics by amphotericin B (yeast-membrane permeability-ribosomal RNA-eukaryotic cell-synergism). Proc. Natl. Acad. Sci., 1972. **69**(1): p. 196-9.

84. Pfaller, M., Reference method for broth dilution antifungal susceptibility testing of yeasts : approved standard. 2002 ed. NCCLS, M27-A2. Vol. 22 no. 15. 2002, Wayne, Pa.: National Committee for Clinical Laboratory Standards.

Chapter 2:

PEG-phospholipid micelles for the delivery of amphotericin B

Portions of this chapter related to AmB solubilization in polymeric micelles and effects on drug self-aggreation have been published in Vakil R., Kuldipkumar A., Andes D., Tan Y., Kwon G., "Polymeric Micelles for the Delivery of Polyene Antibiotics", in S. Svenson (Ed.), Polymeric Drug Delivery Vol. I – Particulate Drug Carriers, ACS Symposium Series Vol. 923, New York (2006): p. 14-26

2.1 Introduction

We have studied PEG-DSPE micelles for the delivery of AmB, owing to the presumed compatibility between the drug and phospholipid and proven safety profile of polymer (1, 2). In this work, we have evaluated the ability of polymeric micelles formed from PEG-DSPE to deaggregate AmB and reduce its toxicity. AmB has been incorporated in PEG-DSPE micelles (AmB|PEG-DSPE) by a method that involves solvent evaporation and dissolution of co-precipitated drug and polymer in buffer. The formation of micelles and drug loading has been confirmed using size-exclusion chromatography. It appears that AmB is deaggregated on incorporation in these micelles, based on results from absorption spectroscopy. The effect of micelle encapsulated AmB on mammalian cell-membranes was assessed using hemolysis. Additionally, we have determined cytotoxicity of AmB|PEG-DSPE against HK-2 cell-cultures. Susceptibility of three fungal isolates to AmB|PEG-DSPE, relative to deoxycholate-AmB (D-AmB) has been tested using a broth microdilution method.

2.2 Materials

AmB was obtained as a gift from Alpharma (Copenhagen, Denmark) and was stored at -20°C until use. D-AmB was purchased from Sigma (Saint Louis, MO). 1,2-Distearoyl-*sn*-glycero-3-phosphoethanolamine-*N*-methoxy(polyethylene glycol) (PEG-DSPE) (M_n = 5800 g/mol) was obtained from Avanti Polar Lipids (Alabaster, AL). All reagents used were of analytical grade and were used without further purification.

Murine erythrocytes were obtained from Harlan Bioproducts (Indianapolis, IN). The HK-2 cell-line was purchased from American Type Culture Collection (ATCC, Manassas, VA). Fungal isolates were obtained from Dr. David Andes (Deparment of Medicine, University of Wisconsin – Madison) and were propagated on Difco Sabouraud Dextrose Agar (Becton, Dickinson and Company, Sparks, MD).

2.3 Incorporation of AmB in PEG-DSPE micelles

Stock solutions of PEG-DSPE (6.0 mg/mL) and AmB (0.3 mg/mL) prepared in chloroform/methanol (1:2) were mixed in a round bottom flask, to obtain varying ratios of AmB: PEG-DSPE. The mixed solvent was evaporated under vacuum to produce a thin film of co-precipitated drug and polymer. This film was dissolved in 10 mM PBS (pH 7.4) and was incubated at 25 °C for 5 min, to allow for complete dissolution. Unincorporated AmB was removed by filtration through a 0.45-μm polyethersulfone membrane. Empty PEG-DSPE micelles were prepared using a similar method without AmB.

2.4 Micelle Characterization

2.4.1 Dynamic light scattering

Size measurements were performed on the NICOMP 380ZLS particle sizer (Particle Sizing Systems, Santa Barbara, CA). Data was acquired to have at least 100k counts in channel 1. A Gaussian fit to the raw data was performed and the particle sizes were expressed as volume-weighted mean diameters.

2.4.2 Spectroscopic analysis of AmB

The level of AmB in solution was evaluated by adding an equal volume of N,N-dimethylformamide (DMF) and monitoring absorbance of the drug at 413.5 nm. Encapsulation yield was calculated as the the ratio of solubilized AmB relative to the initial amount of drug. Additionally, absorbance spectrum of ca. 10 μg/mL micelle encapsulated AmB in 10 mM PBS was recorded to determine the extent of AmB self-aggregation. Absorbance spectra were acquired at room temperature from 300 to 450 nm with a scan step of 0.1 nm.

2.4.3 Size-exclusion chromatography

AmB encapsulated in PEG-DSPE micelles (40 μg/mL AmB at AmB: PEG-DSPE = 0.5, 4.0) was injected in a Shodex PROTEIN KW-804 SEC column (Showa Denko, Japan). The samples were eluted by phosphate buffer (50 mM, pH 7.4) at a flow rate of 0.75 mL/min. The elution of PEG-DSPE micelles was monitored by refractive index and AmB absorbance (300 – 450 nm) was observed using a diode array detector (Agilent 1100).

2.5 Evaluation of *in vitro* toxicity of PEG-DSPE incorporated AmB

2.5.1 Hemolytic activity of AmB against murine erythrocytes

Erythrocytes from female ICR mice were obtained as packed cells in 1 % EDTA. The RBC were washed and diluted in PBS to prepare a stock solution containing 1.6 x 10^8 RBC/mL. AmB was solubilized in PEG-DSPE micelles on the day of the experiment. A stock solution containing 0.1 mg/mL free AmB was

prepared by first dissolving AmB in DMSO, followed by addition to PBS. The final DMSO content was less than 0.2 % v/v. Solutions containing varying levels of AmB were prepared from these concentrated stock solutions. 1.0 mL RBC stock was mixed with 1.0 mL AmB solution and incubated at 37 °C for 30 min. The samples were then centrifuged at 3000 RPM for 5 min to sediment intact RBC. The supernatant was analyzed for absorbance at 576.5 nm and the percentage lysis was calculated by the equation:

$$Percent\ lysis = \frac{A - A_0}{A_{100} - A_0} x100$$

where A, A_0, A_{100} are the absorbances of the supernatant for sample, drug-free control, and control for complete lysis (hypotonic hemolysis), respectively.

2.5.2 Cell viability studies using HK-2 cells

The human proximal tubular kidney cell-line HK-2 (ATCC CRL-2190) was cultured at 37 °C/ 5 % CO_2 in "Defined Keratinocyte Serum Free Medium" (K-SFM) supplemented with L-glutamine, penicillin and streptomycin according to procedures recommended by ATCC. Cells were harvested in the pre-confluence stage using 0.05 % typsin/ 0.53 mM EDTA and placed in 96-well plates at a density of 1.5 x 10^4 cells/ well. The cells were allowed to attain confluence over 72 h, with daily media changes. Solutions containing varied levels of AmB were prepared from stock solutions in DMEM (supplemented with 10 % fetal bovine serum, buffered to pH 5.8), instead of PBS. For the experiment, media in each well was replaced with 200 µL AmB solution. Cell-viability after a 90 min exposure to AmB was determined

using a MTS-based assay kit (CellTiter 96 AQueous One, Promega). HK-2 cells were washed with fresh media and were incubated with test reagents (diluted to recommended levels in DMEM, pH 7.4) for 1 h. Absorbance of the resulting formazan product at 490 nm was determined using the Microplate EL 312e absorbance plate reader. Percent cell-viability was calculated using the following equation:

$$Percent\ viability = \frac{A - A_0}{A_{100} - A_0} x100$$

where A, A_{100}, A_0 are the absorbances of the sample, drug-free control and cell-free control (blank), respectively.

2.6 *In vitro* susceptibility of yeast isolates against PEG-DSPE incorporated AmB

Three bloodstream isolates of *Candida* albicans (K-1, 98-17, 98-234) were maintained on SDA plates. Susceptibility testing of yeast isolates was performed using a broth microdilution method, according to recommendations in the NCCLS M27-A2 protocol (3). Dilutions containing varying levels of AmB were prepared in RPMI-1640 (supplemented with 0.165 M morpholinepropanesulfonic acid, buffered to pH 7.0) from the initial stock solutions. AmB solutions in the range 0.0001 – 2 µg/mL were incubated in 96-well plates for 24 h at 35 °C with yeast inoculum, which was standardized spectrophotometrically. Fungal growth in different wells was visually compared and the minimum inhibitory concentration was defined as the lowest concentration of AmB which completely inhibited fungal growth relative to drug-free control.

2.7 Results and Discussion

2.7.1 Micelle characterization and drug loading

We were unable to directly dissolve AmB and PEG-DSPE in water and obtain appreciable solubilization of drug. Instead, we have dissolved AmB and PEG-DSPE in a chloroform/methanol mixture and have removed the solvent by rotoevaporation to make a solid film of drug and polymer. This film was dissolved in buffer which gave a clear yellow solution of solubilized drug. The yield of AmB (level of incorporated drug/initial level of drug) was about 80 % (Table 2.1). The final ratio of PEG-DSPE to AmB ranged from 0.6 to 5.2 mol:mol, depending on the starting level of PEG-DSPE. Dynamic light scattering results indicated that drug loaded PEG-DSPE micelles were small i.e. ca. 20 nm in size. The level of AmB solubilized in water typically ranged from 0.32 to 0.4 mg/mL. This however does not represent the upper limit of AmB solubilization in PEG-DSPE micelles, as levels in excess of 1000 μg/mL AmB could be solubilized at higher polymer concentrations (data not shown).

[PEG-DSPE] (mg/mL)[a]	PEG-DSPE: AmB (mol/mol)	PEG-DSPE: AmB (w/w)	[AmB] (mg/mL)	Yield of AmB[b]	Hydrodynamic Diameter[c] (nm)
1.26	0.64 ± 0.02	4.03	0.38 ± 0.12	0.78 ± 0.03	21.8 ± 6.1
5.02	5.20 ± 0.05	32.61	0.4 ± 0.02	0.77 ± 0.01	19.3 ± 4.4

Table 2.1. Solubilization of AmB by PEG-DSPE micelles[d]
[a] assuming no loss on filtration [b]AmB solubilized/initial AmB [c]volume-weighted diameter
[d]n=3

2.7.2 AmB self-aggregation in PEG-DSPE micelles

The direct dissolution of AmB as Fungizone (2:1 molar ratio of sodium deoxycholate to AmB) in water produces some monomeric drug and various species of soluble aggregates of the drug combined with sodium deoxycholate. A similar distribution of AmB in various states of self-association is obtained on addition of AmB (dissolved in an organic solvent such as DMSO) to excess water. The proportion of these species of AmB depends on the method of dissolution, temperature and concentration (4). In both cases, given sufficient time, AmB precipitates. The absorption spectrum of deoxycholate AmB is characterized by a broad band centered at 328 nm, corresponding to the soluble aggregated species of AmB (Figure 2.1). In contrast, AmB is entirely monomeric in methanol or DMF, and it has a characteristic spectrum with four well-separated bands at 348, 365, 385 and 409 nm. The relative intensity ratio of the first to the fourth band, often referred to as the I/IV ratio, serves as a measure for the extent of AmB self-association. This ratio is less than 0.25 for monomeric AmB and may be higher than 2.0 for highly aggregated species (5).

The extent of AmB self-association in PEG-DSPE micelles depended on the molar ratio of PEG-DSPE to AmB (Figure 2.2). A broad band at 331 nm that is characteristic of aggregated species of AmB was predominant at a molar ratio of 0.5. With an increase in PEG-DSPE content, sharp bands at 368, 388, and 417 nm increased in intensity and were predominant. The ratio of the intensity at 331 nm to 417 nm, i.e., I/IV ratio, decreased from 2.66 to 0.23 with an increase in PEG-DSPE content, consistent with drug deaggregation.

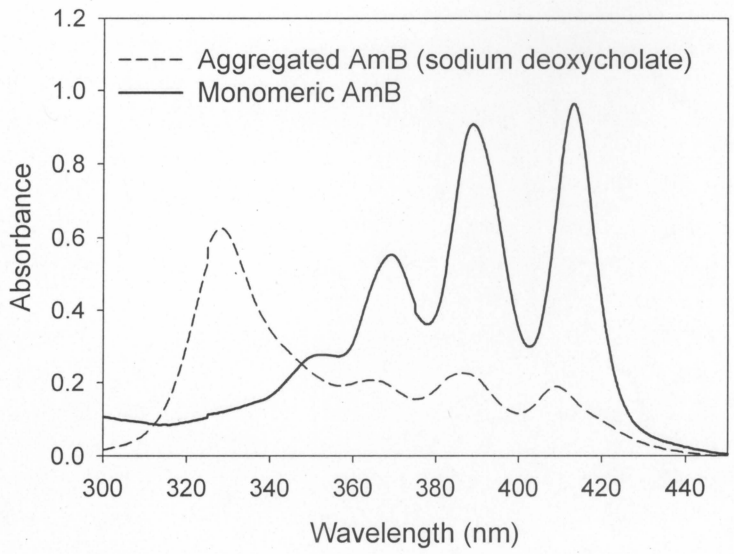


Figure 2.1. Absorption spectra of monomeric[a] and self-aggregated[b] AmB
[a] in DMF [b]D-AmB

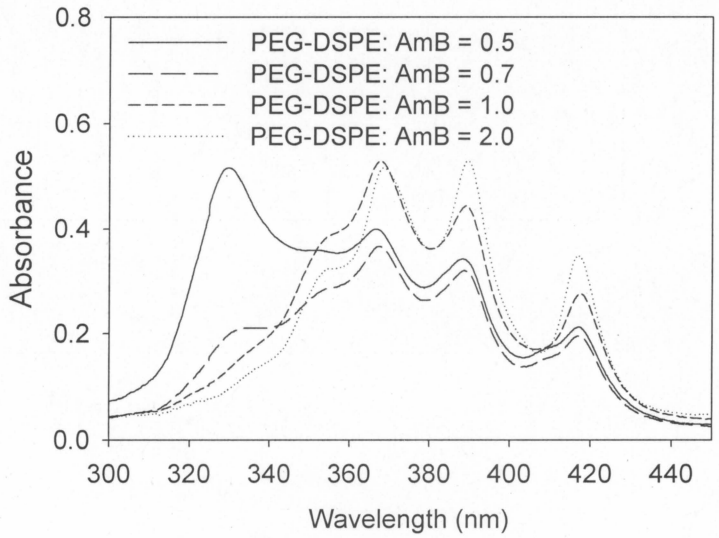


Figure 2.2. Absorption spectra of AmB solubilized by PEG-DSPE at varied mole ratios of PEG-DSPE to AmB

Size exclusion chromatography results reveal that the deaggregation of AmB occurs as a result of its incorporation in PEG-DSPE micelles. Empty PEG-DSPE micelles eluted at 7.68 mL (data not shown). Similarly, PEG-DSPE micelles with AmB eluted at 7.70 mL at a ratio of polymer to drug at 4.0, according to refractive index and absorbance (Figure 2.3a). In contrast, AmB determined to be predominantly self-aggregated by absorbance spectroscopy, at a molar ratio of 0.5, eluted as three species, one at 6.05 mL and a second at 6.91 mL, both corresponding to aggregated species of AmB, and a third at 7.93 mL, corresponding to PEG-DSPE micelles with incorporated AmB in a monomeric state (Figure 2.3b). At a ratio of 0.5, a relatively high level of AmB, it appears that the capacity of the PEG-DSPE micelles for the drug was exceeded, and as a result, AmB assembles into several species of water-soluble aggregates.

The deaggregation of AmB in PEG-DSPE micelles likely occurs by a strong interaction between AmB and distearoyl lipid chains. A slight bathochromic shift and a difference in the intensity of bands associated with monomeric AmB in cores relative to the drug in methanol was an indication of this interaction. In particular, the intensity of the band at 417 nm was less than the intensity of bands at 368 and 388 nm for monomeric AmB in PEG-DSPE micelles. For AmB in methanol, the opposite was observed, and bands, II, III, and IV, were present at 365, 385, and 409 nm.

Several strategies have been studied to deaggregate and thus lower the toxicity of polyene antibiotics. While nontoxic poloxamers are unable to deaggregate AmB, they were able to deaggregate nystatin, a structurally related polyene antibiotic, and thus reduce its toxicity in terms of hemolysis (6). Gruda at al. added excess surfactant

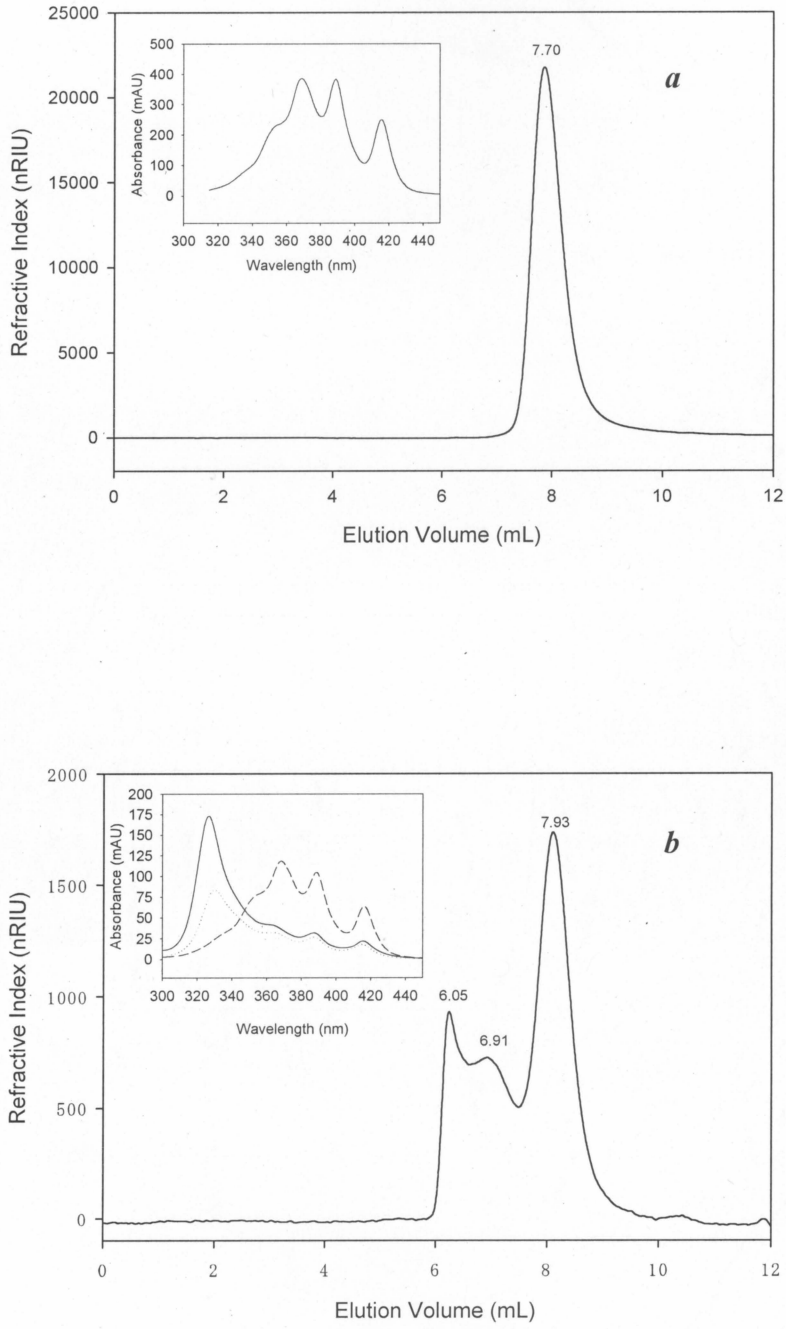


Figure 2.3 . SEC-HPLC of AmB in PEG-DSPE micelles[a]

[a] mole ratio of PEG-DSPE to AmB was ***a***. 4.0 ***b***. 0.5. Absorption spectra of eluting AmB were obtained by a photo diode array detector (inset).

such as sodium deoxycholate or lauryl sucrose to AmB and obtained reduced self-aggregation (7). Tassett et al. have added excess Myrj 59, a PEG derivative of stearic acid, to AmB and have obtained a reduction in self-aggregation (8). In both cases, however, high levels of surfactant (mol ratio > 50) needed to deaggregate AmB are likely to be too toxic for parenteral use.

The side chains of PEG-b-poly(N-hexyl-L-aspartamide) could be adjusted to vary the properties of the resulting polymeric micelles, enhance drug incorporation and gain some measure of controlled release. In these studies, the length of the acyl side chain attached to PEG-b-poly(N-hexyl-L-aspartamide) was found to govern the extent of interaction, incorporation, and release of AmB (5). In particular, the stearic acid ester of PEG-*b*-p(N-hexyl-L-aspartamide) was the most efficient in deaggregating AmB.

2.7.3 In vitro toxicity and efficacy studies

Membrane disruptions in mammalian cells may be assessed using red blood cells (RBCs), measuring hemolysis. AmB in PEG-DSPE micelles caused low degree of hemolysis (< 10 %) up to 50 μM, regardless of the aggregation state of AmB (Figure 2.4). In contrast, free AmB induced hemolysis beyond its critical aggregation concentration, ca. 1 μM, and reaching 90 % at about 10 μM. The reason for low levels of hemolysis with self-aggregated AmB (at PEG-DSPE: AmB = 0.5) is not entirely clear. It appears that there was very little release of AmB over 30 min pointing to the stable incorporation in these polymeric micelles, even in an aggregated state. It is interesting to note that while Pluronic F127 and L92 could

successfully solubilize AmB, these micelles were unable to protect RBC from hemolysis (9). AmB encapsulated in micelles formed from PEG-*b*-p(N-hexyl-L-aspartamide) acyl esters exerted reduced hemolytic activity compared with free AmB. The extent of hemolysis was found to depend on the length of acyl chain attached and the substitution level (5, 10).

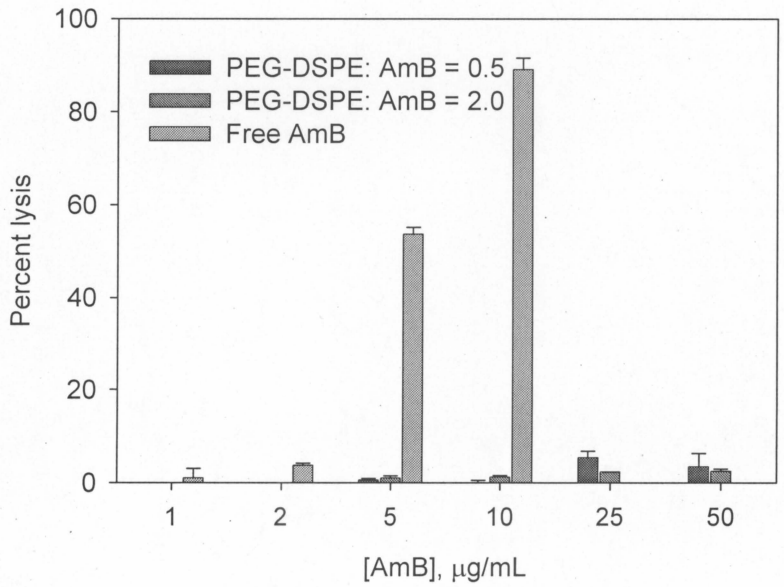


Figure 2.4. Hemolytic activity[a,b] AmB against murine erythrocytes[c]
[a] pH 7.4 [b] incubation for 30 min [c] n=3

Dose-limiting AmB nephrotoxicity has been partly attributed to the membrane-level damage caused by the polyene to the kidney epithelium (11-13). We have assessed AmB mediated toxicity in HK-2 cells, which are epithelial cells derived from the proximal tubule in a normal human kidney (14). On exposure to low levels of free AmB, there was a concentration-dependant decrease in the fraction of viable cells, indicating extensive damage to these cells (Figure 2.5). Remarkably,

micelle encapsulated AmB caused no cytotoxicity even at 1000 μg/mL. These results clearly illustrate the ability of PEG-DSPE micelles to prevent toxicity of AmB, in an *in vitro* setting.

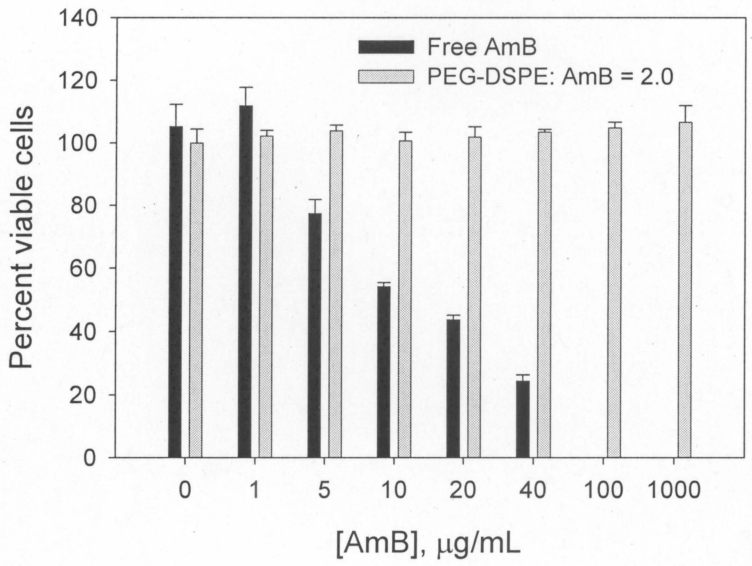


Figure 2.5. HK-2 cell-viability on exposure [a,b] to AmB[c]
[a] pH 5.8 [b] incubation for 90 min [c] n=3

Despite the dramatic reduction in toxicity, AmB in PEG-DSPE micelles completely inhibited fungal growth at concentrations ranging from 0.03 – 0.06 μg/mL. The MIC for D-AmB was 0.25 μg/mL; consistent with earlier results in the literature. PEG-DSPE did not possess intrinsic antifungal activity (MIC > 10 μg/mL). Espuelas et al. have shown a similar potentiation of AmB activity on incorporation into mixed micelles formed from poly(ε-caprolactone) and polaxamer 188. In this form, AmB exerted diminished toxicity against LLC-PK1 cultures while inhibiting

Candida albicans growth at 0.02 – 0.16 μg/mL AmB (15). We speculate that the increased potency of AmB on incorporation in PEG-DSPE micelles reflects the release of monomeric AmB, as opposed to aggregated species of drug, which would reduce the number of AmB entities in solution available for activity.

	C. albicans strain		
	K-1	98-17	98-234
Deoxycholate AmB	0.25	0.25	0.25
AmB: PEG-DSPE = 0.5	0.03	0.03	0.06
AmB: PEG-DSPE = 2.0	0.03	0.06	0.06

Table 2.2. Minimum Inhibitory Concentration (MIC) in mg/L of AmB against *Candida albicans*

2.8 Conclusions

In summary, we have incorporated AmB in PEG-DSPE micelles by a procedure based on solvent evaporation. High levels of AmB were solubilized in water, which would allow adequate doses for testing in rodent models. The extent of AmB self-aggregation, determined using absorbance spectroscopy depended on the ratio of polymer to AmB. Size exclusion chromatography revealed that at a high level of drug loading, the capacity of PEG-DSPE micelles to solubilize AmB is exceeded. Interestingly, PEG-DSPE protected against AmB induced hemolysis, regardless of aggregation state. Micelle encapsulated AmB exerted minimal toxicity to HK-2 cells relative to free drug while retaining potent activity against the fungal isolates tested. Low MIC values and diminished toxicity point to the stable incorporation of AmB, *in vitro*, and release of monomeric AmB from PEG-DSPE micelles.

2.9 References

1. Torchilin, V., Structure and design of polymeric surfactant-based drug delivery systems. J. Controlled Release, 2001. **73**(2-3): p. 137-72.

2. Kwon, G., Polymeric micelles for delivery of poorly water-soluble compounds. Crit. Rev. Ther. Drug Carrier Syst., 2003. **20**(5): p. 357-403.

3. Pfaller, M., Reference method for broth dilution antifungal susceptibility testing of yeasts : approved standard. 2002 ed. NCCLS, M27-A2. Vol. 22 no. 15. 2002, Wayne, Pa.: National Committee for Clinical Laboratory Standards.

4. Brajtburg, J., Bolard, J., Carrier effects on biological activity of amphotericin B. Clin. Microbiol. Rev., 1996. **9**(4): p. 512-31.

5. Adams, M., Kwon, G., Relative aggregation state and hemolytic activity of amphotericin B encapsulated by poly(ethylene oxide)-block-poly(N-hexyl-L-aspartamide)-acyl conjugate micelles: effects of acyl chain length. J. Controlled Release, 2003. **87**(1-3): p. 23-32.

6. Croy, S., Kwon, G., The effects of Pluronic block copolymers on the aggregation state of nystatin. J. Controlled Release, 2004. **95**(2): p. 161-71.

7. Barwicz, J., Christian, S., Gruda, I., Effects of the aggregation state of amphotericin B on its toxicity to mice. Antimicrob. Agents Chemother., 1992. **36**(10): p. 2310-2315.

8. Tasset, C., Preat, V., Roland, M., The influence of Myrj 59 on the solubility, toxicity and activity of amphotericin B. J. Pharm. Pharmacol., 1991. **43**(5): p. 297-302.

9. Forster, D., Washington, C., Davis, S., Toxicity of solubilized and colloidal amphotericin B formulations to human erythrocytes. J. Pharm. Pharmacol., 1988. **40**(5): p. 325-8.

10. Lavasanifar, A., Samuel, J., Sattari, S., Kwon, G., Block copolymer micelles for the encapsulation and delivery of amphotericin B. Pharm. Res., 2002. **19**(4): p. 418-22.

11. Yano, Y., Monteiro, J., Seguro, A., Effect of amphotericin B on water and urea transport in the inner medullary collecting duct. J. Am. Soc. Nephrol., 1994. **5**(1): p. 68-74.

12. Walev, I., Bhakdi, S., Possible reason for preferential damage to renal tubular epithelial cells evoked by amphotericin B. Antimicrob. Agents Chemother., 1996. **40**(5): p. 1116-20.

13. Sawaya, B., Briggs, J., Schnermann, J., Amphotericin B nephrotoxicity: the adverse consequences of altered membrane properties. J. Am. Soc. Nephrol., 1995. **6**(2): p. 154-64.

14. Ryan, M., Johnson, G., Kirk, J., Fuerstenberg, S., Zager, R., Torok-Storb, B., HK-2: an immortalized proximal tubule epithelial cell line from normal adult human kidney. Kidney Int., 1994. **45**(1): p. 48-57.

15. Espuelas, M., Legrand, P., Campanero, M., Appel, M., Cheron, M., Gamazo, C., Barratt, G., Irache, J.,, Polymeric carriers for amphotericin B: In vitro activity, toxicity and therapeutic efficacy against systemic candidiasis in neutropenic mice. J. Antimicrob. Chemother., 2003. **52**(3): p. 419-27.

Chapter 3:

Structuring effect of cholesterol on PEG-phospholipid micelles: Amphotericin B solubilization and *in vitro* release studies

---

A version of this chapter will be submitted for publication in *Journal of Controlled Release* in December 2006.

3.1 Introduction

We have recently described our efforts to study PEG-DSPE micelles for the delivery of AmB (1). PEG-DSPE micelles could incorporate and deaggregate AmB based on absorption spectroscopy. Also, PEG-DSPE encapsulated AmB exerted diminished hemolytic activity compared to free AmB, while retaining potent antifungal activity – suggesting that AmB is released from PEG-DSPE micelles in a monomeric form, which is selectively active against fungal cells (2-5). However, we found poor correlation between *in vivo* and *in vitro* toxicity results (data not shown). Gruda et al. could deaggregate AmB using excess lauryl sucrose; however they have reported a similar, marginal improvement in survival over AmB sodium-deoxycholate (6). Nystatin, a structurally related polyene antibiotic deaggregated in Pluronic F127 micelles exhibited reduced *in vitro* toxicity but led to in a minor increase in LD_{50} doses in mice (7, 8). It is noted that micelles formed from Pluronic F127, sodium deoxycholate and lauryl sucrose are expected to disassociate rapidly on dilution due to relatively high critical micellar concentrations (CMCs).

It has been recently shown that administration of sodium deoxycholate – AmB as a continuous infusion over 24 h had lower nephrotoxicity and infusion related side-effects compared to an equal dose administered as a standard 2 – 4 hour infusion (9-13). It has been proposed that the continuous infusion of sodium – deoxycholate AmB results in low serum levels of drug, primarily in its soluble "bioactive" form. Infusion of an equal dose of AmB over 2 – 4 h produces a similar level of "bioactive" drug – but results in a higher fraction of protein-bound drug capable of evoking host toxicity (14). Regardless of the mechanism, it is becoming increasingly clear that slow

delivery of AmB reduces toxic manifestations of this important antifungal drug. Hence, from the perspective of AmB delivery using polymeric micelles, we hypothesize that slow release of encapsulated drug is important for lower *in vivo* toxicity.

In this work, we have investigated AmB release in buffer and in serum albumin. PEG-DSPE micelles release AmB slowly in buffer, presumably in a monomeric form. However, serum albumin appears to have a destabilizing effect on these micelles, leading to rapid dissociation of encapsulated AmB. In this context, we have investigated the effect of cholesterol incorporation on the properties of PEG-DSPE micelles. Drug release studies using a dialysis setup indicate that in contrast with PEG-DSPE micelles, AmB release from PEG-DSPE micelles with co-incorporated cholesterol (PEG-DSPE|Cholesterol) is slow in serum albumin. Steady state fluorescence measurements and ^{1}H-NMR spectra point to decreased mobility in the core of PEG-DSPE|Cholesterol micelles. The absorbance spectrum of AmB in PEG-DSPE|Cholesterol micelles displays narrower peaks than in PEG-DSPE micelles – an effect perhaps related to increased rigidity in the micelle core. Results from AmB absorption kinetics in physiological concentrations of serum albumin are in agreement with drug release studies and point to stable incorporation of AmB in PEG-DSPE|Cholesterol micelles. Since albumin is the most abundant serum protein – we anticipate that *in vivo* release of AmB from PEG-DSPE|Cholesterol micelles will be slow, raising promise for lower *in vivo* toxicity.

3.2 Materials

AmB was obtained as a gift from Alpharma (Copenhagen, Denmark) and was stored at -20 °C until use. PEG-DSPE (M_n =5800 g/mol) was obtained from Avanti Polar Lipids (Alabaster, AL). Cholesterol and pyrene were obtained from Aldrich (Milwaukee, WI). 1,3-(1,1'-dipyrenyl) propane (P3P) was obtained as a gift from Dr. M. Yokoyama (Kanagawa Academy of Science and Technology, Japan).

3.3 Micelle preparation and incorporation of AmB

PEG-DSPE (6.0 mg/mL in chloroform), cholesterol (1 mg/mL in chloroform) and AmB (0.25 mg/mL in methanol) stock solutions in methanol were mixed in a round bottom flask. The organic solvent was evaporated under vacuum to produce a thin film of co-precipitated drug and polymer. This film was dissolved in 10 mM HEPES, pH 7.0 and incubated at 50 °C for 10 min to allow for complete equilibration. Unincorporated AmB was removed by filtration through a 0.45-μm polyethersulfone (PES) filter. Empty micelles were prepared using an identical procedure without drug. The concentration of AmB was quantified by diluting a 50 μL aliquot of AmB in 1.95 mL DMF and observing absorbance at 413.5 nm. This assay was tested for linearity in the 0.02 – 0.8 mg/mL range.

3.4 Micelle Characterization

3.4.1 Dynamic Light Scattering

Hydrodynamic diameters were determined using dynamic light scattering using the NICOMP ZLS380 particle sizer (Particle Sizing Systems, Santa Barbara,

CA). Data was acquired to have at least 100k counts in Channel 1. The light scattering data was interpreted using Gaussian and NICOMP analyses. NICOMP analysis permits deconvolution of light scattering data into multimodal distributions. Particle sizes were expressed as volume-weighted diameters.

3.4.2 Core microviscosity measurements using 1,3-(1,1'-dipyrenyl) propane

Microviscosity was estimated by measuring the ratio of the fluorescence intensities of the monomer and excimer i.e. I_M/I_E of P3P measured at 376 and 480 nm respectively (15, 16). Aqueous solutions containing 0.5 mg/mL polymer were aliquoted into tubes containing P3P. The samples were heated to 65 °C for 1 hour and allowed to equilibrate overnight at room temperature. The concentration of P3P in the aqueous solution was 0.2 μM. Samples were excited at 333 nm and fluorescent emission at room temperature was recorded from 350 to 600 nm, using a Fluoromax 3 fluorimeter (Horiba Jobin Yvon, Edison, NJ). The spectra were analyzed using the Datamax software (version 2.20, Horiba Jobin Yvon, Edison, NJ).

3.4.3 ^1H NMR spectroscopy

Samples for ^{1}H-NMR were prepared by dissolution of the co-precipitated film of PEG-DSPE and cholesterol in deuterium oxide (Aldrich, Milwaukee) and were allowed to equilibrate at 50 °C for 10 min. The samples contained 5 mg/mL PEG-DSPE. ^{1}H-NMR spectra were acquired at 25 °C on a 400 MHz Varian spectrometer using the using the standard two pulse sequence (17). Peak line-widths ($\Delta\nu_{1/2}$) were determined using the Varian software (version 6.1 revision C, Palo Alto, CA).

3.4.4 AmB release from PEG-DSPE micelles using equilibrium dialysis

Samples containing 30 μg/mL AmB in dialysis cassettes (MWCO = 7000, Pierce) were placed in a bath buffered to pH 7.0, using 5 mM HEPES. The MWCO of the dialysis membrane was chosen to allow for diffusion of monomeric AmB (molecular weight 924.1) while preventing diffusion of large molecules such as bovine serum albumin (molecular weight 66 kDa) or intact micelles (molecular weight > 100 kDa). Near-sink conditions for AmB were maintained by performing the release experiment in 100-fold excess dialysis buffer. Since AmB is susceptible to oxidation by molecular oxygen, the dialysis buffer was degassed overnight and 20 μg/mL propyl gallate was added as an antioxidant (18, 19). At predetermined time intervals, 100 μL samples were taken and AmB concentration in dialysis cassettes was determined using reversed-phase HPLC. Protein from samples containing serum albumin was first precipitated by addition of 400 μL cold methanol. After centrifugation at 13,200 RPM (16.1 x 10^3 *g*) for 10 min, the supernatant was extracted and analyzed for AmB content, using reversed-phase HPLC.

For quantification of AmB content, 15 μL samples were injected into a 4.6 mm x 150 mm Eclipse XDB-C8 column (Agilent Technologies, Palo Alto, CA) and AmB absorbance observed at 412 nm. The flow rate of the eluent consisting of a methanol – (5 % v/v acetic acid) mixture was maintained at 2 mL/min. The eluent composition was maintained at 5 % methanol for 2 min, then linearly varied from 5 % to 90 % methanol content over 2 min using a program. The assay was tested for linearity in the 0.1 – 100 μg/mL range.

AmB release was fit to a first-order process of the form $A_t/A_0 = a.e^{-k.t}$, where A_0 and A_t correspond to the initial AmB concentration in the dialysis cassette at and time t. The rate constant k, was determined using non-linear regression. The half-life for AmB release was calculated using, $t_{1/2} = 0.693/k$.

3.4.5 Electronic absorption kinetics

Stock solutions containing micelle encapsulated AmB (0.4 mg/mL) were added to 4 % bovine serum albumin (BSA), buffered to pH 7.0 with 10 mM HEPES. For association kinetics for free drug, AmB dissolved in DMSO was similarly added to BSA (final DMSO < 0.2 %). The final AmB concentration was 10 μg/mL. Absorbance spectra were recorded from 300 to 450 nm at room temperature using the Cary 50 spectrophotometer (Varian, Palo Alto, CA). Sequential spectra were acquired at 15 s intervals for the first 5 min; and at 1 minute intervals for an additional 40 minutes. A scan for baseline absorbance was taken before addition of AmB and was subtracted from each spectrum. We have used a method similar to Witzke et al.(18) to estimate apparent rate parameters for interaction of free and micelle encapsulated AmB with serum albumin. The change in absorbance at 412 nm, $\Delta A_t = A_\infty - A_t$ was fit to a first-order process of the form $A_\infty - A_t = a.e^{-k.t}$ and parameters a, k and A_∞ were estimated using non-linear regression. The half-life was calculated using , $t_{1/2} = 0.693/k$.

3.5 Results and Discussion

3.5.1 Micelle preparation and characterization

PEG-DSPE and PEG-DSPE|Cholesterol micelles were prepared using a simple solvent evaporation method. PEG-DSPE micelles with a narrow size distribution could be obtained by dissolving the film of co-precipitated drug and polymer at 25 °C, as described earlier (1). Samples incorporating cholesterol had a broad particle size distribution when prepared in a similar manner, resulting in turbid solutions with variable mean particle sizes. PEG-DSPE|Cholesterol micelles with a narrow particle distribution were obtained when the polymer film was dissolved at 50 °C, allowing 10 min for equilibration, presumably due to greater mobility of lipid chains at this elevated temperature.

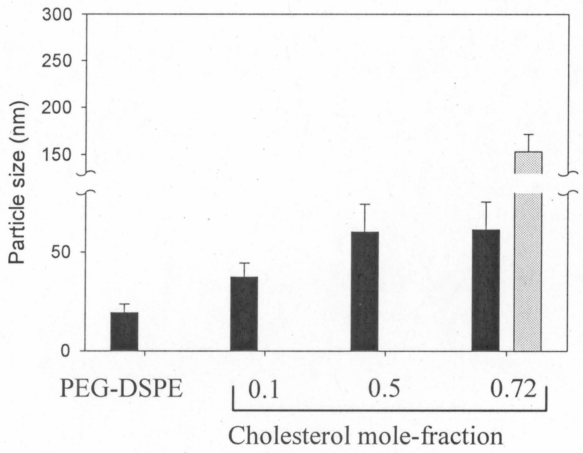


Figure 3.1. Effect of cholesterol content on size of PEG-DSPE|Cholesterol micelles
[a]cholesterol: PEG-DSPE ratio (mol:mol) [b]volume-weighted NICOMP average

Mean diameter for empty PEG-DSPE micelles was ca. 16 nm for empty PEG-DSPE micelles, determined using dynamic light scattering. The hydrodynamic

diameter of PEG-DSPE|Cholesterol micelles increased in a composition dependent manner and reached ca. 60 nm with a cholesterol mole-fraction of 0.5 (Figure 3.1). For higher fractions of cholesterol incorporation, dynamic light scattering reported two populations – corresponding to PEG-DSPE micelles incorporating cholesterol (ca. 60 nm) and aggregates with sizes >150 nm.

Restricted mobility in the core of polymeric micelles results in broadened line-widths in a ^{1}H-NMR spectrum (17, 20). Figure 3.2 shows the ^{1}H-NMR spectrum of PEG-DSPE micelles in D_2O. Peaks at 1.26 and 0.88 ppm were attributed to protons from diacyl chains of PEG-DSPE. These peaks were relatively sharp ($\Delta\nu_{1/2}$ ~ 8.9 Hz, 13.7 Hz) – indicative of high mobility in the core of PEG-DSPE micelles. These results were consistent with electron spin resonance studies reported by Belsito et al. with 1,2-Dipalmitoyl-*sn*-glycero-3-phosphoethanolamine-N-methoxy(poly-ethylene glycol) (DPPE-PEG) micelles (21). Belsito et al. have attributed increased segmental mobility in PEG-lipid micelles than comparable lipid bilayers to decreased lipid packing induced by the bulky poly(ethylene glycol) head group (21-23). The incorporation of cholesterol in PEG-DSPE micelles resulted in a broadening of ^{1}H-NMR signals at 1.26 ppm and 0.88 ppm respectively ($\Delta\nu_{1/2}$ ~ 55.3, 31.9 Hz), pointing to hindered motion in the micelle core.

Intramolecular excimer formation of the lipophilic fluorescent probe P3P depends on flexibility of the propylene chain between the pyrene moieties in the molecule. Since such conformational changes are restricted in environments of high viscosity, the I_M/I_E ratio is useful in determining the fluidity of the microenvironment sensed by these probes (15, 24). The I_M/I_E ratio increased with increasing cholesterol

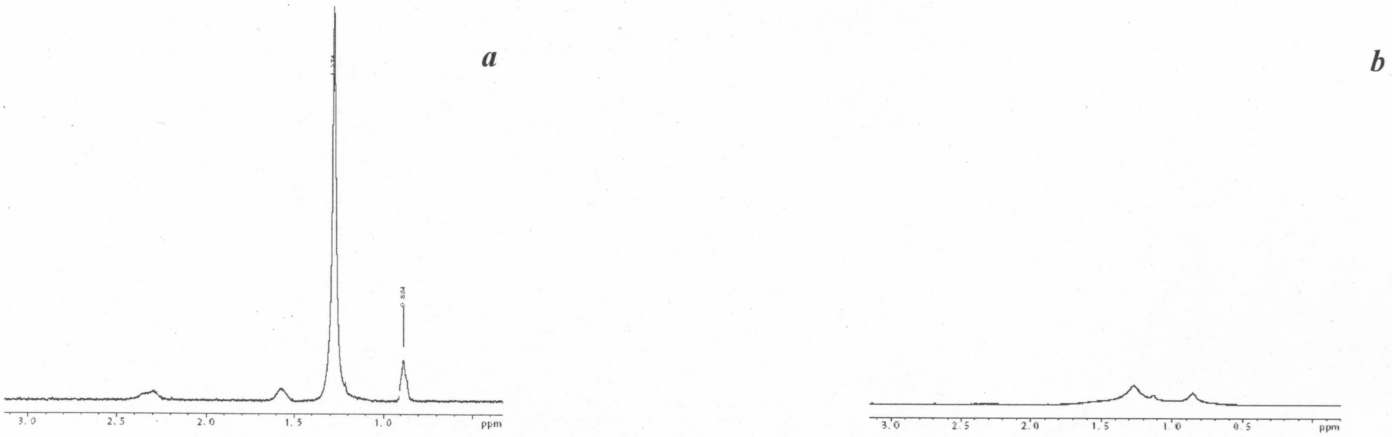


Figure 3.2 ^{1}H NMR spectra for ***a.*** PEG-DSPE micelles ***b.*** PEG-DSPE|Cholesterol micelles (PEG-DSPE: cholesterol = 1:1) at 25 °C

content from 6.2 ± 0.13 in PEG-DSPE micelles to 6.8 ± 0.17 ($p<0.05$) at 50 % cholesterol incorporation (Figure 3.3). The I_M/I_E ratio for P3P fluorescence in PEG-DSPE and PEG-DSPE|Cholesterol micelles was intermediate between the sodium dodecyl sulfate micelles ($I_M/ I_E \sim 2$) with a liquid-like core and that of PEG-b-poly(ε-caprolactone) micelles which have rigid, presumably partially crystalline core ($I_M/ I_E \sim 22$).

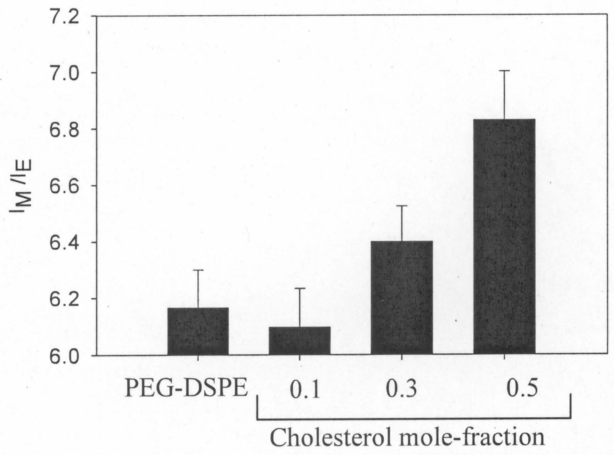


Figure 3.3. I_M/ I_E ratios for P3P fluorescence emission[a] in PEG-DSPE|Cholesterol micelles
[a]λ_{ex} = 333 nm [b] n=3

FTIR studies with DPPC vesicles incorporating cholesterol by Davies et al. indicated that cholesterol is intercalated in the bilayer and the rigid sterol head interacts with diacyl chains closer to the phospholipid head group. Cholesterol incorporation in DPPC vesicles resulted in restricted trans-gauche isomerization in diacyl chains via hydrophobic interaction (25). The ordering of diacyl chains by cholesterol is not uniform through the DPPC bilayer; diacyl chains retain greater mobility away from the phospholipid head group (towards the centre of the bilayer) due to interaction with the cholesterol side-chain with higher flexibility. Molecular

dynamics simulations performed by Hofsas et al. are consistent with observations in FTIR studies and further demonstrate that the average area per phospholipid molecule in the DPPC bilayer is significantly decreased on account of interaction with cholesterol (26).

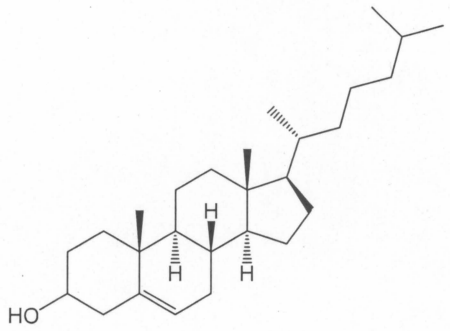


Figure 3.4 Chemical structure of cholesterol

The structuring effects of cholesterol in phospholipid vesicles has been reviewed in detail by Ohvo-Rekila et al. (27) and McConnell et al. (28). We have extended these observations for interpretation of ^{1}H-NMR and P3P fluorescence results in PEG-DSPE|Cholesterol micelles. Broadened line-widths in ^{1}H-NMR spectra of PEG-DSPE|Cholesterol micelles were consistent with decreased mobility in diacyl lipid chains on cholesterol incorporation, possibly via a hydrophobic interaction similar to that observed in DPPC vesicles. Further, the peak in the ^{1}H-NMR spectrum corresponding terminal CH_3- protons (0.88 ppm) was narrower compared to methylene protons (1.26 ppm) from the diacyl chains. This result reflects higher mobility in diacyl chains away from the phospholipid head-group, presumably

due to interaction with the cholesterol side-chain with greater flexibility. We expect the P3P probe to be localized in the interior core of the PEG-DSPE|Cholesterol micelle due to its extreme hydrophobic nature. The modest increase in the I_M/I_E ratio is consistent with higher mobility toward the interior of PEG-DSPE|Cholesterol micelles, determined from ^{1}H-NMR.

High levels of AmB could be incorporated in PEG-DSPE micelles using a solvent evaporation method (Table 3.1). The yield of AmB increased moderately from 78% in PEG-DSPE micelles to 84% in PEG-DSPE|Cholesterol micelles. The particle size of PEG-DSPE|Cholesterol micelles was dependant on the level of cholesterol incorporation and reached ca. 60 nm at 50% cholesterol (mol:mol). The small size of these polyethylene-glycol based micelles raises potential for escape from rapid macrophage uptake and prolonged circulation times (20).

Molar ratio AmB: PEG-DSPE: Cholesterol[a]	Fraction of initial AmB encapsulated	AmB loading % w/w	[AmB], mg/mL[b]	Hydrodynamic Diameter (nm)
1: 0.5	0.78	24.2	0.39 ± 0.02	21.8 ± 6.1[c]
1: 2	0.78	7.21	0.38 ± 0.12	19.3 ± 4.4[c]
1: 2: 0.25	0.82	7.53	0.41 ± 0.09	39.3 ± 4.7[d]
1: 2: 0.5	0.88	7.93	0.44 ± 0.12	64.6 ± 9.2[d]
1: 2: 2	0.84	7.27	0.42 ± 0.02	64.0 ± 9.6[d]

Table 3.1 Solubilization of AmB by PEG-DSPE and PEG-DSPE|Cholesterol micelles
[a]initial ratios [b] n=3 [c]volume-weighted Gaussian average [d]volume-weighted NICOMP average

The absorbance spectra for AmB (10 μg/mL) encapsulated in PEG-DSPE micelles in 10 mM HEPES buffer was sensitive to initial AmB: PEG-DSPE ratio. At low levels of AmB incorporation (AmB: PEG-DSPE = 1:2) three prominent bands were observed at 368, 388 and 417 nm (Figure 3.5). At higher levels of AmB incorporation (AmB: PEG-DSPE = 1: 0.5) the band at 328 nm was prominent relative to higher wavelengths, indicative of AmB self-association. Incorporation of cholesterol into PEG-DSPE micelles (AmB: PEG-DSPE: Cholesterol = 1:2:2) led to narrowing of AmB absorption bands, while retaining low peak I/IV ratio – characteristic of diminished AmB self-aggregation.

The width-at-half-height for peak IV in the AmB absorbance spectrum was estimated by fitting to a Gaussian curve, $A = A_0 + A_{max}.\exp\left(\frac{-(\lambda - \lambda_{max})^2}{2w^2}\right)$ where A_0 and A_{max} are baseline and peak absorbance values, λ_{max} is wavelength corresponding to peak IV maximum and w is the width-at-half-height in nm.

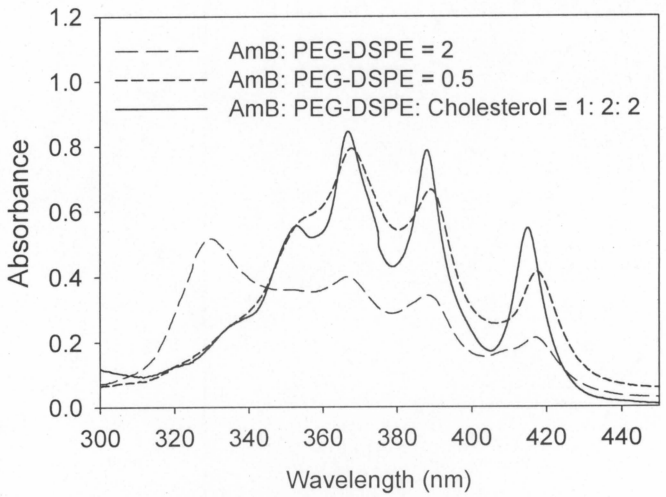
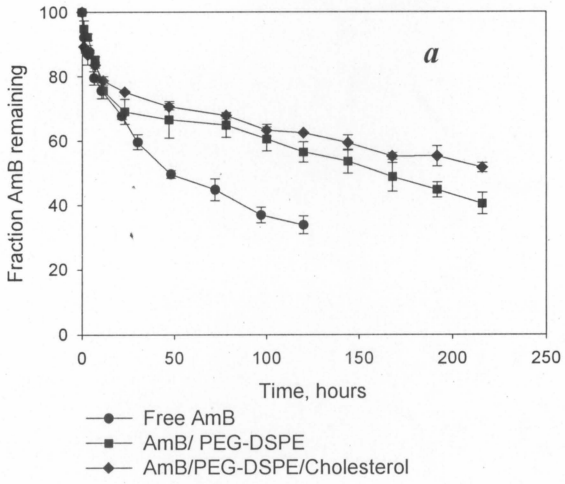


Figure 3.5. Absorption spectra of AmB solubilized by PEG-DSPE and PEG-DSPE|Cholesterol micelles

The λ_{max} was shifted from 417.2 ± 0.04 nm in PEG-DSPE micelles to 415.1 ± 0.03 nm on cholesterol incorporation. Also, *w* decreased from 6.34 ± 0.04 nm in PEG-DSPE micelles to 4.66 ± 0.04 nm in PEG-DSPE|Cholesterol. The absorption spectrum of AmB - cholesterol mixtures in propanol-water mixtures (Charbonneau et al. (29), Barwicz et al. (30)) presented features similar to that in PEG-DSPE|Cholesterol micelles. Barwicz et al. have reported that the *w* for AmB absorbance in 10 % n-propanol/ water decreased from 16.0 nm for AmB to 8.7 nm for a 5:1 ratio of cholesterol: AmB (30). Bolard et al. have suggested that a direct binding between cholesterol and AmB in lipid vesicles is extremely weak (3). Castanho et al. have shown using fluorescence decay measurements that the chromophore in a structurally related polyene, nystatin was sensitive to rigidity in DPPC vesicles induced by cholesterol (31). We attribute changes in AmB absorbance spectrum in PEG-DSPE|Cholesterol micelles to an altered packing on account of higher rigidity in these micelles.

3.5.2 AmB release from PEG-DSPE micelles using equilibrium dialysis

AmB release from PEG-DSPE micelles was studied using a dialysis setup as described in the literature (32, 33). AmB release profiles are shown in Figure 3.6 and corresponding rate parameters are in Table 3.2. AmB release from PEG-DSPE and PEG-DSPE|Cholesterol micelles was slow ($t_{1/2}$ = 184, 259 h) in HEPES. In contrast, AmB is almost completely dissociated from D-AmB reflecting weak AmB – carrier interaction (4). Free AmB is highly self-associated at 30 μg/mL i.e. above its critical aggregation concentration (CAC) in water ca. 1 μM. The CAC of AmB in 4 % BSA



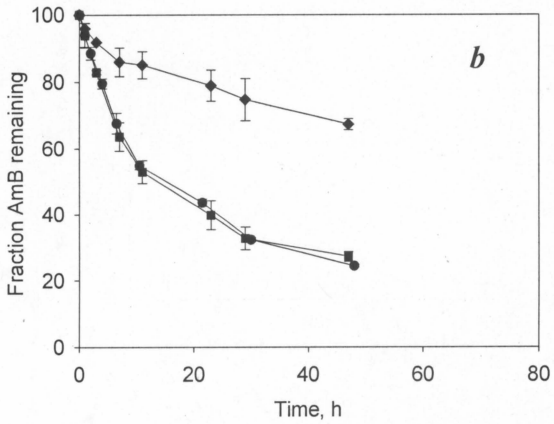


Figure 3.6 AmB release profiles at 25 °C ***a.*** in 5 mM HEPES ***b.*** 4 % BSA

	5 mM HEPES			4 % BSA		
	100.k (h^{-1})	$t_{1/2}$ (h)	R^2	100.k (h^{-1})	$t_{1/2}$ (h)	R^2
Free AmB	1.01 ± 0.10	68.5	0.94	3.72 ± 0.04	18.6	0.96
AmB: PEG-DSPE 1:2	0.38 ± 0.04	183.9	0.90	3.75 ± 0.52	18.4	0.94
AmB: PEG-DSPE: Cholesterol 1:2:2	0.27 ± 0.03	259.2	0.89	8.08 ± 0.08	85.8	0.94

Table 3.2. Fit parameters for AmB release from PEG-DSPE micelles at 25 °C

is ca. 10 μM (34). The release of free AmB in HEPES ($t_{1/2}$ = 69 h) was slower compared to 4 % BSA ($t_{1/2}$ = 18.6 h) presumably limited by the equilibrium between monomeric and self-aggregated AmB. AmB release from PEG-DSPE micelles in BSA was identical to that for free AmB ($t_{1/2}$ = 18.4 h). AmB release from PEG-DSPE|Cholesterol micelles in 4 % BSA was significantly slower compared to PEG-DSPE micelles ($t_{1/2}$ = 85.4 h).

Our results were consistent with reports describing AmB incorporation in lipid vesicles containing cholesterol. Bolard et al. and Hsu Chen et al. have proposed that the incorporation of polyene antibiotics is favored in ordered lipid bilayers such as those containing cholesterol (3, 35). Witzke et al. have estimated using absorption kinetics that the association of AmB in egg-PC vesicles with cholesterol was 35 times stronger compared to vesicles without sterol (18). Slow release of deaggregated AmB from PEG-DSPE|Cholesterol micelles is a significant result, since this raises the prospect of lowering *in vivo* toxicity if our hypothesis concerning slow AmB release from polymeric micelles is valid.

3.5.3 Electronic absorption kinetics in serum albumin

The electronic absorption spectrum of AmB is uniquely sensitive to the environment of the molecule. The absorbance at peak IV increases on AmB dissociation from vesicles or micelles and association with serum albumin. Sequential absorbance spectra were taken upon addition of free or micelle encapsulated AmB in 4 % BSA. Increase in absorbance intensity at 412 nm was used to evaluate drug dissociation from PEG-DSPE micelles and quantify apparent rate constants. Figures

3.7a-c show representative AmB absorbance spectra over time. Figures 3.7d-f show the corresponding changes in the absorbance at 412 nm. Kinetic rate parameters obtained by fitting absorbance values in figures 3.7d-f to a first-order process are shown in Table 3.3.

Free AmB led to the formation of an initial broad band at ca. 350 nm, which is attributed to self-aggregated AmB, when added to 4 % BSA (Figure 3.7a). The intensity of this band diminished over time, with increasing intensity at higher wavelengths – consistent with drug deaggregation in 4 % BSA (34). We have estimated half-life for this association as 2.1 min.

Peak IV absorbance of AmB encapsulated in PEG-DSPE micelles increased over 45 min upon dilution in 4 % BSA and absorbance maxima for peaks III and IV were minimally shifted (~ 2 nm) (Figure 3.7b). The dissociation half-life, assuming first-order kinetics was estimated as 10.5 min. This result was consistent with rapid AmB release from PEG-DSPE micelles in the presence of 4 % BSA observed in dialysis studies. In contrast, there were minimal changes in the absorbance spectrum of AmB in PEG-DSPE|Cholesterol micelles in serum albumin (Figure 3.7c), indicating that AmB incorporated in PEG-DSPE|Cholesterol micelles was not free to interact with serum albumin. The slow release of AmB from these micelles occurs presumably through a simple diffusion process.

3.5.4 In vitro toxicity and efficacy studies

HK-2 cell-viability and susceptibility of fungal isolates on exposure to AmB was determined as described in chapter 2. The *in vitro* toxicity results were similar to

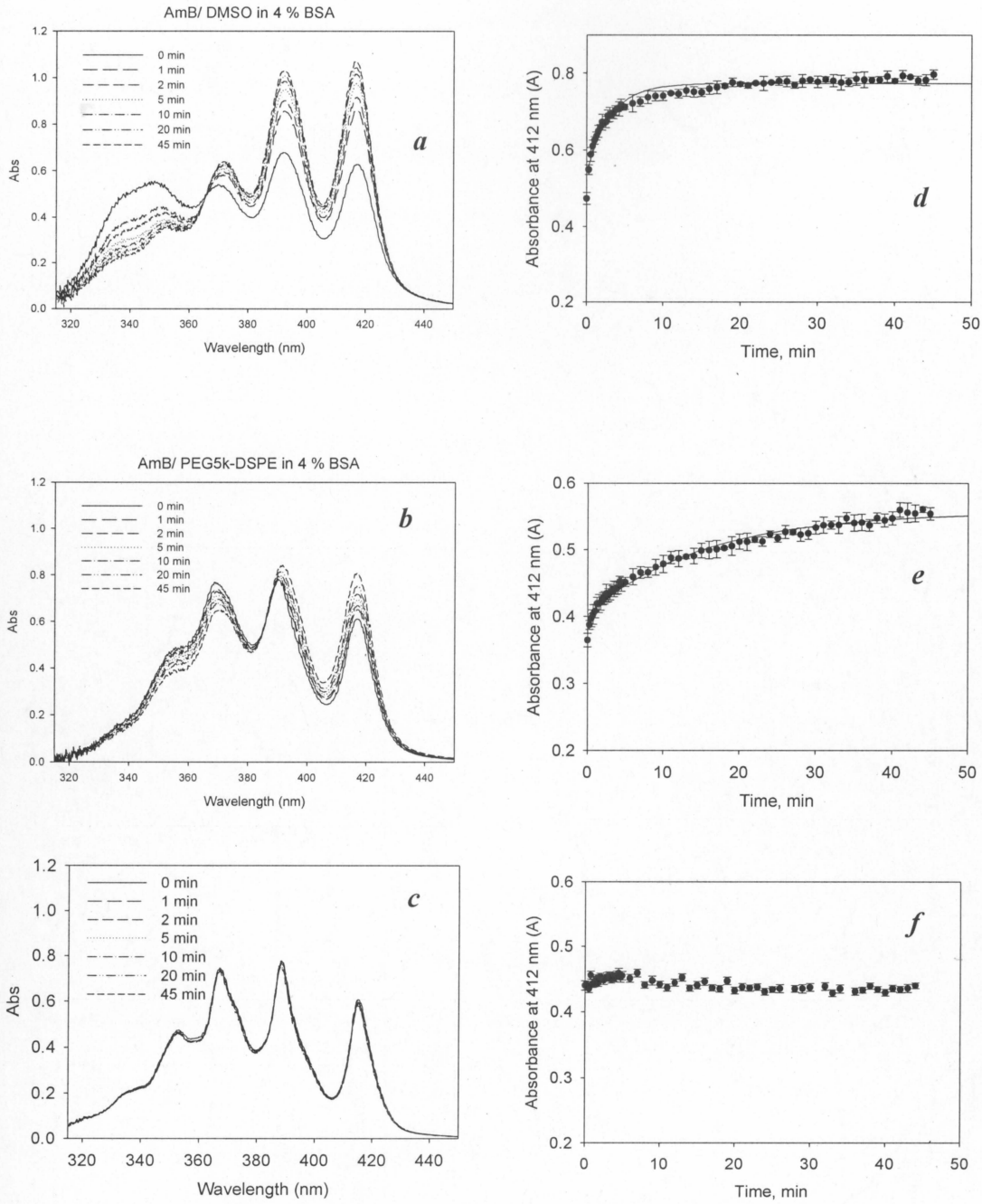


Figure 3.7. Absorbance spectra of micelle encapsulated AmB in 4 % BSA[a].
a. Unencapsulated AmB (in DMSO) ***b.*** AmB in PEG-DSPE micelles (AmB: PEG-DSPE = 1: 2) ***c.*** AmB in PEG-DSPE|Cholesterol micelles (AmB: PEG-DSPE: Cholesterol = 1: 2: 2) ***d-f.*** Absorbance at 412 nm for as a function of incubation time corresponding to figures a-c.
[a] AmB concentration was 10 μg/mL

that for AmB in PEG-DSPE micelles. There was no loss in cell-viability on exposure to 1000 μg/mL AmB encapsulated in PEG-DSPE|Cholesterol micelles. Cholesterol co-incorporation in PEG-DSPE micelles did not decrease AmB efficacy *in vitro*. The MIC values for AmB encapsulated in PEG-DSPE|Cholesterol micelles ranged from 0.03 – 0.06 μg/mL for *Candida albicans* K-1, 98-17 and 98-234.

	100 k (min^{-1})	$t_{1/2-1}$ (min)	R^2	A_∞
Unencapsulated AmB	3.25 ± 0.23	2.1	0.94	0.77
AmB: PEG-DSPE 1:2	6.63 ± 0.53	10.46	0.98	0.56
AmB: PEG-DSPE: Cholesterol 1:2:2	-	-	-	0.42

Table 3.3 Fit parameters for absorbance change for PEG-DSPE incorporated AmB at 412 nm upon dilution in 4 % BSA (figures 3.7d-f)

3.6 Conclusions

PEG-DSPE|Cholesterol micelles prepared using the solvent evaporation method could solubilize high levels of deaggregated AmB. Cholesterol incorporation increased rigidity in the PEG-DSPE micelle core, possibly due to a structuring effect induced by hydrophobic interactions. The narrowed absorption bands in the AmB absorption spectrum indicate modified packing into PEG-DSPE|Cholesterol micelles. While AmB in PEG-DSPE was free to interact with serum albumin, the drug was stably incorporated in cholesterol containing PEG-DSPE micelles apparent from the association kinetics and dialysis experiments. These results were consistent with greater interaction of the polyene with such structured lipids proposed by other researchers.

3.7 References

1. Vakil, R., Kwon, G., PEG-phospholipid micelles for the delivery of amphotericin B. J. Controlled Release, 2005. **101**(1-3): p. 386-9.

2. Barwicz, J., Tancrede, P., The effect of aggregation state of amphotericin B on its interactions with cholesterol- or ergosterol-containing phosphatidylcholine monolayers. Chem. Phys. Lipids, 1997. **85**(2): p. 145-55.

3. Bolard, J., Legrand, P., Heitz, F., Cybulska, B., One-sided action of amphotericin B on cholesterol-containing membranes is determined by its self-association in the medium. Biochemistry, 1991. **30**(23): p. 5707-15.

4. Brajtburg, J., Bolard, J., Carrier effects on biological activity of amphotericin B. Clin. Microbiol. Rev., 1996. **9**(4): p. 512-31.

5. Gruda, I., Dussault, N., Effect of the aggregation state of amphotericin B on its interaction with ergosterol. Biochem. Cell Biol., 1988. **66**(3): p. 177-83.

6. Barwicz, J., Christian, S., Gruda, I., Effects of the aggregation state of amphotericin B on its toxicity to mice. Antimicrob. Agents Chemother., 1992. **36**(10): p. 2310-2315.

7. Croy, S., Kwon, G., The effects of Pluronic block copolymers on the aggregation state of nystatin. J. Controlled Release, 2004. **95**(2): p. 161-71.

8. Croy, S., Effects of nonionic surfactants on nystatin aggregation state and toxicity, in Pharmaceutical Sciences. 2005, University of Wisconsin - Madison.

9. Imhof, A., Walter, R.B., Schaffner, A., Continuous infusion of escalated doses of amphotericin b deoxycholate: an open-label observational study. Clin. Infect. Dis., 2003. **36**: p. 943-951.

10. Eriksson, U., Seifer, B., Schaffner, A., Comparison of effects of amphotericin b deoxycholate infused over 4 to 24 hours: Randomized controlled trial. Br. Med. J., 2001. **322**: p. 579-582.

11. Peleg, A., Woods, M., Continuous and 4 h infusion of amphotericin B: a comparative study involving high-risk haematology patients. J. Antimicrob. Chemother., 2004. **54**(4): p. 803-8.

12. Hiemenz, J., Amphotericin B deoxycholate administered by continuous infusion: does the dosage make a difference? Clin. Infect. Dis., 2003. **36**(8): p. 952-3.

13. Schulenburg, A., Sperr, W., Rabitsch, W., Knobl, P., Thalhammer, F., Brief report: Practicability and safety of amphotericin b deoxycholate as continuous infusion in neutropenic patients with hematological malignancies. Leukemia & Lymphoma, 2005. **46**: p. 1163-1167.

14. Lewis, R., Wiederhold, N., The solubility ceiling: a rationale for continuous infusion of amphotericin b therapy? Clin. Infect. Dis., 2003. **37**: p. 871-872.

15. Lavasanifar, A., Samuel, J., Kwon, G., The effect of alkyl core structure on micellar properties of poly(ethylene oxide)-block-poly(L-aspartamide) derivatives. Colloids Surf. B, 2001. **22**(2): p. 115-126.

16. Winnik, F., Photophysics of preassociated pyrenes in aqueous polymer solutions and in other organized media. Chem. Rev., 1993. **93**(2): p. 587 - 614.

17. Claridge, T., High-Resolution NMR Techniques in Organic Chemistry. 1999: Pergamon.

18. Witzke, N., Bittman, R., Dissociation kinetics and equilibrium binding properties of polyene antibiotic complexes with phosphatidylcholine/sterol vesicles. Biochemistry, 1984. **23**(8): p. 1668-74.

19. Beggs, W., Antioxidant-stabilized amphotericin B. Diagn. Microbiol. Infect. Dis., 1983. **1**(4): p. 339-341.

20. Kwon, G., Kataoka, K., Block copolymer micelles as long-circulating drug vehicles. Adv. Drug Del. Rev., 1995. **16**(2-3): p. 295-309.

21. Montesano, G., Bartucci, R., Belsito, S., Marsh, D., Sportelli, L., Lipid membrane expansion and micelle formation by polymer-grafted lipids: scaling with polymer length studied by spin-label electron spin resonance. Biophys. J., 2001. **80**(3): p. 1372-83.

22. Hristova, K., Needham, D., Phase behavior of a lipid/polymer-lipid mixture in aqueous medium. Macromolecules, 1995. **28**: p. 991-1002.

23. Belsito, S., Bartucci, R., Montesano, G., Marsh, D., Sportelli, L., Molecular and mesoscopic properties of hydrophilic polymer-grafted phospholipids mixed with phosphatidylcholine in aqueous dispersion: interaction of dipalmitoyl N-poly(ethylene glycol)phosphatidylethanolamine with dipalmitoylphosphatidylcholine studied by spectrophotometry and spin-label electron spin resonance. Biophys. J., 2000. **78**(3): p. 1420-30.

24. Wolszczak, M., Miller, J., Characterization of non-ionic surfactant aggregates by fluorometric techniques. J. Photochem. Photobiol. A, 2002. **147**(1): p. 45-54.

25. Davies, M., Schuster, H., Brauner, J., Mendelsohn, R., Effects of cholesterol on conformational disorder in dipalmitoylphosphatidylcholine bilayers. A quantitative IR study of the depth dependence. Biochemistry, 1990. **29**(18): p. 4368-73.

26. Hofsass, C., Lindahl, E., Edholm, O., Molecular dynamics simulations of phospholipid bilayers with cholesterol. Biophys. J., 2003. **84**(4): p. 2192-206.

27. Ohvo-Rekila, H., Ramstedt, B., Leppimaki, P., Slotte, J., Cholesterol interactions with phospholipids in membranes. Prog. Lipid Res., 2002. **41**(1): p. 66-97.

28. Mcconnell, H., Radhakrishnan, A., Condensed complexes of cholesterol and phospholipids. Biochim. Biophys. Acta, 2003. **1610**(2): p. 159-73.

29. Charbonneau, C., Fournier, I., Dufresne, S., Barwicz, J., Tancrede, P., The interactions of amphotericin B with various sterols in relation to its possible use in anticancer therapy. Biophys. Chem., 2001. **91**(2): p. 125-33.

30. Barwicz, J., Gareau, R., Audet, A., Morisset, A., Villiard, J., Gruda, I., Inhibition of the interaction between lipoproteins and amphotericin B by some delivery systems. Biochem. Biophys. Res. Comm., 1991. **181**(2): p. 722-728.

31. Castanho, M., Coutinho, A., Prieto, M., Absorption and fluorescence spectra of polyene antibiotics in the presence of cholesterol. J. Biol. Chem., 1992. **267**(1): p. 204-9.

32. Forrest, M., Won, C., Malick, A., Kwon, G., In vitro release of the mTOR inhibitor rapamycin from poly(ethylene glycol)-b-poly(epsilon-caprolactone) micelles. J. Controlled Release, 2006. **110**(2): p. 370-7.

33. Lim Soo, P., Luo, L., Maysinger, D., Eisenberg, A., Incorporation and release of hydrophobic probes in biocompatible polycaprolactone-block-poly(ethylene oxide) micelles: Implications for drug delivery. Langmuir, 2002. **18**(25): p. 9996-10004.

34. Aramwit, P., Yu, B., Lavasanifar, A., Samuel, J., Kwon, G., The effect of serum albumin on the aggregation state and toxicity of amphotericin B. J. Pharm. Sci., 2000. **89**(12): p. 1589-1593.

35. Hsu Chen, C., Feingold, D., Polyene antibiotic action on lecithin liposomes: effect of cholesterol and fatty acyl chains. Biochem. Biophys. Res. Commun., 1973. **51**(4): p. 972-8.

Chapter 4:

Characterization of mixed polymeric micelles formed from PEG-b-poly(ε-caprolactone) and PEG-phospholipid

---

A version of this chapter has been published in Vakil R., Kwon G., "Poly(ethylene glycol)-b-poly(ε-caprolactone) and PEG-phospholipid form Stable Mixed Micelles in Aqueous Media". Langmuir, 2006. **22**: p 9723-9

4.1 Introduction

Amphiphilic block copolymers (ABC) assemble into nanoscopic core-shell structures, micelles, which are of considerable interest for the delivery of poorly water soluble anticancer and antibiotic drugs (1, 2). The shell of ABC micelles considered for drug delivery usually consists of poly(ethylene glycol). However, various hydrophobic blocks have been studied for drug solubilization to fill requirements of biocompatibility, carrier stability and slow drug release (3). Poly(ethylene glycol)-b-poly(ε-caprolactone) (PEG_{5000}-b-PCL_x) and 1,2-Distearoyl-*sn*-glycero-3-phosphoethanolamine-N-methoxy(polyethylene glycol) (PEG-DSPE), (Figure 4.1) are biocompatible, amphiphilic polymers, which form micellar structures in aqueous media. Various drugs and diagnostic agents with limited aqueous solubility have been incorporated into PEG-DSPE (4-6) and PEG_{5000}-b-PCL_x (7-10) micelle cores.

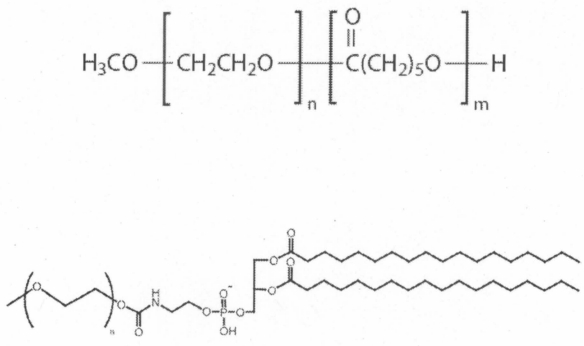


Figure 4.1 Chemical structures of PEG_{5000}-b-PCL_x and PEG-DSPE

Binary surfactant mixtures may form aggregates with greater thermodynamic stability through a cooperative interaction between components (11). Such cooperativity has also been observed in mixtures of polymers and surfactants (12). Polymer-surfactant mixtures have found extensive use in catalysis, painting and detergency (13). Micelles assembled from mixtures of ABCs have been investigated in both organic and aqueous media. Pacovska et al. have shown a spontaneous but gradual formation of unimodal mixed micelles of polystyrene-*b*-polyisoprene and polystyrene-*b*-poly(ethylene-*co*-propylene) in decane (14). Interestingly, spontaneous demixing of block copolymers has been demonstrated by Esselink et al. in which there is a slow evolution of a bimodal distribution from an initial broad distribution in the case of poly(2-vinylpyridine)-b-poly(styrene) with different lengths of poly(2-vinylpyridine) blocks (15). Mixed micelles formed from diblock and triblock copolymers consisting of poly(ethylene glycol), poly(propylene oxide) and poly(butylene oxide) have been extensively characterized using various techniques (16, 17). Stepanek et al. have demonstrated the gradual formation of hybrid micelles formed from poly(methacrylic acid)-b-poly(styrene) and poly(ethylene oxide)-b-poly(styrene) in aqueous media (18).

In the context of drug delivery, mixed Pluronic-105 and PEG-DSPE micelles have been investigated for the delivery of the poorly water soluble antineoplastic doxorubicin. These mixed polymeric micelles resulted in greater tumor accumulation of doxorubicin than Pluronic-105 micelles alone (19, 20). Lee et al. have prepared mixed micelles from PEG-b-poly(L-lactic acid) and folate-PEG-b-poly(L-histidine). The release rate of doxorubicin from these mixed polymeric micelles showed an

interesting dependence on pH as well as fraction of PEG-b-poly(L-lactic acid) in the mixed polymeric micelle (21). Incorporation of various hydrophobic substances such as lipids (22, 23) and vitamin E (8) into PEG-DSPE and PEG_{5000}-b-PCL_x micelles leads to interesting modifications of micelle properties, however we are reluctant to classify them with the foregoing mixed polymeric micelles due to vastly differing sizes of the head groups compared to the poly(ethylene glycol) unit in ABCs.

The objective of our work was to investigate the formation of novel mixed polymeric micelles from the biocompatible polymers PEG_{5000}-b-PCL_x and PEG-DSPE, i.e. PEG-DSPE|PEG_{5000}-b-PCL_x, in the context of drug delivery. These structures possess nanomolar critical micellar concentrations through a cooperative interaction between hydrophobic segments, which may be of significant advantage considering that these carriers are extensively diluted in the body (1). Size-exclusion chromatography and dynamic light scattering have been used to obtain evidence for the formation of small unimodal structures. The microenvironment of the micelle cores was characterized using steady state fluorescence measurements. ^{1}H-NMR and steady state fluorescence measurements indicate that the addition of PEG-DSPE to PEG_{5000}-b-PCL_x micelles results in a highly modified core microenvironment due to interpenetration of hydrophobic segments of the ABCs. Contrary to PEG_{5000}-b-PCL_{4000} micelles, mixed PEG-DSPE|PEG_{5000}-b-PCL_{4000} micelles could incorporate high levels of amphotericin B (AmB). Interestingly, AmB incorporation and release was dependent on the level of PEG-DSPE in the mixed polymeric micelle.

4.2 Materials

Poly(ethylene glycol)-block-poly(ε-caprolactone) polymers (PEG_{5000}-b-PCL_x) (x= 2500, 4000 and 6000 g/mol) were purchased from Polymer Source (Montreal, Canada). Polydispersity (M_w/M_n) for PEG_{5000}-b-PCL_x polymers were 1.12, 1.36 and 1.06 respectively. 1,2-Distearoyl-*sn*-glycero-3-phosphoethanolamine-N-methoxy(polyethylene glycol) (M_n =5800 g/mol) (PEG-DSPE) was obtained from Avanti Polar Lipids (Alabaster, AL). Pyrene and 1,3-(1,1'-dipyrenyl) propane (P3P) were purchased from Aldrich (Milwaukee, WI) and Molecular Probes (Eugene, OR) respectively. Amphotericin B (AmB) was obtained as a gift from Alpharma (Copenhagen, Denmark). All other reagents used were of analytical grade and were used without further purification.

4.3 Preparation of mixed PEG_{5000}-b-PCL_x|PEG-DSPE micelles

The PEG_{5000}-b-PCL_x micelles were prepared using the dialysis method (9). 40 mg PEG_{5000}-b-PCL_x was dissolved in 4.0 mL THF and 3.0 mL water was added dropwise (1 drop/ 10-15 s) with stirring. This solution was transferred to a dialysis bag (MWCO 3500 g/mol, Spectra Por) and dialyzed against 2 L water with three water changes over 24 h. The sample was then filtered through a 0.2-μm Nylon filter and additional water was added, such that the final PEG_{5000}-b-PCL_x concentration was 5 mg/mL.

For preparation of empty mixed PEG-DSPE|PEG_{5000}-b-PCL_x micelles, 1.0 mL PEG_{5000}-b-PCL_x micellar solution (prepared by dialysis) was mixed with 10 mg/mL PEG-DSPE solution, prepared by simple dissolution, at a specified PEG-

DSPE:PEG_{5000}-b-PCL_x ratio and sonicated (Ultrasonic Cleaner model G112SP1, 80W at 80 kHz, Laboratory Supplies Company of New York, Hicksville, NY) for 20 minutes. The temperature of water in the sonicating bath was less than 35 °C. The sample was then filtered through a 0.2-μm Nylon filter.

4.4 Micelle characterization

4.4.1 Size exclusion chromatography

Aqueous micellar solutions were diluted to 1.0 mg/mL polymer content in water. 100 μL samples were injected in triplicate onto a Shodex SB-806M HQ OHpak size exclusion column (Showa Denko, Japan). The column was equilibrated using a 50 mM phosphate buffer (pH = 7.2). The flow rate was maintained at 0.75 mL/min and column compartment maintained at 10 °C. The elution of empty polymeric micelles was monitored using refractive index. Elution of polymeric micelle incorporated AmB was detected using its absorbance at 412 nm.

4.4.2 Dynamic light scattering

Diffusion coefficient measurements were performed on the NICOMP 380ZLS particle sizer (Particle Sizing Systems, Santa Barbara, CA) using a 639 nm laser at a fixed angle of 90°. Data was acquired to have at least 100k counts in channel 1. A Gaussian fit to the raw data was performed by the ZW380 software (v. 1.61A, Particle Sizing Systems, Santa Barbara, CA) and results reported as intensity weighted hydrodynamic diameters.

4.4.3 Critical micellization concentration and core polarity using pyrene fluorescence

The critical micellar concentration (CMC) and core micropolarity of mixed micelles were determined using pyrene fluorescence (24-28). Aqueous solutions containing decreasing polymer concentrations were prepared from a 1.0 mg/mL stock and transferred into tubes containing pyrene to a final concentration of 0.6 μM. The samples were heated to 65 °C for 1 h and allowed to cool to room temperature overnight for pyrene to equilibrate between the aqueous media and the micellar core. The final pyrene concentration was 6×10^{-7} M. Steady state fluorescence measurements were taken at room temperature using a Fluoromax 3 fluorimeter (Horiba Jobin Yvon, Edison, NJ). The sample was excited at 335 nm and emission recorded from 360 to 450 nm, with both bandwidths set to 1.5 nm. A plot of the ratio of the intensity ratio of the first to third peak of the emission spectrum (I_1/I_3) versus the logarithm of the total polymer concentration was prepared and CMC determined using linear regression. Core polarity values are reported as I_1/I_3 ratios of the pyrene fluorescence spectrum, upon complete partitioning into micelle cores (29).

4.4.4 Core microviscosity measurements using 1,3-(1,1'-dipyrenyl) propane

The microviscosity in the micelle cores was estimated by measuring the ratios of the fluorescence intensities of the monomer and excimer i.e. I_M/I_E of 1,3-(1,1'-dipyrenyl) propane (P3P) measured at 376 and 480 nm respectively (29, 30). P3P was dissolved in chloroform and transferred to tubes such that its final concentration was 2×10^{-7} M. All microviscosity determinations were made in samples containing 0.5 mg/mL polymer. The P3P was allowed to partition into the hydrophobic micellar core

and emission spectra were obtained at 25 °C, using an excitation wavelength of 333 nm on a Fluoromax DM3000 fluorimeter. For comparison, core viscosities for PEG_{5000}-b-PCL_{4000} and SDS micelles were determined in a similar manner.

4.4.5 Diffusion coefficients using pulsed field gradient (PFG) spin echo

The PFG spin echo ^{1}H-NMR measurements were performed on a 500 MHz Varian spectrometer equipped with Varian hcx4765 inverse detection probe (Varian, Palo Alto, CA). The maximum gradient strength obtained with this configuration was 0.67 T/m with a current of 10 A. Intensities for 20 increments of gradient strength were used for each diffusion coefficient measurement. Data were subjected to a polynomial baseline correction to avoid distortion of measured peak area. The gradient strength was calibrated with a sample of known diffusion coefficient (1% H_2O in D_2O with a diffusion coefficient of 1.9 x 10^{-9} m^2/s). All PFG measurements were obtained using a diffusion time Δ, of 100 ms.

4.4.6 Spin lattice relaxation (T_1) measurements

Spin-lattice relaxation (T_1) determinations were made on the 500 MHz Varian spectrometer using the using the inversion-recovery sequence (31). Intensities for 20 increments of recovery times were used for each measurement. Relaxation times for protons in the hydrophobic segments of ABC micelles were estimated by fitting to an exponential model

$$I/I_0 = \exp(-t/T_1)$$

where, t is the recovery time and I_0 is the intensity immediately after the 180_x pulse.

4.4.7 NOE measurements

Two dimensional NOE data for one component and mixed micelles were obtained at 25 °C on a 500 MHz Varian spectrometer using the standard three-pulse sequence (31). The mix time and recovery delay was optimized at 400 ms and 4 s using data from spin-lattice relaxation measurements. 2048 points were collected for 256 slices with 8 transients. In both dimensions, the FIDs were apodized using Gaussian functions.

4.8 AmB incorporation and *in vitro* release studies

4.8.1 AmB incorporation into PEG-DSPE, PEG_{5000}-b-PCL_{4000} and PEG-DSPE\| PEG_{5000}-b-PCL_{4000} micelles

PEG-DSPE micelles incorporating AmB (AmB/PEG-DSPE) were formed by dissolution of a thin film of coprecipitated AmB and polymer. Stock solutions of AmB (0.3 mg/mL) in methanol and PEG-DSPE (6 mg/mL) in chloroform were mixed. The organic solvent was evaporated under vacuum using a rotoevaporator forming a thin film of coprecipitated drug and polymer. This film was dissolved in water and unincorporated drug removed by filtration through a 0.2-μm filter.

The dialysis method was investigated for AmB loading into PEG_{5000}-b-PCL_{4000} micelles (9). 40 mg PEG_{5000}-b-PCL_{4000} and 2 mg AmB were dissolved in 4.0 mL DMF and 3.0 mL water was added in a dropwise manner. This solution was similarly transferred to a dialysis bag and dialyzed against 2 L water. After adjusting for volume such that the final polymer concentration was 5 mg/mL, the sample was filtered through a 0.2-μm filter to remove unincorporated drug.

Mixed PEG-DSPE|PEG_{5000}-b-PCL_{4000} micelles incorporating AmB were prepared by sonicating 0.25 mL AmB/PEG-DSPE solutions with empty PEG_{5000}-b-PCL_{4000} (5 mg/mL) micelles for 20 min at room temperature at the specified PEG-DSPE:PEG_{5000}-b-PCL_{4000} ratio. The samples were filtered through a 0.2-μm filter to remove unincorporated drug.

4.8.2 HPLC assay for estimation of AmB content

For determination of AmB content, 25 μL samples were injected into 4.6mm x 150mm Eclipse XDB-C8 reversed-phase column (Agilent Technologies) and AmB absorbance detected at 412 nm using the diode array detector. The column was maintained at 25 °C and a flow rate of 1 mL/min using a methanol – (5 % v/v acetic acid) gradient over 9 min. The assay was tested for linearity in the 0.1 - 100 μg/mL range.

4.8.3 In vitro release study of micelle encapsulated AmB using equilibrium dialysis

Drug release under sink-conditions was assessed using a setup similar to that described in the literature (8, 9) 30 μg/mL free or polymeric micelle encapsulated AmB solutions were put into dialysis cassettes (MWCO 7000 g/mol, Pierce). These dialysis cassettes were placed in a well mixed, temperature controlled water bath at 37 °C. The pH of the temperature bath was maintained at 7.2 ± 0.1 by the addition of sodium phosphate solutions under computer control. AmB concentrations in the dialysis cassettes were determined at fixed time points using the reversed-phase HPLC method.

4.8.4 Electronic absorbance kinetics in serum albumin

Stock solutions containing AmB encapsulated in mixed PEG-DSPE|PEG_{5000}-b-PCL_{4000} micelles were added to 4 % bovine serum albumin solution, such that the final AmB concentration was 10 μg/mL. AmB absorbance spectra were recorded from 300 to 450 nm using the Cary 50 spectrophotometer, as described in chapter 3. The change in absorbance at 412 nm was fit to a first-order process of the form, $A_\infty - A_t = a.e^{-k.t}$ and parameters a, k, and A_∞ were estimated using non-linear regression using SigmaPlot (v. 9.0).

4.9 Results, Analysis and Discussion

4.9.1 Micelle Characterization

Mixed micelles of PEG-DSPE| PEG_{5000}-b-PCL_x were prepared using a simple sonication procedure from a mixture of their corresponding one component systems. The resulting mixed polymeric micelle solutions were clear, indicating the absence of polymer precipitation. Simple mixing of PEG-DSPE and PEG_{5000}-b-PCL_x micelles did not result in complete formation of mixed polymeric micelles, as evidenced by multimodal distribution from size-exclusion chromatography (Figure 4.2a). However, upon sonication of this solution for 20 min a single peak was observed in the SEC chromatograph, indicating the formation of a unimodal population of mixed polymeric micelles (Figure 4.2b). One component PEG_{5000}-b-PCL_{4000} and PEG-DSPE micelles differ in size and produced narrow peaks at 10.57 and 11.15 min respectively (Figure 4.2c). The elution times for the mixed PEG-DSPE|PEG_{5000}-b-PCL_x micelles containing equal weight proportions of PEG-DSPE and PEG_{5000}-b-PCL_x ranged from

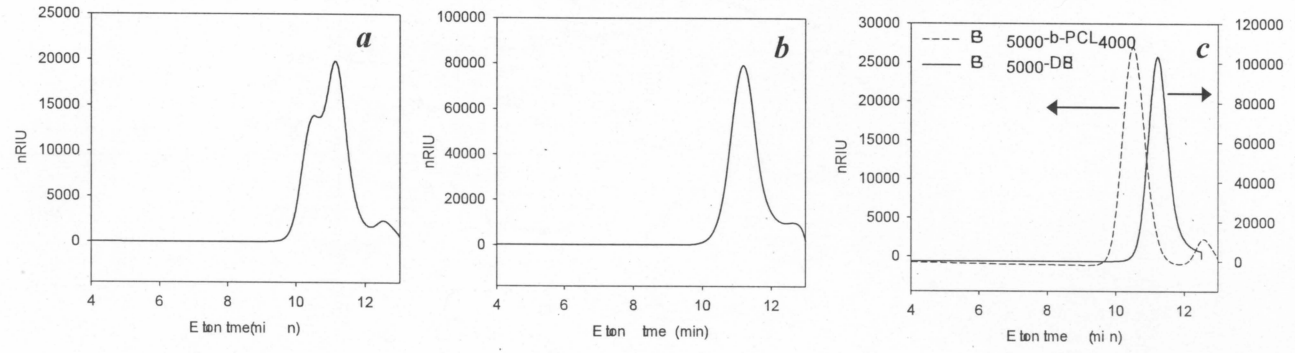


Figure 4.2. Size exclusion chromatographs for one-component and mixed micelles.
a. Simple mixing of PEG-DSPE and PEG_{5000}-b-PCL_{4000} micelles ***b.*** PEG-DSPE| PEG_{5000}-b-PCL_{4000} (1:1) mixed micelles after sonication for 20 min. ***c.*** PEG-DSPE and PEG_{5000}-b-PCL_{4000} micelles.

11.05 to 11.17 min (Table 4.1). Dynamic light scattering was used to estimate hydrodynamic diameters of ABC micelles. Consistent with literature reports, the hydrodynamic diameter for empty PEG-DSPE micelles was 15 nm (23), whereas for PEG_{5000}-b-PCL_x micelles, the diameters increased from 35 to 75 nm, with increasing length of the poly(ε-caprolactone) block (32). SEC and DLS measurements suggested that PEG-DSPE|PEG_{5000}-b-PCL_x micelles are smaller than PEG_{5000}-b-PCL_x micelles and their size increases with PCL block length.

	Elution time (min) [a]	Hydrodynamic diameter (nm) [b]
PEG-DSPE	11.15 ± 0.04	15.1 ± 1.0
PEG_{5000}-b-PCL_{2500}	10.77 ± 0.01	35.3 ± 0.1
PEG_{5000}-b-PCL_{4000}	10.57 ± 0.01	40.7 ± 0.3
PEG_{5000}-b-PCL_{6000}	10.27 ± 0.02	75.4 ± 0.7
PEG-DSPE | PEG_{5000}-b-PCL_{2500} (1:1)	11.16 ± 0.01	16.0 ± <0.1
PEG-DSPE | PEG_{5000}-b-PCL_{4000} (1:1)	11.17 ± 0.02	17.5 ± <0.1
PEG-DSPE | PEG_{5000}-b-PCL_{6000} (1:1)	11.05 ± 0.01	28.2 ± 0.3

Table 4.1. Particle sizing of one-component and mixed micelles using dynamic light scattering and size exclusion chromatography. [a]Shodex SB-806M HQ OHpak column. Eluent: 50 mM phosphate buffer, pH 7.2 [b]intensity weighted gaussian averages.

Pulsed field gradient spin echo (PGSE-NMR) measurements were used to measure self-diffusion coefficients for PEG-DSPE, PEG_{5000}-b-PCL_{4000} and PEG-DSPE|PEG_{5000}-b-PCL_{4000} micelles. Micelle diffusion coefficients were estimated in D_2O at 25 °C using attenuation in the intensity of the PEG peak (3.6 ppm) using the basic spin-echo sequence (32). The signal attenuation is related to the displacement

along the gradient (z-axis) over the period Δ by the Stejskal-Tanner relationship (33). For a single diffusing species the echo intensity A is given by,

$$A = A_0 . \exp\left(- D.(\Delta - \frac{\delta}{3}).(\delta . G_z . \gamma)^2 \right)$$

where A_0 is the intensity immediately after the 90_x pulse, D is the self-diffusion coefficient, Δ is the time between the gradient pulses of length δ and strength G_z, γ is the gyromagnetic ratio (for ^1H, $\gamma = 2.67 \times 10^8$ rad T^{-1} s^{-1}). The echo attenuation data for the single component PEG-DSPE system gave an excellent fit to the above equation. For PEG_{5000}-b-PCL_{4000} and mixed PEG-DSPE|PEG_{5000}-b-PCL_{4000} micelles, however, we could not obtain a satisfactory fit to the equation for a single diffusing population (Figure 4.3). For a multi-component mixture, the echo attenuation can be expressed as a weighted sum of individual contributions (34)

$$A = \sum_i A_i . \exp\left(- D_i . (\Delta - \frac{\delta}{3}).(\delta . G_z . \gamma)^2 \right).$$

A_i is dependent on the relative fraction of the population, and the relevant T_2 relaxation times. Hence for two independently diffusing populations in solution (34, 35)

$$A = A_1 . \exp\left(- D_1 . (\Delta - \frac{\delta}{3}).(\delta . G_z . \gamma)^2 \right) + A_2 . \exp\left(- D_2 . (\Delta - \frac{\delta}{3}).(\delta . G_z . \gamma)^2 \right)$$

where D_1 and D_2 are diffusion coefficients for the fast and slow diffusing populations, estimated using non-linear regression.

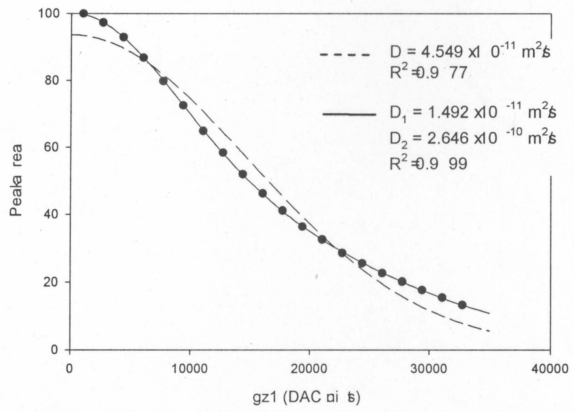


Figure 4.3. Pulsed-field gradient echo attenuation for PEG_{5000}-b-PCL_{4000} micelles in D_2O
[a] PEG peak (3.6 ppm) for [b] 25 °C.

Table 4.2 summarizes the diffusion coefficients obtained after fitting the signal attenuation data for single and two diffusing populations. Excellent fits to the model were obtained as judged by R^2 values close to 1. The diffusion coefficients for the two populations were in the 10^{-10} and 10^{-11} m^2/s range. Number weighted particle diameters were calculated using the Stokes-Einstein equation, $R = \frac{k.T}{6\pi\eta D}$ where R is the hydrodynamic radius, k is the Boltzmann constant, T is the temperature in K, η is the viscosity for D_2O (1.09 mPa.s at 25 °C) and D is the diffusion coefficient determined above. The diffusion coefficients and particle diameters obtained for the slow diffusing population were comparable to those reported by dynamic light scattering. For the fast diffusing component, the analysis yielded particle sizes ranging from 1.5 to 2.4 nm, which is close to the Flory radius of PEG_{5000} (36) and hence may be attributed to unimers. The measured self-diffusion coefficients provide further evidence that the resulting mixed polymeric micelles are smaller than

PEG_{5000}-b-PCL_x micelles. A reduction in size in comparison with PEG_{5000}-b-PCL_x micelles may improve tumor accumulation by the enhanced permeability retention (EPR) effect (37).

	$D_1 \times 10^{-11}$ m^2/s	$2R_1$ (nm)	$D_2 \times 10^{-10}$ m^2/s	$2R_2$ (nm)	R^2	$D \times 10^{-11}$ m^2/s (DLS)
PEG-DSPE	3.143 ± 0.024	12.7	-	-	0.999	2.8
PEG_{5000}-b-PCL_{4000}	1.492 ± 0.036	26.8	2.646 ± 0.028	1.5	0.999	1.1
PEG-DSPE | PEG_{5000}-b-PCL_{4000} (1:1)	3.065± 0.014	13.1	1.664 ± 0.048	2.4	0.999	2.5
PEG-DSPE | PEG_{5000}-b-PCL_{4000} (5:1)	3.118 ± 0.025	12.9	2.272± 0.714	1.8	0.999	-

Table 4.2. Diffusion-coefficient measurements using pulsed-field gradient echo (PGSE-NMR) attenuation data

The vibrational structure of the pyrene fluorescence, specifically the ratio of the intensity of the 0-0 band (I_1) to the intensity of the 0-737 band of b_{1g} vibration (I_3) depends on local polarity (26). The I_1/I_3 ratio changes on micelle assembly and pyrene uptake and hence can be used to determine CMCs of ABC micelles (38). The CMC for PEG_{5000}-b-PCL_x micelles decreased from ca. 910 nM to 300 nM with increasing hydrophobic poly(ε-caprolactone) block length from 2500 to 6000 g/mol. The CMC for PEG-DSPE was ca. 1400 nM, consistent with previous reports (5). The CMC for the binary system of PEG-DSPE|PEG_{5000}-b-PCL_x micelles was significantly lower than PEG-DSPE micelles ($p<0.05$); decreasing from ca. 470 nM to 240 nM with increasing poly(ε-caprolactone) block length (Figure 4.4). Also, the CMC of PEG-DSPE|PEG_{5000}-b-PCL_{6000} mixed micelles was composition dependent and decreased with increasing proportion of PEG_{5000}-b-PCL_{6000} (Figure 4.5).

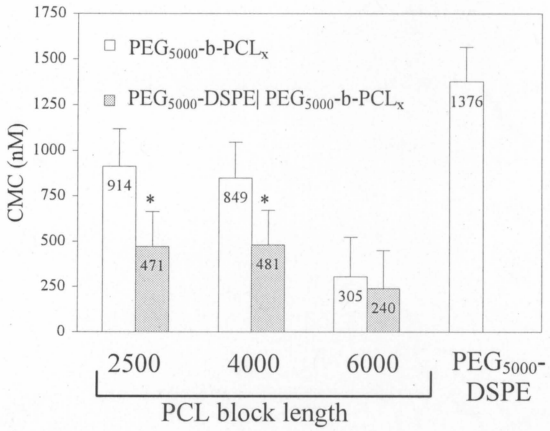


Figure 4.4 Effect of PCL block length on CMC of PEG-DSPE|PEG_{5000}-b-PCL_{6000} (1:1) micelles. * $p<0.05$

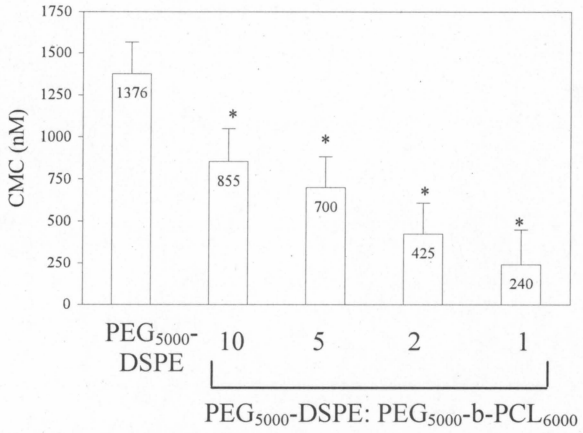


Figure 4.5 Effect of PEG-DSPE: PEG_{5000}-b-PCL_{6000} ratio on the effective CMC of PEG-DSPE| PEG_{5000}-b-PCL_{6000} micelles. * $p<0.05$

In its empirical form, the pseudophase model with the regular solution approximation has been remarkably successful in modeling non-ideal behavior of surfactant mixtures (39, 40). The CMC of the mixed micelle (C_M) can be expressed as

$$\frac{1}{C_M} = \frac{y_1}{f_1.C_{M_1}} + \frac{1-y_1}{f_2.C_{M_2}}$$

where y_1 is the mole fraction of polymer 1 in solution, C_{M1} and C_{M2} are CMCs for one- component micelles 1 and 2. Micellar activity coefficients f_1 and f_2 are expressed using the regular solution approximation as $f_1 = \beta.\exp(1-x_1)^2$ and $f_2 = \beta.\exp x_1^2$ where x_1 is the mole fraction of polymer 1 in the mixed micelle and β is the dimensionless interaction parameter, interpreted generally as the excess free energy of mixing (39, 40). For the ideal mixing, β = 0. Cooperative interactions between individual micelle components result in depressed CMCs and negative values for β. Based on a large number of CMC measurements reported in the literature, binary non-ionic/anionic surfactant mixtures show strong negative deviations from ideal mixing, hence β values are in the range $-5 \leq \beta \leq -1$ (39). For the PEG-DSPE|PEG_{5000}-b-PCL_{6000} mixed micelles, β was determined using an iterative procedure from the following equations (39, 40)

$$\frac{x_1^2.\ln(y_1.C_M / x_1.C_{M_1})}{(1-x_1)^2.\ln[C_M(1-y_1)/C_{M_2}(1-x_1)]} = 1 \quad \text{and}$$

$$\beta = \frac{\ln(C_M.y_1 / C_{M_1}.x_1)}{(1-x_1)^2} = \frac{\ln(C_M.(1-y_1)/C_{M_1}.(1-x_1))}{x_1^2}$$

The best-fit value for the interaction parameter, β for PEG-DSPE|PEG_{5000}-b-PCL_{6000} was determined to be -4.06. The large negative value of β indicated that the mixed micelle formation is accompanied by a relatively large decrease in free energy. This non-ideal mixing points to a cooperative interaction between the hydrophobic segments of PEG-DSPE and PEG_{5000}-b-PCL_{6000}.

The determination of I_1/I_3 values for pyrene partitioned into PEG-DSPE|PEG_{5000}-b-PCL_{6000} permits estimation of the core polarity as a function of core composition. The I_1/I_3 value was 1.28 for PEG-DSPE micelles, consistent with low core polarity owing to alkyl chains (Figure 4.6). As the content of PEG_{5000}-b-PCL_{6000} increased, the I_1/I_3 value rose, indicating an increase in polarity with PEG_{5000}-b-PCL_{6000} content. The I_1/I_3 value for PEG_{5000}-b-PCL_{6000} micelles was 1.36, presenting a slightly more polar environment than PEG-DSPE micelles. Hence, core polarity can be modulated in mixed polymer micelles by varying the ratio of the binary components.

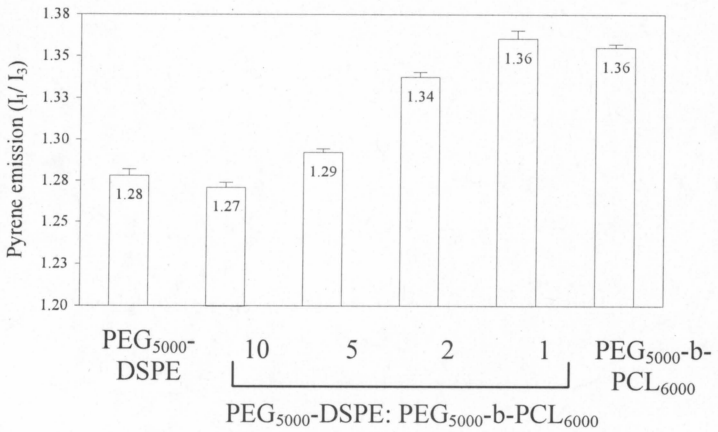


Figure 4.6 Core micropolarity of PEG-DSPE| PEG_{5000}-b-PCL_{6000} micelles. λ_{ex} = 335 nm

The ratio of the fluorescence intensities due to P3P excimer and monomer I_M/I_E, is sensitive to microenvironment viscosity in micellar aggregates (24, 30). Core viscosity of PEG-DSPE|PEG_{5000}-b-PCL_{4000} micelles, as revealed by the intramolecular excimer formation of P3P was only slightly higher than the core viscosity of PEG-DSPE micelles (Figure 4.7). The core viscosity of PEG-DSPE

micelles was higher than low molecular weight surfactant sodium dodecyl sulfate micelles, but lower than PEG_{5000}-b-PCL_{4000} micelles, which have low excimer formation, I_M/I_E ca. 22. This high value of I_M/I_E may reflect partial crystallinity in the core of the PEG_{5000}-b-PCL_{4000} micelles. The presence of PEG-DSPE in the mixed polymeric micelles reduces the I_M/I_E values closer to PEG-DSPE micelles, presumably due to an inhibition of poly(ε-caprolactone) crystallization. Nonetheless, core mobility of PEG-DSPE is relatively low and is an important factor influencing the kinetic stability in an *in vivo* setting (5).

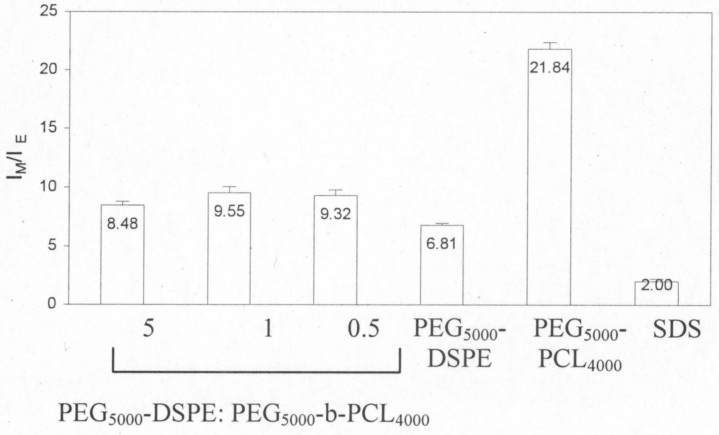


Figure 4.7. I_M/I_E ratios for 1,3-(1,1'-dipyrenyl) propane fluorescence emission in PEG-DSPE|PEG_{5000}-b-PCL_{4000} micelles at 25 °C. λ_{ex} = 333 nm

Spin lattice relaxation time (T_1) measurements provide useful information about local mobility in polymer segments (31, 41). Relaxation times (T_1) at 25 °C were measured for protons in the hydrophobic components of PEG-DSPE, PEG_{5000}-b-PCL_{4000} and PEG-DSPE|PEG_{5000}-b-PCL_{4000} micelles (Table 4.3). Short relaxation times, <1 s, for protons from the hydrophobic components of the polymers indicate a

restricted mobility consistent with the core-shell model for polymeric micelles. The relaxation times for methylene protons (2.26, 1.58, 1.33 ppm) of the poly(ε-caprolactone) segment in PEG-DSPE|PEG_{5000}-b-PCL_{4000} micelles are higher compared with PEG_{5000}-b-PCL_{4000} micelles and increase with increasing PEG-DSPE content. Also, relaxation times for the alkyl chain protons (1.26, 0.88 ppm) decreased compared to one component PEG-DSPE micelles. These results are consistent with results obtained from P3P photophysical experiments, which indicate that there is greater polymer mobility in PEG-DSPE|PEG_{5000}-b-PCL_{4000} micelle cores compared to PEG_{5000}-b-PCL_{4000} micelles.

Peak (ppm)	Spin lattice relaxation (T_1) times (ms)			
	PEG_{5000}-b-PCL_{4000}	PEG-DSPE	PEG-DSPE| PEG_{5000}-b-PCL_{4000} (5:1)	PEG-DSPE| PEG_{5000}-b-PCL_{4000} (1:1)
α -CH_2- (2.26)	441.7 ± 30.3	-	483.3 ± 15.5*	466.6 ± 16.5
β,δ -CH_2- (1.58)	394.6 ± 10.9	-	420 ± 11.6*	408.6 ± 10.5
γ -CH_2- (1.33)	427.8 ± 29.9	-	456.1 ± 17.6	424.7 ± 20.0
-CH_2- (1.26)	-	504.1 ± 9.5	489.2 ± 6.46*	502.5 ± 18.7
CH_3- (0.88)	-	925.5 ± 88.6	731.2 ± 26.4*	753.2 ± 58.3*

Table 4.3. Spin lattice relaxation (T_1) measurements for one-component and mixed micelles in D_2O at 25 °C. *$p < 0.05$

Since NOE cross-peaks arise between nuclei in close proximity (31), ^1H NOESY is a useful tool in studying spatial relationships in mixed micelles (12, 41). The cross peaks between methylene protons from PEG-DSPE (1.26 ppm) and those in the PCL block (2.26, 1.58, 1.33 ppm) in the NOE spectrum of PEG-DSPE|PEG_{5000}-b-PCL_{4000} may indicate that these are in close proximity, pointing to the formation of a homogeneous core due to polymer interpenetration (Figure 4.8). The cross peak

between protons from the ethylene oxide repeat unit (3.6 ppm) and those from the core forming blocks (1.58, 1.26 ppm) may give some evidence to suggest penetration of the poly(ethylene glycol) corona into the micelle core.

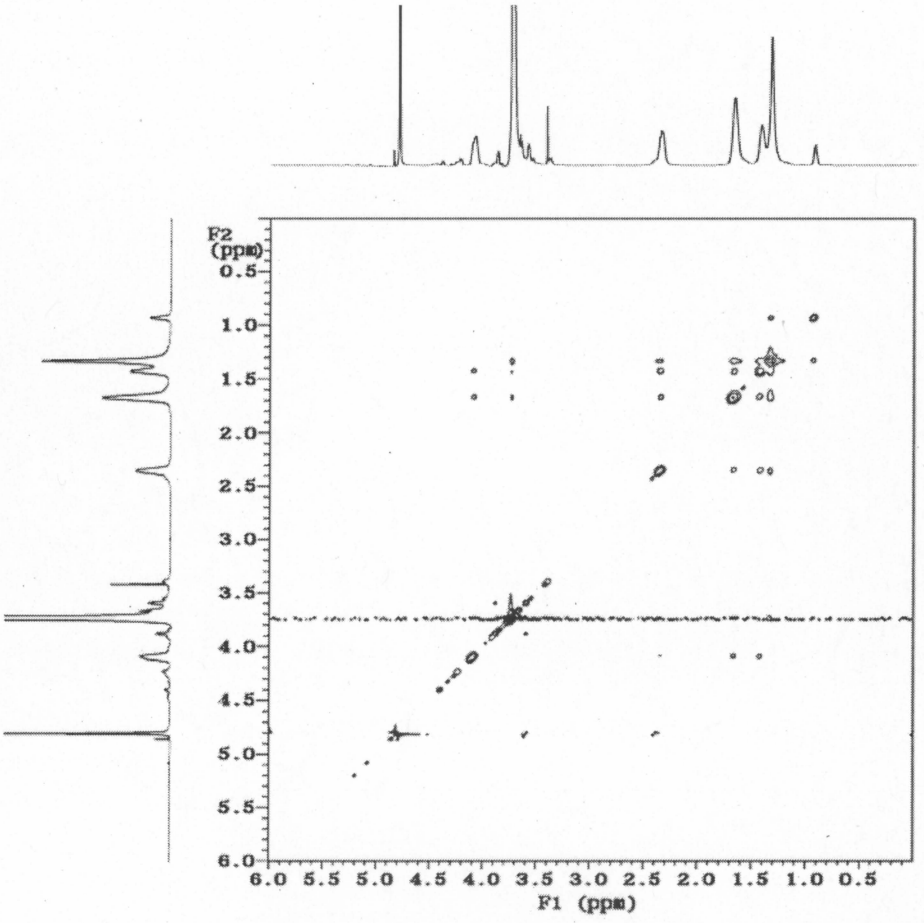


Figure 4.8 Contour plot of the NOE spectrum at 25 °C of a mixture of PEG-DSPE|PEG_{5000}-b-PCL_{4000} (1:1) mixed micelles in D_2O.

4.9.2 AmB encapsulation and release

Table 4.4 summarizes the result of AmB incorporation into PEG-DSPE, PEG_{5000}-b-PCL_{4000} and PEG-DSPE|PEG_{5000}-b-PCL_{4000} micelles. PEG-DSPE micelles could be loaded with high levels of AmB, consistent with our previous report (42). Surprisingly, one component PEG_{5000}-b-PCL_x micelles did not load AmB to any appreciable extent. Clinically relevant levels of AmB could be incorporated into PEG-DSPE|PEG_{5000}-b-PCL_{4000} micelles by sonicating AmB/PEG-DSPE with empty PEG_{5000}-b-PCL_{4000} micelles. The fraction of initial AmB encapsulated decreased from 91.5 to 83.5 % with increasing PEG_{5000}-b-PCL_{4000} content, at a constant AmB:PEG-DSPE ratio. AmB incorporation into the composite structure was verified by using size exclusion chromatography (Figure 4.9). The drug, monitored using absorbance at 412 nm, eluted with the micelle at 9.99 min. From DLS measurements, PEG-DSPE micelles increased in size from 15 to 42 nm on incorporation of AmB. The particle size of AmB loaded PEG_{5000}-b-PCL_{4000} micelles was comparable to empty micelles, possibly due to low levels of drug incorporation. The size for PEG_{5000}-b-PCL_{4000} rich PEG-DSPE|PEG_{5000}-b-PCL_{4000} micelles increased to 69 nm on AmB incorporation. For PEG-DSPE|PEG_{5000}-b-PCL_{4000} micelles containing a 5:1 weight-ratio of PEG-DSPE:PEG_{5000}-b-PCL_{4000}, the size was comparable to AmB/PEG-DSPE micelles.

AmB release from PEG-DSPE|PEG_{5000}-b-PCL_{4000} micelles was studied at 37 °C and pH 7.2 for two ratios of PEG-DSPE:PEG_{5000}-b-PCL_{4000} (Figure 4.10). Unencapsulated AmB was rapidly released from the dialysis cassette. A release profile for PEG_{5000}-b-PCL_{4000} micelles could not be obtained, since these micelles did not take up AmB to any appreciable extent. AmB release was slowest for PEG-DSPE

Weight ratio of PEG-DSPE: PEG_{5000}-b-PCL_{4000}	[AmB] mg/mL	AmB loading % w/w	Fraction of initial AmB encapsulated	Particle size (nm)
0.1	0.025	0.6 ± 0.01	83.5 ± 1.06	69 ± 1.0
0.25	0.055	1.35± 0.04	84.8 ± 0.29	57 ± 0.8
1	0.118	3.22 ± 0.01	80.8 ± 0.31	68 ± 1.3
5	0.199	6.08 ± 0.03	91.5 ± 0.41	42 ± 1.6
PEG-DSPE	0.249	7.95 ± 0.2	62.4 ± 1.2	41 ± 2.3
PEG_{5000}-b-PCL_{4000}	0.0013	0.02	0.065	44 ± 0.1

Table 4.4. AmB loading into PEG-DSPE|PEG_{5000}-b-PCL_{4000} mixed micelles.

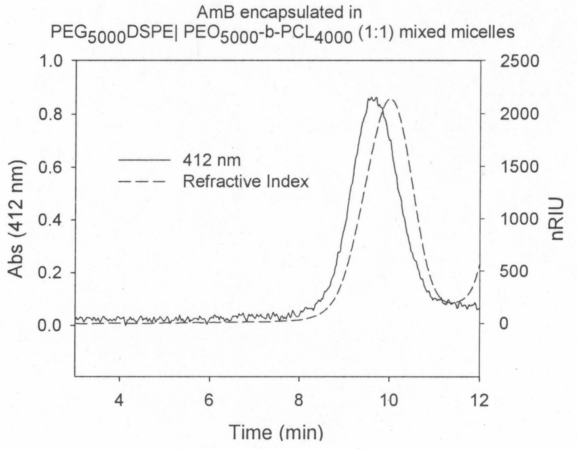


Figure 4.9. SEC of AmB encapsulated in PEG-DSPE| PEG_{5000}-b-PCL_{4000} (1:1) mixed micelles detected by absorbance at 412 nm and refractive index.

micelles consistent with our previous report (42). This slow release may be explained by the high compatibility of AmB with alkyl chains in PEG-DSPE, consistent with its antifungal activity at the membrane level. AmB release from the mixed PEG-DSPE|PEG_{5000}-b-PCL_{4000} micelles increased with increasing PEG_{5000}-b-PCL_{4000} fraction in the mixed micelle, pointing to decreased interaction of AmB with the micelle core.

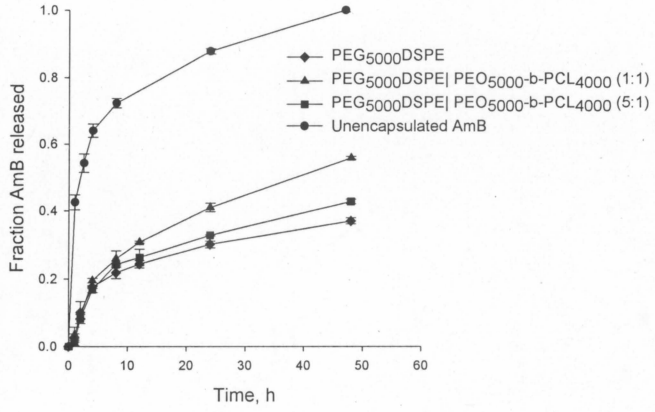


Figure 4.10. AmB release from PEG-DSPE | PEG_{5000}-b-PCL_{4000} mixed micelles under sink condition at 37 °C.

4.9.3 Electronic absorption kinetics in serum albumin

The absorbance spectrum of AmB encapsulated in PEG-DSPE|PEG_{5000}-b-PCL_{4000} mixed micelles (PEG-DSPE: PEG_{5000}-b-PCL_{4000} = 5:1) was identical to the spectrum of AmB solubilized in one-component PEG-DSPE micelles. However, the spectrum of AmB encapsulated in mixed micelles with higher proportion of PEG_{5000}-b-PCL_{4000} (PEG-DSPE: PEG_{5000}-b-PCL_{4000} = 1:1) has a peak at 328 nm, which is attributed to self-aggregated AmB. It appears that the solubilization capacity of the

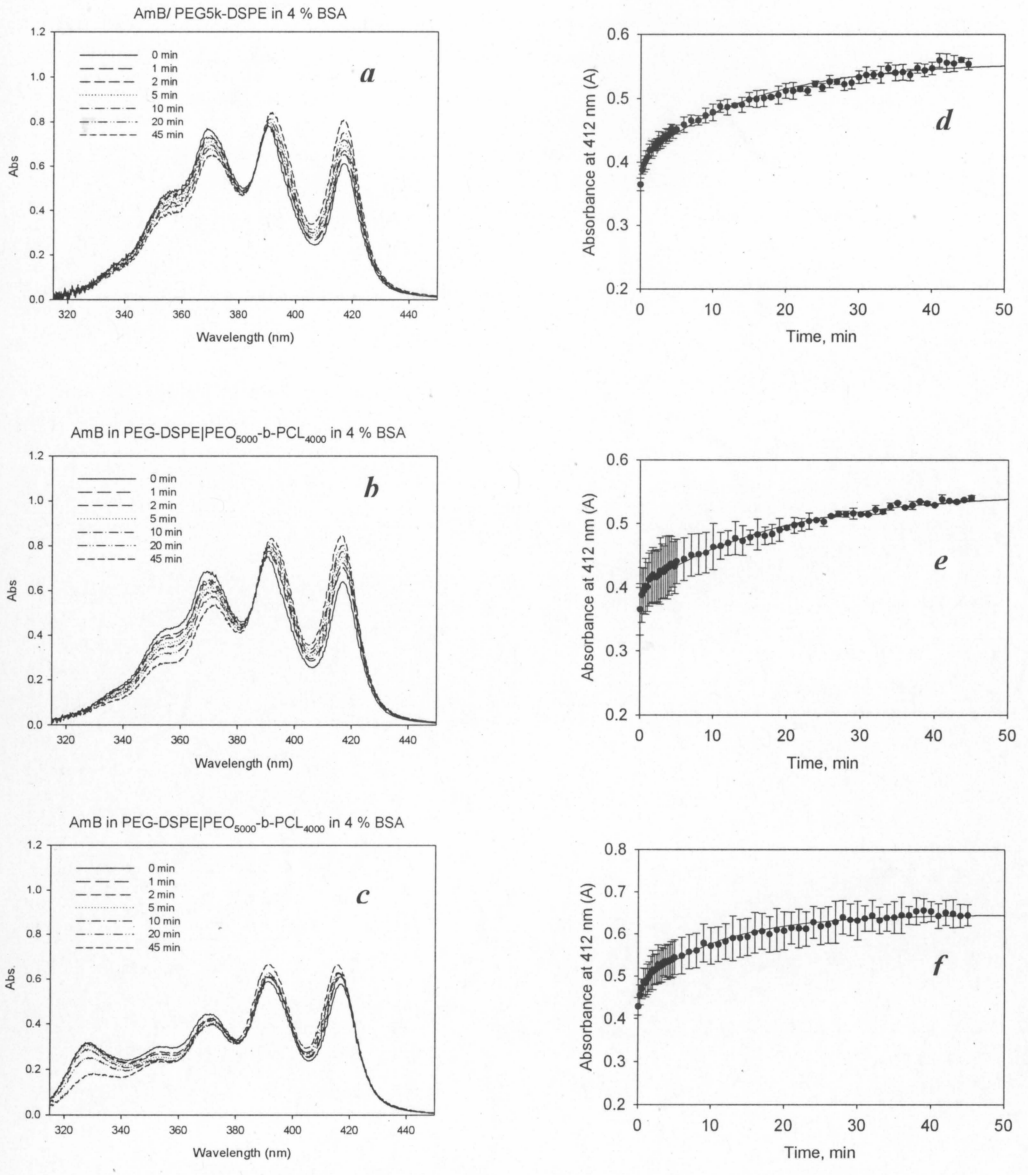


Figure 4.11. Absorbance spectra of micelle encapsulated AmB in 4 % BSA.
a. AmB in PEG-DSPE micelles (AmB: PEG-DSPE = 1: 2) ***b.*** AmB in PEG-DSPE|PEG_{5000}-b-PCL_{4000} micelles (PEG-DSPE: PEG_{5000}-b-PCL_{4000} = 1: 1) ***c.*** AmB in PEG-DSPE|PEG_{5000}-b-PCL_{4000} micelles (PEG-DSPE: PEG_{5000}-b-PCL_{4000} = 5: 1) ***d-f.*** Absorbance at 412 nm for as a function of incubation time corresponding to figures a-c.
[a] AmB concentration was 10 μg/mL

mixed micelles for AmB is decreased at higher PEG_{5000}-b-PCL_{4000} content, leading to drug self-aggregation.

	100 k (min^{-1})	$t_{1/2-1}$ (min)	R^2	A_∞
AmB: PEG-DSPE 1:2	6.63 ± 0.53	10.46	0.98	0.56
AmB: (PEG-DSPE: PEG_{5000}-b-PCL_{4000} 1:1)	5.39 ± 0.41	12.85	0.99	0.55
AmB: (PEG-DSPE: PEG_{5000}-b-PCL_{4000} 1:1)	9.04 ± 0.67	7.39	0.97	0.64

Table 4.5. Fit parameters for absorbance change for PEG-DSPE incorporated AmB at 412 nm upon dilution in 4 % BSA (figures 7d-f)

The absorption spectrum of AmB is sensitive to dissociation from micelles and association with serum albumin. Hence, sequential absorbance spectra of micelle encapsulated AmB were acquired upon the addition to bovine serum albumin, as described in chapter 3. Peak IV absorbance of AmB encapsulated in PEG-DSPE|PEG_{5000}-b-PCL_{4000} micelles increased over 45 min upon dilution in 4 % BSA, regardless of the polymer ratio, representative of AmB interaction with serum albumin. The dissociation half-life estimated assuming first-order kinetics was 12.8 and 7.4 minutes respectively, which was similar to PEG-DSPE micelles (10.5 min). It appears that AmB in mixed PEG-DSPE|PEG_{5000}-b-PCL_{4000} micelles is free to interact with serum albumin. Hence, we expect to see quick dissociation of encapsulated AmB from these mixed micelles in serum albumin, a likely situation *in vivo*.

4.10 Conclusions

We have prepared novel mixed polymeric micelles from PEG_{5000}-b-PCL_x and PEG-DSPE using a sonication procedure. These composite aggregates consist of a poly(ethylene glycol) corona and a hydrophobic core. These mixed polymeric micelles demonstrate synergistic lowering of CMCs due to a cooperative interaction between hydrophobic segments of the two polymers. Steady state fluorescence measurements indicate the mixed micelle core presents an environment of intermediate polarity possibly due to interpenetration of the hydrophobic segments of the polymers. PEG-DSPE|PEG_{5000}-b-PCL_x mixed micelles solubilize the poorly water soluble antibiotic AmB, at clinically relevant levels. AmB release from these mixed polymeric micelles was dependent on the fraction of PEG_{5000}-b-PCL_x, pointing to an interesting composition-dependant interaction of the drug with the micelle core. In the context of AmB delivery, it appears that AmB encapsulated in PEG-DSPE|PEG_{5000}-b-PCL_x mixed micelles is free to interact with serum albumin in a manner similar to PEG-DSPE solubilized AmB. However, due to their biocompatible nature, small size and high thermodynamic stability, these novel carriers are interesting for the delivery of other drugs with limited aqueous solubility.

4.11 References

1. Kwon, G., Polymeric micelles for delivery of poorly water-soluble compounds. Crit. Rev. Ther. Drug Carrier Syst., 2003. **20**(5): p. 357-403.

2. Kataoka, K., Kwon, G., Yokoyama, M., Okano, T., Sakurai, Y., Block copolymer micelles as vehicles for drug delivery. J. Controlled Release, 1993. **24**(1-3): p. 119-132.

3. Torchilin, V., Structure and design of polymeric surfactant-based drug delivery systems. J. Controlled Release, 2001. **73**(2-3): p. 137-72.

4. Lukyanov, A., Gao, Z., Mazzola, L., Torchilin, V., Polyethylene glycol-diacyllipid micelles demonstrate increased acculumation in subcutaneous tumors in mice. Pharm. Res., 2002. **19**(10): p. 1424-9.

5. Lukyanov, A., Torchilin, V., Micelles from lipid derivatives of water-soluble polymers as delivery systems for poorly soluble drugs. Adv. Drug Deliv. Rev., 2004. **56**(9): p. 1273-89.

6. Torchilin, V., PEG-based micelles as carriers of contrast agents for different imaging modalities. Adv. Drug Deliv. Rev., 2002. **54**(2): p. 235-52.

7. Allen, C., Han, J., Yu, Y., Maysinger, D., Eisenberg, A., Polycaprolactone-b-poly(ethylene oxide) copolymer micelles as a delivery vehicle for dihydrotestosterone. J. Controlled Release, 2000. **63**(3): p. 275-286.

8. Forrest, M., Won, C., Malick, A., Kwon, G., In vitro release of the mTOR inhibitor rapamycin from poly(ethylene glycol)-b-poly(epsilon-caprolactone) micelles. J. Controlled Release, 2006. **110**(2): p. 370-7.

9. Lim Soo, P., Luo, L., Maysinger, D., Eisenberg, A., Incorporation and release of hydrophobic probes in biocompatible polycaprolactone-block-poly(ethylene oxide) micelles: Implications for drug delivery. Langmuir, 2002. **18**(25): p. 9996-10004.

10. Lim Soo, P., Lovric, J., Davidson, P., Maysinger, D., Eisenberg, A., Polycaprolactone-block-poly(ethylene oxide) micelles: A nanodelivery system for beta-estradiol. Mol. Pharm., 2005. **2**(6): p. 519-527.

11. Nagarajan, R., Thermodynamics of nonionic polymer-micelle association. Colloids Surf., 1985. **13**: p. 1-17.

12. Vangeyte, P., Leyh, B., Auvray, L., Grandjean, J., Misselyn-Bauduin, A., Jerome, R., Mixed self-Assembly of poly(ethylene oxide)-b-(epsilon-caprolactone) copolymers and sodium dodecyl sulfate in aqueous solution. Langmuir, 2004. **20**(21): p. 9019-9028.

13. Goddard, E., Ananthapadmanabhan, K., Applications of polymer-surfactant systems, in Polymer-surfactant systems, J. Kwak, Editor. 1998. p. 22-64.

14. Pacovska, M., Prochazka, K., Tuzar, Z., Munk, P., Formation of block copolymer micelles: A sedimentation study. Polymer, 1993. **34**(21): p. 4585-4588.

15. Esselink, F., Dormidontova, E., Hadziioannou, G., Redistribution of block copolymer chains between mixed micelles in solution. Macromolecules, 1998. **31**(15): p. 4873-4878.

16. Mingvanish, W., Chaibundit, C., Booth, C., Mixed micellisation of oxyethylene-oxybutylene diblock and triblock copolymers in water studied by light scattering. Phys. Chem. Chem. Phys., 2002. **4**(5): p. 778-784.

17. Liu, T., Nace, V., Chu, B., Self-assembly of mixed amphiphilic triblock copolymers in aqueous solution. Langmuir, 1999. **15**(9): p. 3109-3117.

18. Stepanek, M., Podhajecka, K., Tesarova, E., Prochazka, K., Tuzar, Z., Brown, W., Hybrid polymeric micelles with hydrophobic cores and mixed polyelectrolyte/nonelectrolyte shells in aqueous media. 1. Preparation and basic characterization. Langmuir, 2001. **17**(14): p. 4240-4244.

19. Gao, Z., Fain, H., Rapoport, N., Ultrasound-enhanced tumor targeting of polymeric micellar drug carriers. Mol. Pharm., 2004. **1**(4): p. 317-330.

20. Gao, Z., Fain, H., Rapoport, N., Controlled and targeted tumor chemotherapy by micellar-encapsulated drug and ultrasound. J. Controlled Release, 2005. **102**(1): p. 203-222.

21. Lee, E., Na, K., Bae, Y-H.,, Polymeric micelle for tumor pH and folate-mediated targeting. J. Controlled Release, 2003. **91**(1-2): p. 103-113.

22. Krishnadas, A., Rubinstein, I., Onyuksel, H., Sterically stabilized phospholipid mixed micelles: in vitro evaluation as a novel carrier for water-insoluble drugs. Pharm. Res., 2003. **20**(2): p. 297-302.

23. Ashok, B., Arleth, L., Hjelm, R., Rubinstein, I., Onyuksel, H., In vitro characterization of PEGylated phospholipid micelles for improved drug

solubilization: effects of PEG chain length and PC incorporation. J. Pharm. Sci., 2004. **93**(10): p. 2476-2487.

24. Wolszczak, M., Miller, J., Characterization of non-ionic surfactant aggregates by fluorometric techniques. J. Photochem. Photobiol. A, 2002. **147**(1): p. 45-54.

25. Zhao, C., Winnik, M., Riess, G., Croucher, M., Fluorescence probe techniques used to study micelle formation in water-soluble block copolymers. Langmuir, 1990. **6**: p. 514.

26. Kalyanasundaram, K., Thomas, J., Environmental effects on vibronic band intensities in pyrene monomer fluorescence and their application in studies of micellar systems. J. Am. Chem. Soc., 1977. **99**: p. 2039.

27. Winnik, F., Regismond, S., Fluorescence methods in the study of polymer-surfactant systems, in Polymer-surfactant systems, J. Kwak, Editor. 1998. p. 267-315.

28. Dong, D., Winnik, M., The Py scale of solvent polarities. Can. J. Chem., 1984. **62**: p. 2560-2565.

29. Lavasanifar, A., Samuel, J., Kwon, G., The effect of alkyl core structure on micellar properties of poly(ethylene oxide)-block-poly(L-aspartamide) derivatives. Colloids Surf. B, 2001. **22**(2): p. 115-126.

30. Winnik, F., Photophysics of preassociated pyrenes in aqueous polymer solutions and in other organized media. Chem. Rev., 1993. **93**(2): p. 587 - 614.

31. Claridge, T., High-Resolution NMR Techniques in Organic Chemistry. 1999: Pergamon.

32. Garasanin, T., Cosgrove, T., Marteaux, L., Kretschmer, A., Goodwin, A., Zick, K.,, NMR self-diffusion studies on PDMS oil-in-water emulsion. Langmuir, 2002. **18**(26): p. 10298-10304.

33. Stejskal, E., Tanner, J., Spin diffusion measurements: Spin echoes in the presence of a time-dependent field gradient. The Journal of Chemical Physics, 1965. **42**(1): p. 288-292.

34. Ambrosone, L., Ceglie, A., Colafemmina, G., Palazzo, G., Resolving complex mixtures by means of pulsed gradient spin-echo NMR experiments. Phys. Chem. Chem. Phys., 2002. **4**: p. 3040-3047.

35. Griffiths, P., Stilbs, P., Adsorption fractionation studies by size-resolved pulsed-gradient spin-echo-NMR. Langmuir, 1995. **11**: p. 898-904.

36. Tirosh, O., Barenholz, Y., Katzhendler, J., Priev, A., Hydration of polyethylene glycol-grafted liposomes. Biophys. J., 1998. **74**(3): p. 1371-9.

37. Torchilin, V., Trubetskoy V., Which polymers can make nanoparticulate drug carriers long-circulating? Adv. Drug Deliv. Rev., 1995. **16**: p. 141-155.

38. Adams, M., Kwon, G., The effects of acyl chain length on the micelle properties of poly(ethylene oxide)-block-poly(N-hexyl-L-aspartamide)-acyl conjugates. J. Biomater. Sci., Polym. Ed., 2002. **13**(9): p. 991-1006.

39. Holland, P., Modeling mixed surfactant systems, in Mixed surfactant systems, P. Holland, Rubingh, D., Editor. 1992. p. 31-44.

40. Nishikido, N., Thermodynamic models for mixed micellization, in Mixed surfactant systems, K. Ogino, Abe, M., Editor. 1993. p. 23-61.

41. Nagayama, T., Hashidzume, A., Morishima, Y., Characterization of self-association in water of polycations hydrophobically modified with hydrocarbon and siloxane chains. Langmuir, 2002. **18**(18): p. 6775-6782.

42. Vakil, R., Kwon, G., PEG-phospholipid micelles for the delivery of amphotericin B. J. Controlled Release, 2005. **101**(1-3): p. 386-9.

Chapter 5:

Polymeric micelles for combination antifungal therapy involving amphotericin B, rapamycin and 5-fluorocytosine

---

A version of this chapter will be submitted for publication in *Antimicrobial Agents and Chemotherapy* in December 2006.

5.1 Introduction

The increasing incidence of hospital acquired opportunistic fungal infections is of concern, particularly in the context of a growing population of patients with compromised or suppressed immune systems (1). Amphotericin B solubilized as a colloidal dispersion by sodium deoxycholate (D-AmB) is a first-line antifungal agent administered to most patients with invasive candidiasis, despite severe kidney toxicity (2). Liposomal amphotericin B (L-AmB) is less toxic compared to D-AmB allowing for dose-escalation and improved tolerability; however, L-AmB has lower antifungal activity at equal doses necessitating significantly higher doses for comparable efficacy, raising doubts about a meaningful increase in the therapeutic index (3). Notably, L-AmB has not had a significant impact on the crude or attributable mortality compared to D-AmB (4).

There is a renewed interest in studying combinations of antifungal drugs to explore potential advantages such as broad-spectrum efficacy, indifferent or synergistic potency, improved safety and tolerability and a reduction of resistant organisms (5, 6). There is growing evidence that the combination of D-AmB and 5-fluorocytosine (5-FC) has better activity against candidiasis compared to D-AmB (7-10). The *in vitro* antifungal effects of the combination of D-AmB and 5-FC are synergistic or indifferent, depending on the species of *Candida*: *C. albicans* (synergistic and indifferent), *C. glabrata* (indifferent) and *C. krusei* (indifferent) (6). It is hypothesized that AmB potentiates 5-FC activity by increasing the penetration of 5-FC across fungal membranes, highlighting the value of exposing the fungal pathogen to 5-FC at the same time or after exposure to AmB (11). Recently, D-AmB

in 5 % dextrose and 5-FC in 0.9 % NaCl, injected intraperitoneally as separate and rapid sequential injections showed additive activity in a murine model of candidiasis according to the response-surface model (12).

Rapamycin is a potent antifungal which exerts activity by inhibiting TOR kinases leading to cell cycle arrest (MIC against C. *albicans* < 0.02 mg/L) (13, 14). Early animal experiments showed effectiveness against *Candida* infection, however, enthusiasm for use as an antifungal agent were lowered on emergence of potent immunosuppression in hosts (15). Rapamycin-analogues that selectively bind yeast TOR kinases present a thousand-fold reduction in immunosuppressive activity, while retaining some measure of antifungal activity (MIC < 3 mg/L for C. *albicans* and C. glabrata) (16). The TOR signaling cascade represents a conserved pathway across yeast, involved in eliciting a cellular response to a wide variety of stimuli including nutrients and external stress (17). Considering the unique mechanism of action, this class of antifungal antibiotics has unexplored potential for treatment of systemic fungal disease. The AmB – rapamycin combination has a high potential for cooperative interaction through a simultaneous exposure to cationic stress and ATP depletion induced by AmB, combined with inhibition of yeast survival pathways. Rapamycin is very poorly water-soluble and has proven to be highly challenging for drug solubilization requiring analogues for clinical trials in cancer.

Several strategies have emerged which are beneficial in lowering AmB related toxicities. There is recent clinical evidence which suggests that D-AmB administered as a continuous infusion over 24 h results in a lower incidence of nephrotoxicity and infusion-related side-effects compared to the standard 2 – 4 h infusion at an equal

dose (18-20). Although the mechanism for lowered toxicities is poorly understood, it is proposed that slow infusion results in lower levels of protein-bound drug capable of evoking host toxicity, compared to the standard infusion regimen (21). Saline loading during AmB therapy has been shown to reduce the severity of AmB related toxicities. In a double-blind, placebo-controlled study with human subjects, sodium supplementation has been shown to diminish infusion-related side effects and nephrotoxicity caused by D-AmB (22).

Combination antifungal therapy involving AmB has been restricted by poor physical stability and compatibility with antifungal drugs and vehicles, especially in the form of D-AmB. D-AmB is not compatible with saline and precipitates instantly on dilution (23). Although saline loading has gained some degree of acceptance, this procedure necessitates sequential administration of saline and D-AmB and special care must be taken to adequately flush infusion lines with 5 % dextrose prior to D-AmB administration to avoid potentially hazardous drug precipitation. Multiple-agent therapy with continuous administration of D-AmB would require additional intravenous (IV) access-lines owing to incompatibility, raising concern of increased risk of infection in these critically ill patients.

We have previously reported that micelles formed from the amphiphilic polymer 1,2-Distearoyl-*sn*-glycero-3-phosphoethanolamine-*N*-methoxy poly(ethylene glycol) (PEG-DSPE) readily solubilize AmB (AmB|PEG-DSPE) (24). In this work, we report that PEG-DSPE micelles also encapsulate high levels of rapamycin when prepared using an identical solvent evaporation method (rapamycin|PEG-DSPE). AmB is stably incorporated in PEG-DSPE micelles in a form which is compatible

with rapamycin and 5-FC in 0.9 % NaCl. We have evaluated the *in vitro* activity of two- and three-drug combinations using a broth microdilution method. Interactive effects have been quantified by two methods used in the literature: FIC index, combination index calculated using median dose-effect equation.

5.2 Materials

AmB was obtained as a gift from Alpharma (Copenhagen, Denmark). Rapamycin and 5-FC were purchased from LC Labs (Woburn, MA) and Sigma (St. Louis, MO), respectively. AmB formulated in sodium deoxycholate (conventional AmB, D-AmB) was purchased from Sigma (St. Louis, MO). The drugs were stored at -20 °C until use. PEG-DSPE (M_n =5800 g/mol) was obtained from Avanti Polar Lipids (Alabaster, AL). All other reagents used were of analytical grade and were used without further purification.

5.3 Micelle preparation and incorporation of AmB and rapamycin

PEG-DSPE (6.0 mg/mL in chloroform) was mixed with AmB (0.25 mg/mL in methanol) or rapamycin (1 mg/mL in chloroform) in a round bottom flask. The organic solvent was evaporated under vacuum to produce a thin film of co-precipitated drug and polymer. This film was dissolved in 10 mM HEPES, pH 7.0 and incubated at room temperature for 10 min to allow for complete equilibration. The micellar solution was filtered through a 0.45-μm polyethersulfone (PES) filter. Empty micelles were prepared using an identical procedure without drug. The concentration of AmB was quantified by diluting a 50 μL aliquot of AmB in 1.95 mL

DMF and observing absorbance at 413.5 nm. This assay was tested for linearity in the 0.02 – 0.8 mg/mL range. For determination of rapamycin content, 5 μL samples were injected into 4.6mm x 50mm Ace 3 C18 reversed-phase column and absorbance detected at 277 nm. The column was maintained at 25 °C and eluent flow rate was set at 1 mL/min. The eluent composition was linearly varied by mixing methanol and a 1:1 methanol – 50 mM acetic acid mixture over 4 min. The assay was tested for linearity in the 0.1 - 100 μg/mL range.

5.4 Micelle Characterization

5.4.1 Dynamic Light Scattering

Hydrodynamic diameters were determined using dynamic light scattering using the NICOMP ZLS380 particle sizer (Particle Sizing Systems, Santa Barbara, CA) equipped with a 639 nm laser at a fixed angle of 90°. Data was acquired to have greater than 100k counts in Channel 1. The light scattering data was interpreted using Gaussian and NICOMP analyses. The NICOMP analysis permits deconvolution of light scattering data into multimodal distributions. Particle sizes were expressed as volume-weighted diameters.

5.4.2 Size exclusion chromatography

Aqueous micellar solutions were diluted to 1.0 mg/mL polymer content in water. 100 μL samples were injected in triplicate onto a Shodex PROTEIN KW-804 size exclusion column (Showa Denko, Japan). The column was equilibrated using water. The flow rate was maintained at 0.75 mL/min, and the column compartment

maintained at 10 °C. The elution of empty polymeric micelles was monitored using refractive index. Elution of AmB was detected using its absorbance at 412 nm.

5.5 Solution turbidity measurements

Precipitation of D-AmB was studied by observing solution turbidity (OD_{650nm}) using a Cary 50 UV spectrophotometer equipped with a dip probe. Aqueous solutions containing 0.9 % NaCl or 5 % dextrose were maintained at 25 °C in a water-jacketed beaker. OD_{650nm} was observed for the initial 2.0 min to estimate baseline turbidity. Thereafter, D-AmB was added to aqueous medium and changes in OD_{650nm} were observed over the duration of the experiment. The final concentration of AmB was 0.1 mg/mL. Changes in solution turbidity on the addition of AmB|PEG-DSPE to 0.9 % NaCl and 0.9 % dextrose were similarly measured. Further, the potential for precipitation on mixing AmB|PEG-DSPE, rapamycin|PEG-DSPE and 5-FC was examined using an identical procedure.

5.6 *In vitro* susceptibility of fungal isolates

5.6.1 Estimation of Minimum Inhibitory Concentration (MIC)

C. albicans 98-17, *C. albicans* 98-234 and *C. albicans* K-1 were maintained on SDA plates. Susceptibility of yeast isolates was performed using broth microdilution in RPMI-1640 (supplemented with 0.165 M morpholinepropanesulfonic acid, buffered to pH 7.0) according to procedures recommended in NCCLS M27-A2 (25). Test drug solutions were incubated with yeast inoculum at 35 °C in 96-well plates. All measurements were done in triplicate.

C. *albicans* 98-17 and 98-234 were incubated for a 24 h period, while C. *albicans* K-1 were incubated for 48 h to allow for sufficient growth. Percent yeast growth relative to drug-free control was determined by measuring optical density (OD) at 650 nm, using the Microplate EL 312e plate reader. Minimum inhibitory concentration (MIC) values represent drug concentrations which resulted in > 95 % inhibition of fungal growth relative to drug-free control. The MIC values were expressed as a mean of three determinations.

5.6.2 Interactive effects of drug-combinations

The interactive effects of drug combinations were assessed using a checkerboard layout. For a two-drug combination the concentration of each drug was varied, for a constant level of the other drug. For a three-drug combination, the ratio of AmB|PEG-DSPE: rapamycin|PEG-DSPE was fixed at 1:2 or 2:1 and the levels of 5-FC were varied for a constant level of the AmB|PEG-DSPE - rapamycin|PEG-DSPE combination. Determination of fungal growth in response to drug combinations was performed in triplicate. Interactive effects were interpreted using two methods extensively used in the literature: FIC analysis (6) and calculation of a combination index using a median-effect equation (26, 27).

FIC analysis:

The FIC index (FICI) for a three drug combination is defined by the equation:

$$FICI = \frac{MIC_{A-combination}}{MIC_A} + \frac{MIC_{B-combination}}{MIC_B} + \frac{MIC_{C-combination}}{MIC_C}$$

where, $MIC_{A\text{-combination}}$ and MIC_A represent the concentration of "drug A" which leads to greater than 95 % inhibition of fungal growth in combination with "drug B" and "drug C", and as a single agent, respectively. The FICI values have been interpreted to indicate synergism, additivity or antagonism according to the recommendations in the literature (5, 28-30) for the interpretation of FIC index values and have been shown in Table 5.4.

Combination indices using median-effect response:

Calculation of a combination index for a drug combination was done in two steps. First, inhibition of fungal growth in response to varying concentrations of single-drug was fit to median-effect function:

$$f_a = \frac{1}{1+(D_m/D)^m}$$

where f_a is the mean growth inhibition, relative to drug-free control, D_m is the drug concentration for a 50 % growth inhibition, and m is the slope-factor describing the dose-response curve. Parameter D_m and m for each drug were estimated by non-linear regression using SigmaPlot (v. 9.0).

The combination index was estimated on the assumption of mutually exclusive effects using the CombiTool software using the following equation:

$$CI = \frac{D_{A-combination}}{D_{A,fa}} + \frac{D_{B-combination}}{D_{B,fa}} + \frac{D_{C-combination}}{D_{C,fa}}$$

where $D_{A\text{-combination}}$, $D_{B\text{-combination}}$ and $D_{C\text{-combination}}$ are concentrations of "drug A", "drug B" and "drug C" which in combination produce a growth inhibition, f_a. $D_{A,fa}$, $D_{B,fa}$ and $D_{C,fa}$ are corresponding drug concentrations which produce f_a inhibition by themselves. $D_{A,fa}$, $D_{B,fa}$ and $D_{C,fa}$ were calculated using the median-effect equation, knowing D_m and m. Combination indices were represented as color maps using Origin software (version 7.0). The graphs have been color-coded to represent synergism (dark blue), moderate antagonism (light blue), indifference (green) and antagonism (red), according to the ranges in Table 5.4.

5.7 Results and Discussion

5.7.1 Micelle Characterization

AmB could be efficiently solubilized by PEG-DSPE micelles (AmB|PEG-DSPE) using the solvent evaporation method, as described in chapter 2 (Table 5.1). Additionally, incorporation of AmB in PEG-DSPE micelles resulted in drug deaggregation owing to polymer – drug interactions (24). High levels of rapamycin could be loaded into PEG-DSPE micelles (rapamycin|PEG-DSPE) using a similar procedure. The level of rapamycin solubilized was ca. 0.38 mg/mL, with a high yield (93 % of initial drug). Using dynamic light scattering, the hydrodynamic diameter of AmB|PEG-DSPE micelles (PEG-DSPE: AmB = 2.0) was determined to be 19.3 ± 4.4

nm, slightly larger than empty PEG-DSPE micelles (16.1 ± 2.2 nm). The size of rapamycin|PEG-DSPE micelles was similarly small, 26.4 ± 2.0 nm.

	Fraction of initial drug encapsulated	Drug loading % w/w	Level of drug solubilized, mg/mL	Diameter (nm)[a]
PEG-DSPE	-	-	-	16.1 ± 2.2
AmB|PEG-DSPE	0.78 ± 0.03	7.21	0.38 ± 0.12	19.3 ± 4.4
Rapamycin|PEG-DSPE	0.93 ± 0.15	7.76	0.37 ± 0.06	26.4 ± 2.0

Table 5.1 Solubilization of AmB and Rapamycin by PEG-DSPE micelles
[a] volume-weighted Gaussian average

We have studied changes in solution turbidity on addition of D-AmB to 0.9 % NaCl or 5 % dextrose solutions using a spectrophotometer equipped with a dip-probe assembly. There was an instantaneous increase in solution turbidity on addition of D-AmB to 0.9 % NaCl, indicative of rapid precipitation on mixing (Figure 5.1-a). Addition D-AmB to 5 % dextrose did not result in increased solution turbidity, consistent with the conventional use of 5 % dextrose as acceptable vehicle for dilution of D-AmB (Figure 5.1-b). In contrast, addition of AmB|PEG-DSPE and rapamycin|PEG-DSPE to 5-FC in 0.9 % NaCl led to a minor increase in OD_{650nm}, attributed to light scattering by intact PEG-DSPE micelles (Figure 5.1-c). AmB eluted with intact PEG-DSPE micelles with no appearance of free AmB, when incubated with rapamycin|PEG-DSPE and 5-FC in saline at 37 °C for several hours, indicating that AmB is stably solubilized in PEG-DSPE micelles (Figure 5.2). Results from dynamic light scattering indicated negligible changes in the size of AmB|PEG-DSPE

micelles several hours after mixing with rapamycin|PEG-DSPE and 5-FC in 0.9 % NaCl. Importantly, this study did not find drug aggregates in solution (Figure 5.3).

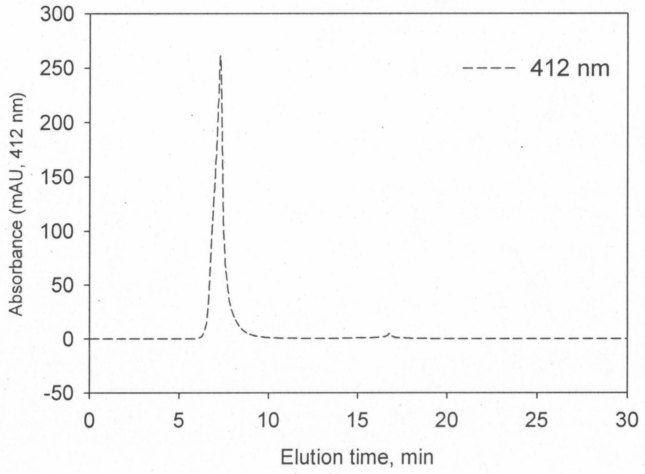


Figure 5.2. SEC of AmB|PEG-DSPE, rapamycin|PEG-DSPE and 5-FC in 0.9 % NaCl[a,b]
[a] incubation at 37 °C for 4.5 h. [b] 40 μg/mL AmB|PEG-DSPE, 40 μg/mL rapamycin|PEG-DSPE, 2 mg/mL 5-FC. Column: Shodex PROTEIN-KW804. Eluent: Water at 0.75 mL/min. Column temperature: 10 °C.

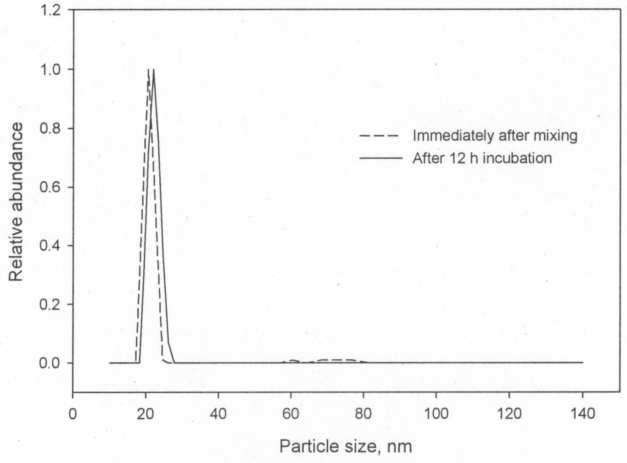


Figure 5.3 Sizing of AmB|PEG-DSPE, rapamycin|PEG-DSPE and 5-FC mixture in 0.9 % NaCl using DLS. ***a.*** immediately after mixing ***b.*** after incubation for 12 h at room temperature.

These results are particularly encouraging from a delivery perspective, since AmB|PEG-DSPE may be suitable for slow infusion over several hours without concern for drug precipitation on dilution. In this form, AmB has a distinct advantage over D-AmB, since it may allow for simultaneous administration of saline via a single IV access-line. Since AmB|PEG-DSPE remains solubilized when mixed with 5-FC and solubilized rapamycin, it may become possible to explore for benefit of drug combinations over monotherapy.

5.7.2 In vitro susceptibility studies

In vitro susceptibility of *C. albicans* 98-17, *C. albicans* 98-234 and *C. albicans* K-1 was evaluated using the broth microdilution method. MIC values for AmB|PEG-DSPE were 0.05 μg/mL. The MIC for D-AmB, in which the drug is highly self-aggregated, was 0.25 μg/mL (Table 5.2).

	Strain of *C. albicans*		
	98-17	98-234	K-1
D-AmB	0.25	0.25	0.25
AmB| PEG-DSPE	0.05	0.05	0.05
Rapamycin| PEG-DSPE	0.05	0.05	0.05
5-FC	0.1	0.1	0.1

Table 5.2. Minimum Inhibitory Concentrations (MIC) in mg/L against C. *albicans* isolates

PEG-DSPE did not exhibit intrinsic antifungal activity (MIC > 10 μg/mL). The reason for enhanced activity of PEG-DSPE encapsulated AmB is unclear – however a similar potentiation of AmB activity has been demonstrated on

encapsulation in mixed micelles formed from poly(ε-caprolactone) and poloxamer 188 (31).We hypothesize that in contrast with D-AmB that produces a mixture of monomers and water soluble aggregates, AmB dissociated from intact PEG-DSPE micelles is predominantly in a monomeric form, which results in a higher number of membrane-active units compared to the D-AmB. The MIC of rapamycin in PEG-DSPE micelles was 0.05 mg/L, which is comparable to that for free rapamycin reported in the literature (14). The MIC for 5-FC, corresponding to complete inhibition of fungal-growth was 0.1 mg/L – consistent with some literature reports (10, 32).

	Strain of *Candida albicans*					
	98-17		98 – 234		K-1	
	$D_m \times 10^3$	m	$D_m \times 10^3$	m	$D_m \times 10^3$	m
AmB| PEG-DSPE	17.3 ± 0.2	6.0 ± 0.2	11.3 ± 0.4	6.5 ± 0.5	19.6 ± 0.4	5.1 ± 0.3
Rapamycin|PEG-DSPE	32.3 ± 2.2	6.5 ± 2.2	24.2 ± 0.9	3.5 ± 0.5	15.4 ± 1.7	6.0 ± 2.4
5-FC	70.7 ± 7.3	2.0 ± 0.8	39.8 ± 0.1	1.9 ± 0.4	54.9 ± 4.9	1.3 ± 0.2

Table 5.3. Best fit parameters to median-effect equation, $f_a = \frac{1}{1+(D_m/D)^m}$

Table 5.3 shows parameters obtained by fitting the dose-response curve for AmB|PEG-DSPE, rapamycin|PEG-DSPE or 5-FC to the median-effect equation. Reasonable fits to the data were obtained using non-linear regression, judged by R^2 values greater than 0.9. D_m represents drug potency, corresponding to the drug concentration for 50 % inhibition and the slope-factor m represents the shape of the

dose-response curve. D_m for AmB|PEG-DSPE and rapamycin|PEG-DSPE varied from 0.01 to 0.02 mg/L or 0.02 to 0.03 mg/L, respectively – consistent with low MIC values. A high value for the shape factor, m for both AmB|PEG-DSPE and rapamycin|PEG-DSPE implied transition from no inhibition to complete growth inhibition over a narrow range of concentration. D_m for 5-FC varied from 0.04 to 0.07 mg/L, depending on the isolate tested and the shape factor ranged from 1.2 to 2.0, lower in comparison with AmB|PEG-DSPE and rapamycin|PEG-DSPE.

We have studied interactive effects of AmB|PEG-DSPE, rapamycin|PEG-DSPE and 5-FC as two- and three-drug combinations using a checkerboard layout. The complexity of assessing drug interactions has been stressed in the literature (5, 10, 33). Calculation of FIC indices have been most extensively used for evaluating interactive effects between antimicrobial combinations. A limitation of the FIC analysis is that this analysis presumes that drug interactions are unvariant and apply across all concentrations. Several methods have been proposed to study drug interactions over an appropriate concentration range and have been reviewed in detail by Greco (34). The response surface method proposed by Greco et al. (35) and the method of Chou and Talalay using the median-effect equation (26, 30) have been frequently used in studying antiviral and antineoplastic drug interactions, each with a set of important underlying assumptions and limitations. An advantage of the method of Chou and Talalay is that it allows visualization of the combination index for different drug ratios – an important goal in studying drug combinations, *in vitro*. This approach has particular utility when the drug combination under study shows cooperativity for some ratios and antagonism at other ratios. We have calculated

allow for an increase in antifungal activity in situations when dose-escalation is not an option. Mechanistic studies of drug-interactions were outside the scope of this work – however, it appears that these antifungal drugs act by relatively independent mechanisms. This combination may present a strategy which combines the rapid fungicidal action of AmB|PEG-DSPE with low doses of rapamycin|PEG-DSPE, which may work well as consolidation or clearance therapy. The temporal effect of drug exposure was also outside the scope of this work, however, represents an exciting avenue for further work.

	C. *albicans* K-1	C. *albicans* 98-17	C. *albicans* 98-234
AmB|PEG-DSPE – Rapamycin|PEG-DSPE	1.1	1.3 (1.1 – 1.6)	1
AmB|PEG-DSPE – 5-FC	1.1 (0.8 – 1.5)	0.6	0.8
Rapamycin|PEG-DSPE – 5-FC	1	1	1
AmB|PEG-DSPE – Rapamycin|PEG-DSPE – 5-FC	1.1 (0.8 – 1.6)	0.7 (0.4 – 0.8)	0.45 (0.4 – 0.5)

Table 5.5. Fractional inhibitory concentration (FIC) analysis for test isolates against AmB – Rapamycin – 5-FC combinations after 24 h. Results are expressed as mean (range) for test-replicates

The 5-FC – AmB combination has been extensively studied *in vitro* and in animal models (5, 12). The FICI values for the 5-FC – AmB|PEG-DSPE ranged from 0.6 – 0.8, for C. *albicans* 98-17 and 98-234, indicating that this combination exerted moderately synergistic behavior. The FICI values for C. *albicans* K-1 ranged from 0.8 – 1.5 indicating indifference for this isolate. The varying nature of the interaction is consistent with earlier reports that indicate that the D-AmB – 5-FC interaction is variable and depends on experimental conditions and on the isolate tested (10, 33). A

majority of the isolates studied in the literature reported indifferent activities, whereas the interaction was synergistic for some isolates. Moderate antagonism has been reported in a small fraction of C. *albicans* isolates tested (37).

Drug combinations with a high proportion of 5-FC relative to AmB|PEG-DSPE had combination index values less than 0.5 indicating synergistic potential. The interaction profile for C. *albicans* K-1 demonstrates moderate antagonism for intermediate concentrations of 5-FC, however, the interaction was synergistic for higher ratios of 5-FC: AmB|PEG-DSPE (Figures 5.4, 5.6, 5.8). The mechanism of cooperative interaction between 5-FC and AmB|PEG-DSPE is not well understood, however, higher penetration of 5-FC through the yeast cell-membrane in the presence of D-AmB has been proposed. It is noted that nystatin, structurally related to AmB exerted an antagonistic interaction with 5-FC (38). Alternatively, D-AmB is thought to influence processes that transport 5-FC out of the yeast cells (5).

The combination of 5-FC with rapamycin|PEG-DSPE was indifferent with FICI equal to 1 for the three isolates tested. The combination index analysis indicated a trend similar to the 5-FC – AmB|PEG-DSPE combination, with a moderately synergistic interaction at high 5-FC: rapamycin|PEG-DSPE ratios for C. *albicans* 98-17 and 98-234. This aspect of the drug interaction was missed by the FIC analysis, which concludes additivity based on concentrations required to completely inhibit fungal growth. The interaction profile for C. *albicans* K-1 was similar to C. *albicans* 98-17 and 98-234, indicating synergy at high 5-FC levels relative to rapamycin|PEG-DSPE.

The three-drug combination of 5-FC, AmB|PEG-DSPE and rapamycin|PEG-DSPE resulted in a moderately synergistic interaction for C. *albicans* 98-17 and 98-234, with the FICI ranging from 0.4 to 0.8, consistently lower than 1. The interaction for C. *albicans* K-1 was variable and indifferent since the FICI ranged from 0.8 to 1.6 (Figures 5.5, 5.7 and 5.9). Moderate synergism is observed at high 5-FC: (AmB|PEG-DSPE + rapamycin|PEG-DSPE) ratios. However it is interesting to note that cooperativity is observed over a greater range of concentrations compared to pair-wise combinations. It appears that while AmB|PEG-DSPE and rapamycin|PEG-DSPE are largely indifferent, the three-drug combination derives synergistic potency from interactions between 5-FC – AmB|PEG-DSPE and 5-FC – rapamycin|PEG-DSPE. We would like to call attention to the fact that complete inhibition of fungal growth was observed for C. *albicans* 98-17 and 98-234 for ternary mixtures containing less than 0.03 mg/L AmB|PEG-DSPE, 0.03 mg/L rapamycin|PEG-DSPE and 0.08 mg/L 5-FC. For C. *albicans* K-1, moderate antagonism was noted at intermediate concentrations of 5-FC, similar to that observed for the 5-FC – AmB|PEG-DSPE combination. It is not clear why the three-drug combination resulted in a higher antagonism compared with AmB|PEG-DSPE in C. *albicans* K-1.

In summary, there was good agreement between results obtained from FIC analysis and those obtained from the method Chou and Talalay, using the median-effect equation. Each drug pair represented indifferent or moderately synergistic interactions. This analysis points to drug combinations with a high 5-FC: AmB|PEG-DSPE and AmB: rapamycin|PEG-DSPE as an interesting area for further exploration. It must be emphasized that although *in vitro* studies provide an excellent frame-work

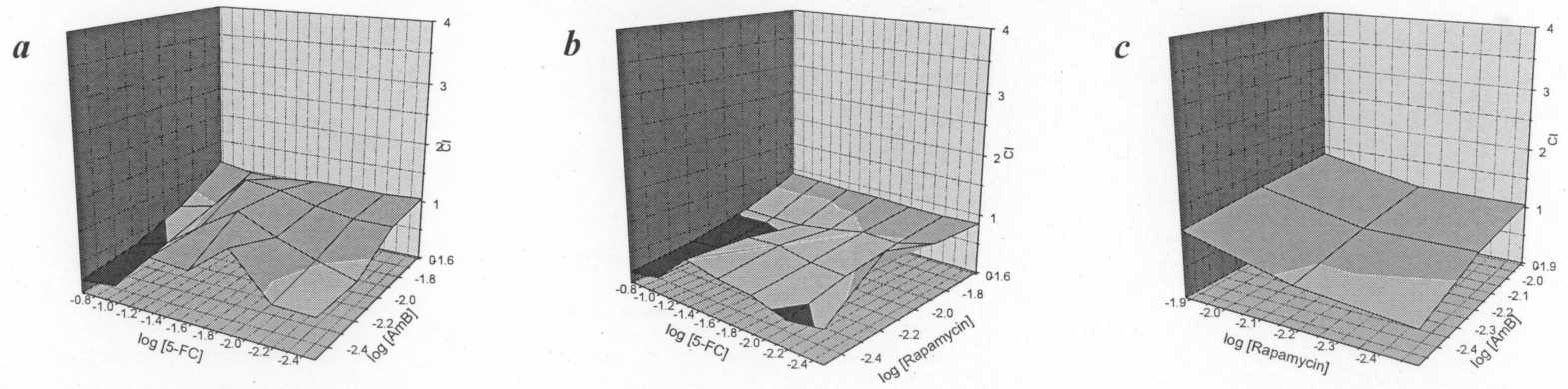


Figure 5.4. Combination index values for ***a.*** 5-FC – AmB|PEG-DSPE ***b.*** 5-FC – rapamycin|PEG-DSPE ***c.*** rapamycin|PEG-DSPE - AmB|PEG-DSPE combinations against C. *albicans* 98-17



Figure 5.5. Combination index values for 5-FC – AmB|PEG-DSPE – rapamycin|PEG-DSPE combinations for AmB|PEG-DSPE : rapamycin|PEG-DSPE ***a.*** 1:2 ***b.*** 2:1 for C. *albicans* 98-17

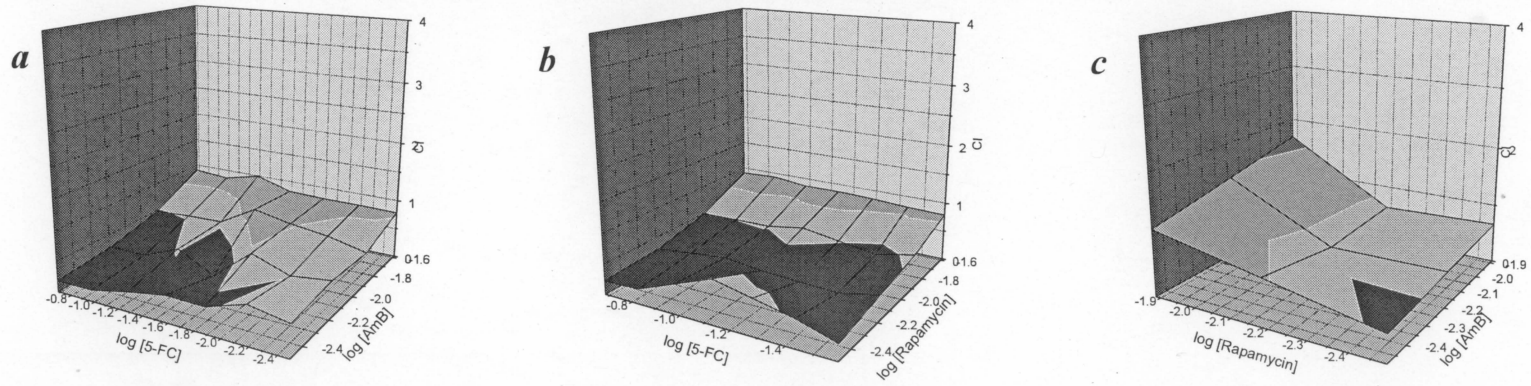


Figure 5.6 Combination index values for ***a.*** 5-FC – AmB|PEG-DSPE ***b.*** 5-FC – rapamycin|PEG-DSPE ***c.*** rapamycin|PEG-DSPE - AmB|PEG-DSPE combinations against C. *albicans* 98-234

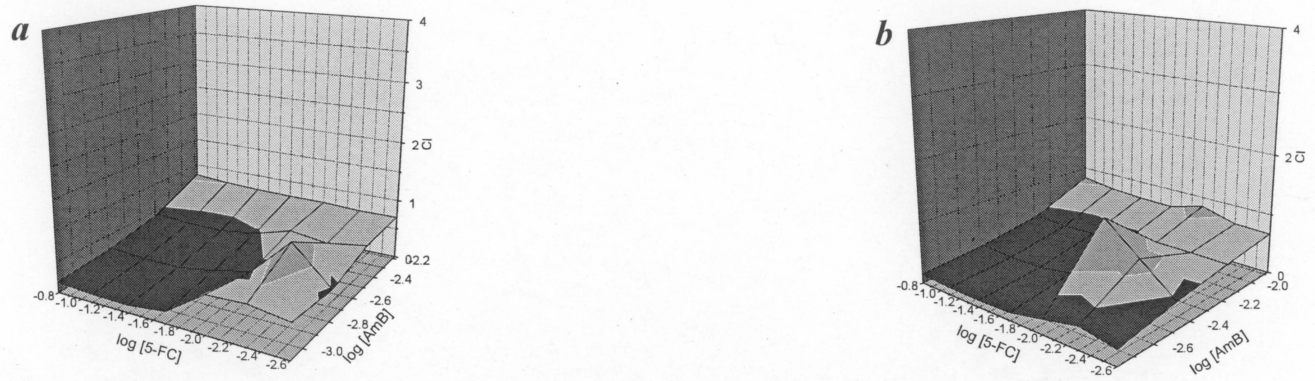


Figure 5.7 Combination index values for 5-FC – AmB|PEG-DSPE – rapamycin|PEG-DSPE combinations for AmB|PEG-DSPE : rapamycin|PEG-DSPE ***a.*** 1:2 ***b.*** 2:1 for C. *albicans* 98-234

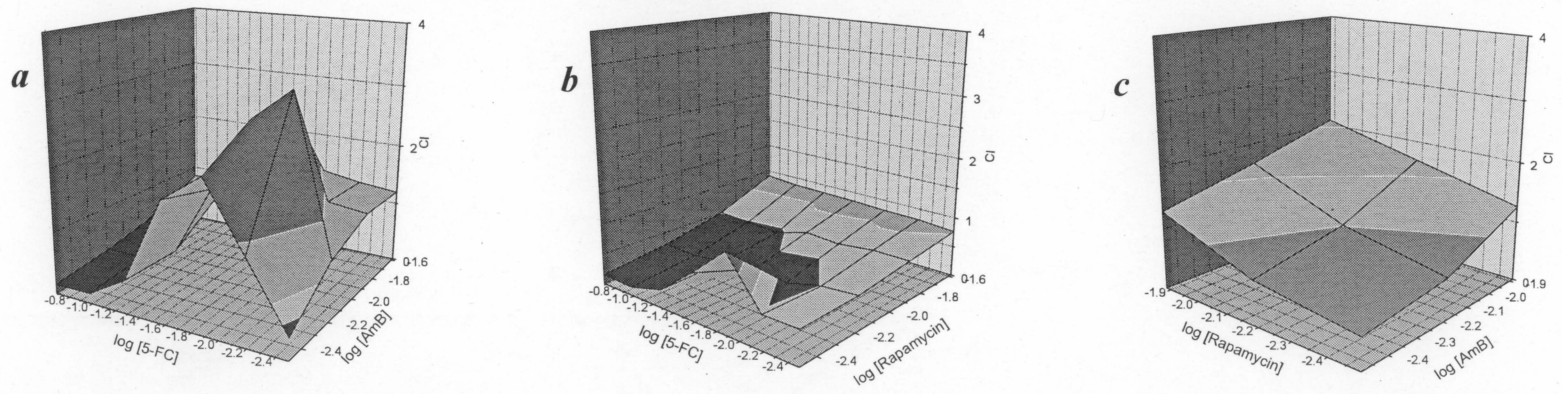


Figure 5.8 Combination index values for ***a.*** 5-FC – AmB|PEG-DSPE ***b.*** 5-FC – rapamycin|PEG-DSPE ***c.*** rapamycin|PEG-DSPE - AmB|PEG-DSPE combinations against C. *albicans* K-1



Figure 5.9 Combination index values for 5-FC – AmB|PEG-DSPE – rapamycin|PEG-DSPE combinations for AmB|PEG-DSPE : rapamycin|PEG-DSPE ***a.*** 1:2 ***b.*** 2:1 for C. *albicans* K-1

for studying drug interactions, there has been poor correlation with results *in vivo* (5). Numerous factors such as drug pharmacokinetics, fungal burden and state of immunosuppression play have been thought to play an important role in outcome *in vivo*. Further experiments in animal models are required to validate our *in vitro* observations.

5.8 Conclusions

AmB|PEG-DSPE represents an interesting alternative to D-AmB, with significant advantages in the context of combination therapy. In this form, AmB is stable against precipitation in a saline vehicle over prolonged periods of time, which may enable slow or continuous administration of AmB with simultaneous sodium supplementation in a single IV access-line. Contrary to L-AmB, which exerts lower activity compared to D-AmB, AmB|PEG-DSPE retains potent antifungal *in vitro* efficacy. Additionally, in this form AmB may be mixed with other antifungal agents such 5-FC and rapamycin|PEG-DSPE, allowing further exploration of combination therapy for the treatment of invasive mycoses in animal models.

In this preliminary investigation, we observed indifferent or moderately synergistic activity for pair-wise drug combinations against C. *albicans* isolates tested. Drug combinations with a high ratio of 5-FC:AmB|PEG-DSPE and 5-FC:rapamycin|PEG-DSPE exhibited cooperative interactions and are of interest since they enable a reduction of 5-FC levels in the presence of low levels of AmB|PEG-DSPE and rapamycin|PEG-DSPE. Additionally, drug combinations may present a broad range activity, particularly in the context of resistant isolates. *In vitro* studies

indicate that the three-drug combination was favorable over a wider range of drug ratios compared to pair-wise combinations, presumably due to cooperative 5-FC – AmB|PEG-DSPE and 5-FC – rapamycin|PEG-DSPE interactions.

This formulation holds promise for efficacy against disseminated candidiasis, with some improvement in toxicity over D-AmB – particularly in conjunction with saline loading and slow administration. Further validation of this hypothesis is required in animal models.

5.9 References

1. Gudlaugsson, O., Gillespie, S., Lee, K., Vande Berg, J., Hu, J., Messer, S., Herwaldt, L., Pfaller, M., Diekema, D., Attributable mortality of nosocomial candidemia, revisited. Clin. Infect. Dis., 2003. **37**(9): p. 1172-7.

2. Spellberg, B., Filler, S., Edwards, J., Current treatment strategies for disseminated candidiasis. Clin. Infect. Dis., 2006. **42**(2): p. 244-51.

3. Dupont, B., Overview of the lipid formulations of amphotericin B. J. Antimicrob. Chemother., 2002. **49 Suppl. 1**: p. 31-6.

4. Walsh, T., Finberg, R., Arndt, C., Hiemenz, J., Schwartz, C., Bodensteiner, D., Pappas, P., Seibel, N., Greenberg, R., Dummer, S., Schuster, M., Holcenberg, J., Dismukes, W., Liposomal amphotericin B for empirical therapy in patients with persistent fever and neutropenia. N. Engl. J. Med., 1999. **340**(10): p. 764-771.

5. Johnson, M., Macdougall, C., Ostrosky-Zeichner, L., Perfect, J., Rex, J.,, Combination antifungal therapy. Antimicrob. Agents Chemother., 2004. **48**(3): p. 693-715.

6. Mukherjee, P., Sheehan, D., Hitchcock, C., Ghannoum, M., Combination treatment of invasive fungal infections. Clin. Microbiol. Rev., 2005. **18**(1): p. 163-94.

7. Kume, H., Murase, S., Mochizuki, M., Combined effect of antifungal agents - fundamental study on amphotericin B and flucytosine. Jpn. J. Med. Mycol., 1985. **26**: p. 126-132.

8. Sobel, J., Combination therapy for invasive mycoses: Evaluation of past clinical trial designs. Clin. Infect. Dis., 2004. **39 Suppl. 4**: p. S224-7.

9. Arroyo, J., Medoff, G., Kobayashi, G. S., Therapy of murine aspergillosis with amphotericin B in combination with rifampin of 5-fluorocytosine. Antimicrob. Agents Chemother., 1977. **11**(1): p. 21-25.

10. Te Dorsthorst, D., Verweij, P., Meletiadis, J., Bergervoet, M., Punt, N., Meis, J., Mouton, J., In vitro interaction of flucytosine combined with amphotericin B or fluconazole against thirty-five yeast isolates determined by both the fractional inhibitory concentration index and the response surface approach. Antimicrob. Agents Chemother., 2002. **46**(9): p. 2982-9.

11. Medoff, G., Kobayashi, G., Kwan, C., Schlessinger, D., Venkov, P., Potentiation of rifampicin and 5-fluorocytosine as antifungal antibiotics by amphotericin B (yeast-membrane permeability-ribosomal RNA-eukaryotic cell-synergism). Proc. Natl. Acad. Sci., 1972. **69**(1): p. 196-9.

12. Hope, W., Warn, P., Sharp, A., Reed, P., Keevil, B., Louie, A., Denning, D., Drusano, G., Surface response modeling to examine the combination of amphotericin b deoxycholate and 5-fluorocytosine for treatment of invasive candidiasis. J. Infect. Dis., 2005. **192**: p. 673-680.

13. Vezina, C., Kudelski, A., Sehgal, S., Rapamycin (AY-22,989), a new antifungal antibiotic I. Taxonomy of the producing streptomycete and isolation of the active principle. J. of Antibiotics, 1975. **28**: p. 721-726.

14. Baker, H., Sidorowicz, A., Sehgal, S.., Vezina, C., Rapamycin (AY-22,989), a new antifungal antibiotic III. In vitro and in vivo evaluation. J. Antibiotics, 1978. **31**: p. 539-545.

15. Kahan, B., Camardo, J., Rapamycin: clinical results and future opportunities. Transplantation, 2001. **72**: p. 1181-1193.

16. Dickman, D., Ding, H., Li, Q., Nilius, A., Balli, D., Ballaron, S., Trevillyan, J., Smith, M., Seif, L., Kim, L., Sarthy, A., Goldman, R., Plattner, J., Bennani Y., Antifungal rapamycin analogues with reduced immunosuppressive activity. Bioorg. Med. Chem Lett., 2000. **10**: p. 1405-1408.

17. Rohde, J., Heitman, J., Cardenas, M., The TOR kinases link nutrient sensing to cell growth. J. Biol. Chem., 2001. **276**(13): p. 9583-6.

18. Imhof, A., Walter, R.B., Schaffner, A., Continuous infusion of escalated doses of amphotericin b deoxycholate: an open-label observational study. Clin. Infect. Dis., 2003. **36**: p. 943-951.

19. Eriksson, U., Seifer, B., Schaffner, A., Comparison of effects of amphotericin b deoxycholate infused over 4 to 24 hours: Randomized controlled trial. Br. Med. J., 2001. **322**: p. 579-582.

20. Peleg, A., Woods, M., Continuous and 4 h infusion of amphotericin B: a comparative study involving high-risk haematology patients. J. Antimicrob. Chemother., 2004. **54**(4): p. 803-8.

21. Lewis, R., Wiederhold, N., The solubility ceiling: a rationale for continuous infusion of amphotericin b therapy? Clin. Infect. Dis., 2003. **37**: p. 871-872.

22. Llanos, A., Cieza, J., Berando, J., Effect of salt supplementation on amphotericin nephrotoxicity. Kidney Int., 1991. **40**: p. 302-308.

23. Jurgens, R., Deluca, P., Papadimitriou D., Compatibility of amphotericin b with certain large-volume parenterals. Am. J. Hospital Pharm., 1981. **38**: p. 377-378.

24. Vakil, R., Kwon, G., PEG-phospholipid micelles for the delivery of amphotericin B. J. Controlled Release, 2005. **101**(1-3): p. 386-9.

25. Pfaller, M., Reference method for broth dilution antifungal susceptibility testing of yeasts : approved standard. 2002 ed. NCCLS, M27-A2. Vol. 22 no. 15. 2002, Wayne, Pa.: National Committee for Clinical Laboratory Standards.

26. Chou, T.-C., Talalay, P., Quantitative analysis of dose-effect relationships: the combined effects of multiple drugs or enzyme inhibitors. Adv. Enzyme Regul., 1984. **22**: p. 27-55.

27. Chou, T.-C., Talalay, P., Generalized equations for the analysis of inhibitions of Michaelis-Menten and higher-order kinetic systems with two or more mutually exclusive and nonexclusive inhibitors. Eur. J. Biochem., 1981. **115**(1): p. 207-16.

28. Instructions to Authors. Antimicrob. Agents Chemother., 2006. **50**(1): p. 1-21.

29. Odds, F., Synergy, antagonism, and what the chequerboard puts between them. J. Antimicrob. Chemother., 2003. **52**(1): p. 1.

30. Chou, T.-C., Theoretical basis, experimental design, and computerized simulation of synergism and antagonism in drug combination studies. Pharmacol. Rev., 2006. **58**(3): p. 621-681.

31. Espuelas, M., Legrand, P., Campanero, M., Appel, M., Cheron, M., Gamazo, C., Barratt, G., Irache, J., Polymeric carriers for amphotericin B: In vitro activity, toxicity and therapeutic efficacy against systemic candidiasis in neutropenic mice. J. Antimicrob. Chemother., 2003. **52**(3): p. 419-27.

32. Nakagawa, Z., Nucci, M., Branchini, M., Salomao, R., Richtmann, R., Colombo, A. In vitro susceptibility patterns of 200 recent bloodstream isolates of Candida species to four antifungal drugs determined by the NCCLS microbroth procedure. in Intersci. Conf. Antimicrob. Agents Chemother. 1998.

33. Ghannoum, M., Motawy, M., Abu Hatab, M., Ibrahim, A., Criddle, R., Multifactorial analysis of effects of interactions among antifungal and

antineoplastic drugs on inhibition of Candida albicans growth. Antimicrob. Agents Chemother., 1989. **33**(5): p. 717-25.

34. Greco, W., Bravo, G., Parsons, J., The search for synergy: a critical review from a response surface perspective. Pharmacol. Rev., 1995. **47**(2): p. 331-85.

35. Greco, W., Park, H., Rustum, Y., Application of a new approach for the quantitation of drug synergism to the combination of cis-diamminedichloroplatinum and 1-beta-D-arabinofuranosylcytosine. Cancer Res., 1990. **50**(17): p. 5318-27.

36. Steinbach, W., Schell, W., Blankenship, J., Onyewu, C., Heitman, J., Perfect, J., In vitro interactions between antifungals and immunosuppressants against Aspergillus fumigatus. Antimicrob. Agents Chemother., 2004. **48**(5): p. 1664-9.

37. Shadomy, S., Wagner, G., Espinel-Ingroff, E., Davis, B. A., In vitro studies with combinations of 5-fluorocytosine and amphotericin B. Antimicrob. Agents Chemother., 1975. **8**(2): p. 117-21.

38. Ghannoum, M., Motawy, M., Abu Hatab, M., Abu Elteen, K., Criddle, R., Interactive effects of antifungal and antineoplastic agents on yeasts commonly prevalent in cancer patients. Antimicrob. Agents Chemother., 1989. **33**(5): p. 726-30.

Chapter 6:

General discussion and conclusions

6.1 Conclusions and primary findings

The potential of polymeric micelles formed from PEG-DSPE as sustained release nanocarriers for amphotericin B has been evaluated in this dissertation. An emphasis has been placed on studying biocompatible or generally regarded as safe (GRAS) materials since further development can proceed without an explicit concern for biocompatibility, which may slow progress of particulate carriers prepared from novel synthetic polymers. PEG-phospholipid is a biocompatible polymer and is approved for use in humans. Similarly, PEG-b-poly(ε-caprolactone) degrades to non-toxic species and hence is expected to be safe for systemic administration.

PEG-DSPE micelles were studied for their ability to solubilize AmB and reduce toxicity. PEG-DSPE micelles clearly prevented AmB induced toxicity pointing to stable incorporation, *in vitro*. However, drug release and absorption kinetics studies revealed that AmB was rapidly dissociated from PEG-DSPE micelles, a likely situation *in vivo*. Cholesterol co-incorporation influenced properties of PEG-DSPE micelles and slowed AmB release in serum albumin raising promise as long-circulating carriers for AmB delivery. Novel polymeric micelles formed from PEG-DSPE and PEG-b-poly(ε-caprolactone) exhibited high thermodynamic stability, but were unable to prevent AmB association with serum albumin raising questions about the utility of these carriers in the context of AmB delivery. AmB in PEG-DSPE micelles was stable against precipitation in saline when combined with 5-fluorocytosine and solubilized rapamycin. PEG-DSPE micelles represented an interesting alternative to D-AmB, particularly in combination therapy involving AmB in conjunction with continuous infusion and sodium supplementation.

The following conclusions were derived from this dissertation:

1. PEG-DSPE micelles could solubilize high levels of AmB, when prepared using the solvent evaporation method. The relative self-aggregation of AmB in PEG-DSPE micelles was influenced by the molar ratio of PEG-DSPE to AmB. Size exclusion chromatography and absorbance spectroscopy revealed that AmB deaggregation occurs on incorporation in PEG-DSPE micelles. Micelle encapsulated AmB exerted low levels of hemolysis regardless of drug aggregation. Also, AmB solubilization in PEG-DSPE micelles caused a significant reduction in HK-2 cytotoxicity relative to free AmB. Despite the reduction in toxicity, potent fungicidal activity was observed *in vitro* for micelle encapsulated AmB. These results pointed to slow release of monomeric AmB from PEG-DSPE micelles in an *in vitro* setting.

2. Cholesterol incorporation in PEG-DSPE micelles resulted in increased rigidity in the micelle core, evident from a dramatic peak broadening in the ^{1}H-NMR spectrum and a moderate decrease in dipyrene excimer emission. The absorption spectrum of AmB in cholesterol containing PEG-DSPE micelles presented narrow peaks compared with AmB in PEG-DSPE micelles, which was taken to be an indication of an altered interaction of the drug with the micelle core. Absorption kinetics revealed that AmB in PEG-DSPE micelles was free to interact with serum albumin, a likely situation *in vivo*. In contrast, there were no changes in the absorption spectrum of AmB in PEG-DSPE micelles with cholesterol on addition to serum albumin. Results from release

studies were consistent with findings from absorption kinetics. Cholesterol incorporation considerably slowed AmB release from PEG-DSPE micelles in serum albumin, raising promise for these micelles as long-circulating carriers *in vivo*.

3. Formation of unimodal mixed polymeric micelles from PEG-DSPE and PEG-b-poly(ε-caprolactone) was verified using size-exclusion chromatography. These mixed micelles had lower CMCs relative to PEG-DSPE or PEG-b-poly(ε-caprolactone) micelles due to a cooperative interaction between hydrophobic segments. NOESY ^{1}H-NMR pointed to an interpenetration of hydrophobic segments of polymers. Contrary to PEG-b-poly(ε-caprolactone) micelles, which did not solubilize AmB to any appreciable extent, mixed polymeric micelles encapsulated clinically relevant levels of AmB. AmB release in buffer depended on the ratio between PEG-DSPE and PEG-b-poly(ε-caprolactone) pointing to a composition dependent drug – micelle interaction. Absorption kinetics studies indicated that AmB encapsulated in these mixed micelles was free to interact with serum albumin and hence is expected to be rapidly dissociated from the carrier, *in vivo*.

4. Size exclusion chromatography, dynamic light scattering and solution turbidity measurements indicated that AmB loaded PEG-DSPE micelles were essentially unchanged in a saline vehicle for prolonged periods of time. Hence, in this form AmB has a distinct advantage over deoxycholate AmB as

it may allow for slow or continuous administration of AmB with simultaneous sodium supplementation in a single IV-access line, without concern for drug precipitation.

5. AmB remained solubilized in PEG-DSPE micelles when combined with 5-fluorocytosine and solubilized rapamycin in saline. This result is important since it enables evaluation of the three-drug combination for the treatment of systemic fungal diseases in conjunction with sodium supplementation. The pair-wise or three-drug interactive effects of the AmB, rapamycin and 5-flucytosine combination indicated an additive or moderately synergistic increase in fungicidal potency.

6.2 Suggestions for future research

6.2.1 Determination of serum lipoprotein distribution of AmB

Wasan et al. have shown that the binding of AmB to lipoproteins may enhance uptake of drug by mammalian cells, hence influencing drug selectivity (1, 2). The formation of LDL – AmB complexes is mediated by the interaction between the carrier and AmB (3). Lipid based carriers that preferentially associate with HDL cause lower nephrotoxicity compared to free AmB (4). Hence, a study defining the interaction of AmB in PEG-DSPE micelles with various lipoprotein fractions is suggested prior to *in vivo* toxicity studies. The lipoprotein in serum may be fractionated using standard density gradient ultracentrifugation methods (4, 5).

6.2.2 In vivo dose escalation studies for AmB in PEG-DSPE|Cholesterol micelles

PEG-DSPE micelles incorporating cholesterol release AmB slowly in physiological concentrations of serum albumin. Hence, sustained release of AmB from these carriers is expected *in vivo*. Studies aimed at defining a maximal tolerated dose of AmB encapsulated in these nanocarriers relative to D-AmB are suggested. Kidney and liver toxicity (acute and 7-day) may be meaningful end-points (6). Blood urea nitrogen (BUN) and serum creatinine levels are markers for AmB induced nephrotoxicity and may be assessed using standard procedures (7, 8). Aspartate aminotransferase (ASAT) and alanine aminotransferase (ALAT) levels may be used to monitor for hepatocellular injury (9-11).

6.2.3 In vivo biodistribution and pharmacokinetic studies with AmB in PEG-DSPE and PEG-DSPE|Cholesterol micelles

Cholesterol containing PEG-DSPE micelles may serve as long-circulating nanocarriers influencing drug pharmacokinetics. The small size of these carriers may enable penetration into deep sites of infection; hence it may be reasonable to expect an altered drug biodistribution. A detailed pharmacokinetic study in a suitable rodent model would enable testing of this hypothesis. A biodistribution study involving the spleen, liver, kidney and lungs is expected to further elucidate the fate of PEG-DSPE micelles *in vivo*. AmB content in plasma and tissue samples may be determined using a HPLC assay (12, 13).

6.2.4 In vivo toxicity studies with PEG-DSPE micelle encapsulated AmB with slow infusion in conjunction with sodium supplementation

There is recent evidence that suggests that AmB toxicity can be reduced by slow administration (14). AmB solubilized in PEG-DSPE micelles presents an interesting alternative to D-AmB for exploring slow infusion in conjunction with sodium supplementation. Moreover, PEG-DSPE is potentially a less toxic vehicle compared with sodium deoxycholate. Since micelle encapsulated AmB is stable in saline solutions for prolonged periods, a study designed to define the dependence of maximal tolerated dose on infusion rate and varied degrees of sodium supplementation would be instructive. Formulations may be administered at specified infusion rates via jugular cannula in rats. Markers for nephrotoxicity and hepatocellular injury suggested in the previous section may be used for these studies.

6.2.5 In vivo toxicity and efficacy studies of of pair-wise and three-drug combinations in a murine model of systemic candidiasis

An experiment exploring the nephrotoxicity of AmB in rats after chronic treatment (7-day) is proposed focusing on the effects of infusion rate, sodium supplementation and co-administered antifungal agents (rapamycin or 5-FC). Since the degree of nephrotoxicity correlates with cumulative dose, a chronic toxicity study would be more relevant compared with an acute toxicity experiment commonly used for AmB (15). Rats may be randomized into appropriate groups receiving AmB, rapamycin and 5-FC as two- or three-drug combinations, with D-AmB as a positive control. Elevation in the serum creatinine and blood urea nitrogen levels may be used as indicators for the onset of kidney toxicity (7, 8). Liver toxicity may be monitored by determining levels of aspartate aminotransferase (ASAT) and alanine aminotransferase (ALAT) (9-11).

Depending on the outcome of toxicity studies, the utility of combining several antifungal drugs may be evaluated *in vivo* in a murine model of systemic candidiasis. Infected mice may be given several doses of AmB, rapamycin and 5-FC as pair-wise or three-drug combinations via a catheter placed in the jugular vein, using a subcutaneously implanted osmotic pump. *In vitro* studies indicate that a high level of 5-FC relative to AmB and rapamycin has potential for synergistic activity. Since kidneys represent a major site for *Candida albicans* colonization, disease progression may be monitored by determining fungal burden in the kidneys using established procedures. Comparative analysis of efficacy may be presented as an area under time-kill curve, relative to D-AmB (16).

6.3 References

1. Wasan, K., Rosenblum, M., Cheung, L., Lopez-Berestein, G., Influence of lipoproteins on renal cytotoxicity and antifungal activity of amphotericin B. Antimicrob. Agents Chemother., 1994. **38**(2): p. 223-7.

2. Wasan, K., Lopez-Berestein, G., Modification of amphotericin B's therapeutic index by increasing its association with serum high-density lipoproteins. Ann. N Y Acad. Sci., 1994. **730**: p. 93-106.

3. Brajtburg, J., Bolard, J., Carrier effects on biological activity of amphotericin B. Clin. Microbiol. Rev., 1996. **9**(4): p. 512-31.

4. Wasan, K., Lopez-Berestein, G., The interaction of liposomal amphotericin B and serum lipoproteins within the biological milieu. J. Drug Target., 1994. **2**(5): p. 373-80.

5. Chapman, M., Goldstein, S., Lagrange, D., Laplaud, P., A density gradient ultracentrifugal procedure for the isolation of the major lipoprotein classes from human serum. J. Lipid Res., 1981. **22**(2): p. 339-358.

6. Van Etten, E., Van Vianen, W., Tijhuis, R., Storm, G., Bakker-Woudenberg, I., Sterically stabilized amphotericin B-liposomes: Toxicity and biodistribution in mice. J. Controlled Release, 1995. **37**: p. 123-129.

7. Larsen, K., Creatinine assay by a reaction-kinetic principle. Clin. Chim. Acta, 1972. **41**: p. 209-17.

8. Chaney, A., Marbach, E., Modified reagents for determination of urea and ammonia. Clin. Chem., 1962. **8**: p. 130-2.

9. Miller, M., Reversible hepatotoxicity related to amphotericin B. Can. Med. Assoc. J., 1984. **131**: p. 1245-1247.

10. Leppanen, E., Grasbeck, R., Experimental basis of standardized specimen collection: the effect of moderate ethanol consumption on some serum components (K, Na, ASAT, ALAT, CK, LD, total protein). Scand. J. Clin. Lab. Invest., 1987. **47**(4): p. 337-43.

11. Amacher, D., Serum transaminase elevations as indicators of hepatic injury following the administration of drugs. Reg. Toxicol. Pharmacol., 1998. **27**(2): p. 119-130.

12. Egger, P., Bellmann, R., Wiedermann, C., Determination of amphotericin B, liposomal amphotericin B, and amphotericin B colloidal dispersion in plasma by high-performance liquid chromatography. J. Chromatogr. B Biomed. Sci. Appl., 2001. **760**(2): p. 307-13.

13. Eldem, T., Arican-Cellat, N., Determination of amphotericin B in human plasma using solid-phase extraction and high-performance liquid chromatography. J. Pharm. Biomed. Anal., 2001. **25**(1): p. 53-64.

14. Peleg, A., Woods, M., Continuous and 4 h infusion of amphotericin B: a comparative study involving high-risk haematology patients. J. Antimicrob. Chemother., 2004. **54**(4): p. 803-8.

15. Deray, G., Amphotericin B nephrotoxicity. J. Antimicrob. Chemother., 2002. **49 Suppl 1**: p. 37-41.

16. Andes, D., Safdar, N., Marchillo, K., Conklin, R., Pharmacokinetic-pharmacodynamic comparison of amphotericin B (AMB) and two lipid-associated AMB preparations, liposomal AMB and AMB lipid complex, in murine candidiasis models. Antimicrob. Agents Chemother., 2006. **50**(2): p. 674-84.